universität wien

# DIPLOMARBEIT

Titel der Diplomarbeit

## Investigating directionality of genome release from Human Rhinovirus A 2

>Band 1 von 1 Bänden<

Verfasserin

Katharina Huszar

angestrebter akademischer Grad

Magistra der Naturwissenschaften (Mag.rer.nat.)

Wien, im Oktober 2013

| | |
|---|---|
| Studienkennzahl lt. Studienblatt: | A 441 |
| Studienrichtung lt. Studienblatt: | Diplomstudium Genetik - Mikrobiologie (Stzw) UniStG |
| Betreuerin / Betreuer: | Univ.-Prof. Dipl.-Ing. Dr. Dieter Blaas |

I thank

Univ.-Prof. Dipl.-Ing. Dr. Dieter Blaas for his guidance and patience

Prof. Dr. Ernst Kenndler for helpful suggestions

Irene Gösler for preparation of virus and mental support

Angela Pickl-Herk for guidance

Gerry Bilek, Victor Weiss and Christoph Weber for helpful suggestions and making me laugh so hard, that I needed to go to the stairwell (not once)

Abdul Ghafoor Khan for support and help during late nights

Xavier Subirats, Nena Matscheko, Shushan Harytyunian and Mohit Kumar for the great Labmosphere

Karin Waclawek for mental support

Nathalie Landstetter, Mohit Kumar, Madeleine Grünwidl and Daniela Klinka (and Bohne) for helpful suggestions about manuscript preparation

Dank an meine Familie, die mich in diese Welt gesetzt hat und mich dabei unterstützt hat der Mensch zu werden, der ich bin. In Gedenken an Opa Nießler und Grossmutti.

*"By perseverance the snail reached the ark"*

*Charles Haddon Spurgeon (1834 – 1892)*

# Table of contents

# 1 Abstract

Human Rhinoviruses (HRVs) are depending on a human cell to generate progeny. The natural host cell of HRV is a ciliated epithelial cell in the respiratory tract; HRV infections are responsible for about 50% of mild infections of the upper respiratory tract. HRVs consist of an RNA genome protected by a protein shell (capsid). The aim of this study was to elucidate the mechanism of uncoating of Human Rhinovirus A2 (HRV2), i.e. the process of genome release from the capsid. Coarsely, HRV2 binds to its cognate receptor and is taken up by the cell via endocytosis. Endocytosed vesicles get acidified, and this drop of pH causes the HRV2 particle to change its morphology. Conformational changes of the viral proteins lead to expansion of the capsid, pores are opened and the RNA is released. The viral capsid is symmetric; therefore several pores are opened simultaneously. We wanted to know: Is the RNA genome ejected by one particular pore, or are several points of egress chosen, with loops protruding from the holey capsid? If one pore is chosen, does the RNA emerge as a single strand, or in a paired conformation? Is there a directionality of egress, i.e. is it regulated that a particular end of the RNA exits first? Those questions were addressed by two different chemical methods that were focused on either quickly capturing a snapshot of RNA in the act of egress or alternatively, halting exit of the genome.

In Selective 2´-Hydroxyl Acylation and Primer Extension (SHAPE) an electrophile reagent reacts with the 2´hydroxyl (2´OH) group of RNA to form an ester; exclusively nucleotides that are not involved in base pairing or tertiary interactions are accessible to modification. Several chemicals were shown to be suitable for SHAPE chemistry; depending on the chemical, the reaction is complete in down to ~1 second. Due to this fast reactivity, a snapshot of RNA release can be taken, determining the length and nature of the protruding part of the genome. Modifications are detected by a halt in reverse transcription, the output of a SHAPE experiment are cDNA fragments of different length. The method was adjusted to allow for the analysis of cDNA fragments by an ABI PRISM®310Genetic Analyzer. However, this change of the protocol did not allow data analysis by the software designed for SHAPE analysis and an alternative program proofed to be unreliable. Therefore, another approach to assessing directionality of RNA release from HRV was chosen. Formaldehyde reacts with both amino acids as well as the bases of nucleic acids. Crosslinking of RNA to the capsid would halt RNA egress and allow characterization of the remaining part of the RNA. Halting egress turned out to be expendable, because the chosen conditions to stimulate RNA release were insufficient. Acidification of HRV2 in plain buffer solution primes the virus for uncoating but is not sufficient to trigger release of the RNA genome. Even following acidification of diluted samples for 30 minutes at 37°C, the majority of the particles did not release their genome, as demonstrated by resistance of the viral RNA to bovine pancreatic ribonuclease A (RNase A).

Using SDS-PAGE and western blotting, the particles generated by acidification were identified to be uncoating intermediates (135S particles) that have lost the small viral protein VP4 but still contain RNA. In the 135S particle, part of the RNA is accessible to digestion by RNase A. Recovery of the RNA and PCR analysis following reverse transcription revealed that the 3´ end of the genome is missing whereas the 5´end is protected.

# 2 Introduction

Human Rhinovirus (HRV) is the causative agent of the common cold and HRV infections are responsible for about 50% of mild infections of the upper respiratory tract (*Heikkinen & Jarvinen,* 2003). Although HRV is rather benign, due to its high infectivity HRV causes a significant economic burden because of large expenditures for medication and sickness absence rates (*Fendrick et al.,* 2003). Further, it has been reported, that HRV is involved in the exacerbation of asthma and chronic obstructive pulmonary disease (*Hayden,* 2004*, Peltola et al.,* 2008, *Jacobs et al., 2013*). There is no vaccine protecting against HRV because of the large number of different serotypes. Understanding the life cycle of rhinoviruses can point up potential therapeutic targets.

## 2.1 Classification of Rhinoviruses

According to the International Committee on Taxonomy of Viruses (ICTV), Human Rhinoviruses (HRVs) belong to the *Picornaviridae* family[1]. *Picornaviridae* are small, non-enveloped viruses consisting of an icosahedral capsid and a single stranded RNA genome of positive polarity. The *Picornaviridae* family currently comprises 17 Genera; Rhinoviruses are classified as a member of the Genus Enterovirus.

Based on sequence similarity, Rhinoviruses are grouped into the major clades HRV-A, -B and –C. A fourth clade, HRV-D was suggested. Each clade comprises a large number of different HRV serotypes; constant mutation as well as recombination between different HRV strains contributes to variation of the HRV genome, generating new serotypes (*Palmenberg et al., 2010*). Rhinoviruses are further classified into a major and a minor group according to their receptor specificity. 12 serotypes of HRV-A bind to members of the low-density lipoprotein receptor (LDLR) super gene family, the remaining strains of HRV-A as well as HRV-B bind to human intercellular adhesion molecule 1 (ICAM-1) (*Abraham & Colonno 1984, Uncapher et al.,* 1991, *Vlasak et al.,* 2005). Receptor usage of the recently classified HRV-C is currently not known (*McErlean et al., 2008*). Additionally, HRVs can be grouped into antiviral groups A and B, depending on differential sensitivity to antiviral compounds (*Andries et al., 1990*).

## 2.2 Composition

HRVs consist of a protein shell (capsid) and a single stranded RNA genome of positive polarity.

### 2.2.1 Capsid

The protein shell, i.e. the capsid, is of icosahedral symmetry and has a diameter of about 30nm. The capsid is composed of 60 units (protomers). Each protomer is built from one copy of the viral proteins (VPs) VP1, VP2 and VP3; VP4 is lining the inner surface of the capsid. Figure 1 shows an example of an icosahedral capsid. At the fivefold axes 5 copies of VP1 are joined and form a star-shaped dome; each dome is surrounded by a depression, the canyon (see Figure 1 c). Residues buried in the canyon are partially protected against immune selection (*Rossmann et al., 1985*). A tryptophan residue at the interior of the particle (Trp2038) conserved among rhinoviruses is in contact with the RNA genome (*Verdaguer et al.,* 2000).

[1] http://www.ictvonline.org/virusTaxonomy.asp?version=2012

A viral capsid has two chores: protection of the genome on the way from host cell to host cell and delivery of the genome when arrived at the host cell (*Skern 2006*). It was proposed for some HRV serotypes that the capsid is stabilized during its spread from cell to cell by (transient) incorporation of a fatty acid into a small cavity at the bottom of the canyon (the hydrophobic pocket) and/ or by coordination of a $Ca^{2+}$ or a $Zn^{2+}$ ion at each fivefold axis (*Zhao et al., 1996; Hadfield et al., 1997, Verdaguer et al.,* 2000, *Hewat et al., 2004*). In order to stick to or even overcome a host cell membrane, capsid proteins of picornaviruses contain hydrophobic sequences and/ or are myristoylated (*reviewed in Tsai 2007*).

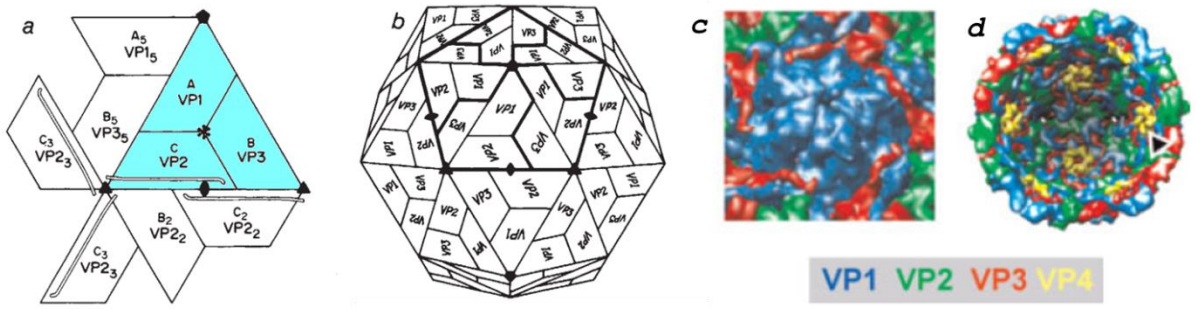


Figure 1: Models of an icosahedral capsid

a: assembly of icosahedral subunits. 3 viral proteins (VP) combine to form a protomer (cyan); protomers assemble to build the capsid. Indicated are the twofold axes (oval, two identical proteins neighboring), threefold axes (triangle, 3 identical proteins neighboring) and fivefold axes (pentagon).
b: model of an icosahedral capsid
c: Close-up of the star-shaped dome at the fivefold axis and the surrounding canyon of the HRV2 capsid.
d: The interior of the HRV2 capsid. VP4 (yellow) is localized at the inner surface, beneath the fivefold axes (arrow head).
Pictures adapted from *Rossmann et al*., 1985 and *Fuchs & Blaas*, 2010.

### 2.2.2 Genome

RNA genomes of picornavirus family members are roughly 7100 bases in length and share a similar organization. A single large open reading frame (ORF) is flanked by a 5´ untranslated region (UTR) and a 3´UTR followed by a poly (A) tail (*Ahlquist & Kaesberg, 1979, Skern et al., 1985*). The 5´and 3´ UTRs are folded into structures that are important for translation and replication.

The 5´ UTR contains a cloverleaf conserved between rhinoviruses; it is involved in initiation of replication. The clover leaf is followed by a spacer tract that is variable even within a given serotype; mutations in this region were suggested to affect virulence. Initiation of translation in eukaryotes usually starts at a 5´terminal cap, which is not present at the 5´end of the HRV genome. Instead, it is attached to the small viral protein VPg. A structure within the 5´UTR called internal ribosome entry site (IRES) is used as platform for binding of host cell translation initiation factors and ribosomes. The IRES of HRV is folded into a stem that includes the start codon for translation. The 3´ UTR of rhinoviruses folds into a stem located at the end of the ORF, aiding termination of translation. This hairpin is extended by a poly(A) tail that is required for replication (*Golini et al., 1978, Palmenberg et al., 2009, Palmenberg et al., 2010*).

The overall folding of picornavirus genomes was calculated to be rather relaxed, with about 63% of the bases involved in paired configurations. According to folding predictions, the RNA adopts an elongated conformation with protruding stems, the two ends of the picornaviral genome being located close to each other (*Palmenberg & Sgro, 1997*).

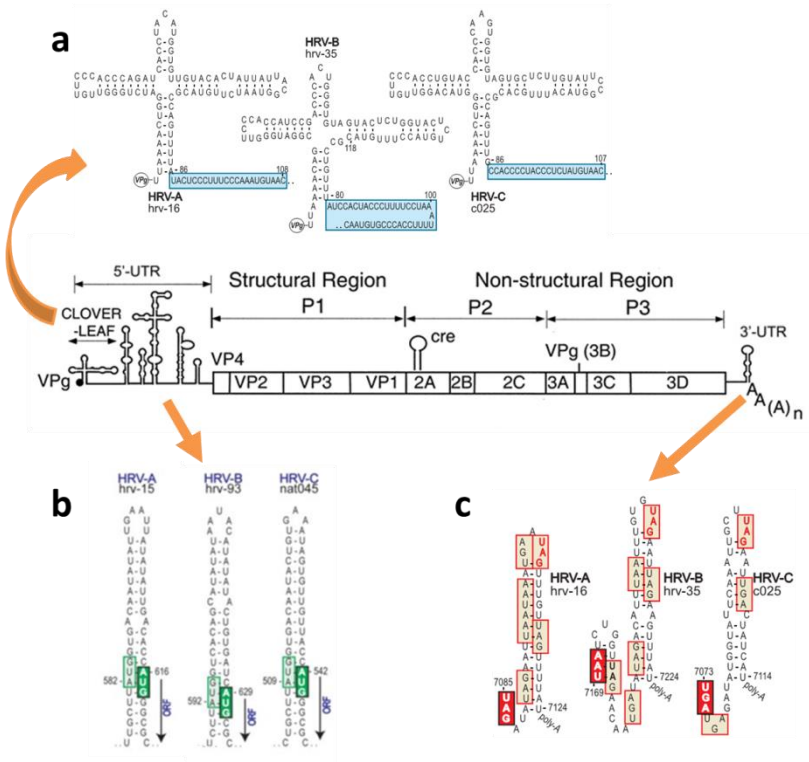


Figure 2: HRV genome, ORF and structure elements required for translation and replication.

The HRV genome consists of a single open reading frame flanked by untranslated regions (UTRs). The open reading frame codes for a polyprotein, which is co- and post-translationally processed to yield the individual viral proteins. The polyprotein is segmented into the structural region P1 and two non-structural regions P2 and P3, the precursors for proteins required for replication and interaction with host cell functions. The UTRs are folded into conserved structures required for translation and replication. Cre, a conserved hairpin structure required for initiation of replication, is located within the coding region.

a: The 5´UTR contains a cloverleaf conserved among picornaviruses that is required for replication. The cloverleaf is followed by a variable pyrimidine tract that might influence infectivity.

b: The viral genome is not capped, unlike host cell mRNAs, instead it is linked to the small protein VPg. A structure within the 5´UTR called internal ribosome entry site is used for recruitment of host cell translation factors and ribosomes. The IRES of HRVs forms an unbranched stem that contains the AUG of the open reading frame. The paired AUG motif is highly conserved among HRVs, but was not found in any other enterovirus genome.

c: HRV 3' UTRs fold into an unbranched stem adjacent to the termination codon. This structure is extended by a poly(A) tail important for replication.

Picture merged from *Gerber et al*., 2001, *Palmenberg et al*., 2009 and *Palmenberg et al*., 2010

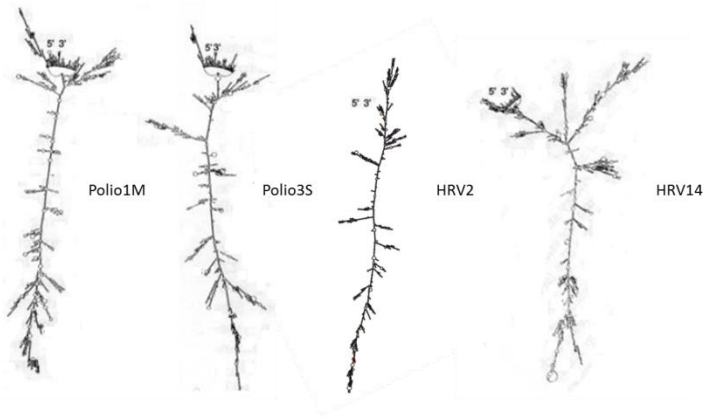


Figure 3: Folding predictions of picornaviral genomes

Picornavirus genomes are calculated to adopt longitudinal structures with protruding stems. In the folding predictions the 5´ and 3´ ends are in close proximity.

The secondary structures of RNAs of Polio1M, Polio3S and HRV14 are adapted from *Palmenberg & Sgro, 1997,* they were calculated by the program mfold Version 2.2. The folding of the HRV2 genome was calculated on the RNAfold Webserver[2]. In the sequence of the HRV2 cDNA (GenBank accession no. X02316) T was replaced by U by using the life science tools of fr33.net[3] and 50 A residues were added prior to calculation.

## 2.3 Viral life cycle

In order to persist, all viruses must:

- Bind to a host cell it can replicate in (attachment)
- Enter the cell (entry)
- Release its genome into the appropriate compartment of the host cell (uncoating)
- Mediate translation of its viral proteins (gene expression)
- Ensure multiplication of its genome (replication)
- Package their genome and, if necessary, proteins into capsids (assembly)
- Escape from the cell (release)
- Prime the capsid for the next round of infection (maturation)

The sequence of replication and gene expression may vary, depending on the type of genome (combined from a presentation of the Hafenstein lab[4] and *Skern, 2006*). Stages in the life cycle of human rhinoviruses are outlined below. The steps leading to release of the genome are covered in more detail since this thesis concentrates on the uncoating step.

### 2.3.1 Attachment

The natural host cell of HRV is a ciliated epithelial cell; HRVs were found to replicate in the upper and lower respiratory tract (*Bardin et al.,* 1994, *Arruda et al.,* 1995, *Gern et al.,* 1997). Major group HRVs bind to intercellular adhesion molecule-1 (ICAM-1), minor group HRVs recognize members of the low- density lipoprotein receptor (LDLR) superfamily (*Greve et al.,*

[2] RNAfold Webserver: http://rna.tbi.univie.ac.at/cgi-bin/RNAfold.cgi [July 2013]
[3] Complementary sequence, T → U http://www.fr33.net/seqedit.php [July 2013]
[4] Outline of a viral life cycle in www.psu.edu/dept/hafenstein/pdfs/organtini.pptx [July 2013]

*1989, Gruenberger et al., 1995*). In addition, certain major group HRVs can also use heparan sulfate (HS) proteoglycan as an alternate receptor (*Khan et al., 2007*). The receptor for HRV-C is not known yet. The N- terminal domain of ICAM-1 interacts with residues hidden in the canyon, whereas VLDL was shown to interact via several domains with residues around the 5-fold axis (*Colonno et al., 1988, Olson et al., 1993*, *Register et al., 1991, Hewat et al., 2000*)

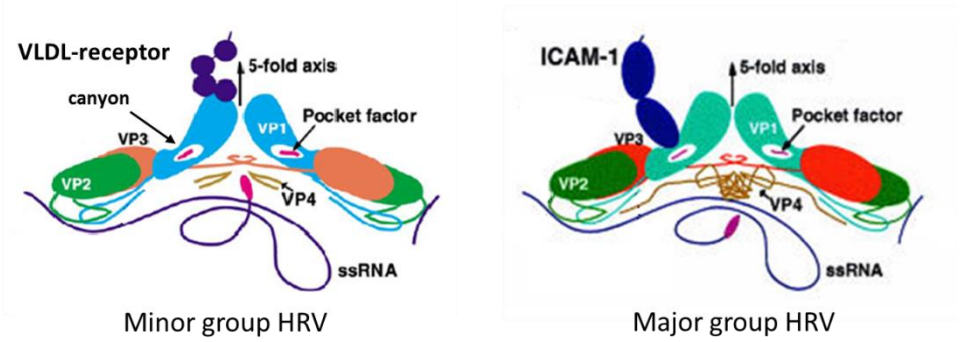


Figure 4: Scheme of receptor binding to minor and major receptor group viruses

Members of the LDLR superfamily recognize residues around the fivefold axes of minor group HRVs. The receptor of major group viruses, ICAM-1, inserts into the canyon. Pictures adapted from *Hewat et al., 2002* & *Hewat et al., 2004*

### 2.3.2 Entry

Enveloped viruses can gain access to the host cell cytoplasm by fusing their membrane with the host cell´s membrane. Nonenveloped viruses lack the lipid envelope and are therefore incapable of fusing with the host cell membrane; they depend on being actively internalized by the host cell by receptor-mediated endocytosis. Since viruses are multivalent, they may be able to stimulate receptor clustering and thereby activate signaling pathways leading to uptake of receptor and ligand. Signaling can be induced either by an inherent activity in the receptor or by formation of lipid rafts that activate signaling molecules on the cytoplasmic side of the membrane.

Four primary endocytic routes have been described to be involved in entry of viruses: Clathrin-mediated endocytosis, caveolae-mediated endocytosis, non-clathrin-, non-caveolae-mediated endocytosis and macropinocytosis. Vesicles internalized by clathrin- dependent and independent pathways as well as by macropinocytosis are targeted to the lysosome and get acidified progressively, thereby travelling through early (pH 6.5-6.0) and late endosomes (pH6.0-5.5). Caveolar/ lipid raft pathways transport cargo to pH-neutral organelles in the cytoplasm (caveosomes) and further to the endoplasmic reticulum. They are not acidified. The formation of entry vesicles is rather heterogeneous; inside the cell the pathways meet, and cargo internalized by different mechanism may end up in the same organelle. Viruses can use multiple pathways, thereby adapting to a range of host cells and various conditions (*reviewed in Sieczkarski & Whittaker, 2005 and Marsh & Helenius, 2006*).

Major group viruses are internalized by clathrin-mediated endocytosis (*Grunert et al., 1997*) as well as by non-clathrin-, non-caveolae-mediated endocytosis (*Khan et al.,* 2010). Minor group viruses preferentially use the clathrin-dependent internalization pathway, which is triggered by

members of the LDLR-family (*Hofer et al., 1994, Snyers et al., 2003*). Both major and minor group viruses initiate formation of membrane rafts and activate raft-dependent signaling (*Dreschers et al., 2007*).

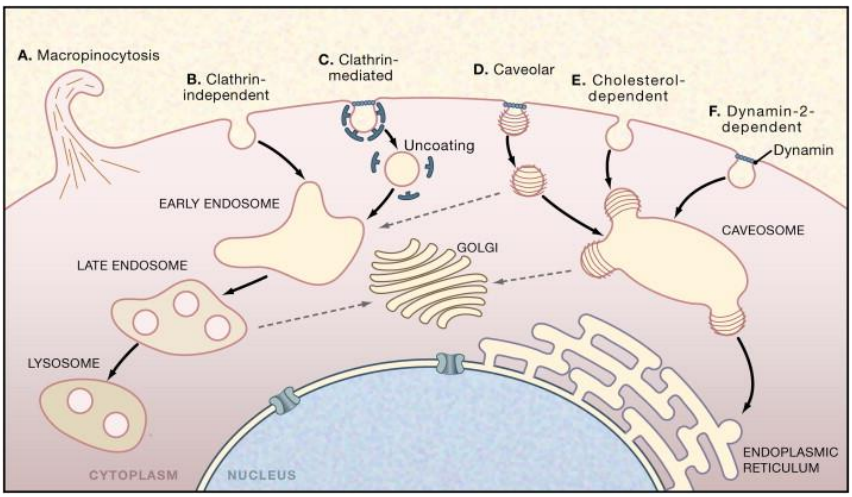


Figure 5: Entry pathways engaged by non-enveloped viruses

Currently, there is evidence for six entry pathways used by viruses. Vesicles internalized by macropinocytosis (A), Clathrin- independent (B), as well as clathrin-mediated endocytosis (C) are acidified during progression to lysosomes. The raft-induced pathways depending on caveolae (D), cholesterol (E) and dynamin-2 (F) are not acidified; they are targeted to the endoplasmic reticulum. Figure taken from *Marsh & Helenius, 2006*

Although internalized, viruses in vesicles are still part of the extracellular space, and must overcome the vesicular membrane. This can be achieved by disruption of the membrane or by pore formation. By membrane disruption, both viral proteins as well as the genome enter the cytoplasm, whereas by pore formation only the genome is delivered into the cytoplasm (*reviewed in Sieczkarski & Whittaker, 2005*). Disruption of the membrane or pore formation is mediated by membrane active peptides that are exposed or released upon arrival of the virus at the site of penetration. Conformational changes that expose the membrane active peptides can be mediated by the receptor or by the chemical environment of the given compartment (*reviewed in Tsai 2007* and *Banerjee & Johnson, 2008*).

Major group HRVs were shown to gain access to the host cell cytoplasm by disrupting the endosomal membrane (*Schober et al., 1998*). Exposal of membrane active peptides is enhanced mainly by the receptor, as HRV14 can escape non-acidified vesicles (*Bayer et al., 1999*). However, contribution of receptor and acidification to induction of structural changes varies among different major group serotypes (*Khan et al., 2007*). In contrast, minor group viruses dissociate from their receptor during the progression from early to late endosomes (*Brabec et al., 2003*); conformational changes releasing membrane active peptides are strictly dependent on acidification (*Prchla et al., 1994*, *Bayer et al., 1998, Bayer et al., 1999*). Minor group viruses were shown to form pores in late endosomes, only the genome accesses the host cell cytoplasm (*Prchla et al., 1994, Prchla et al., 1995*, *Brabec et al., 2005*).

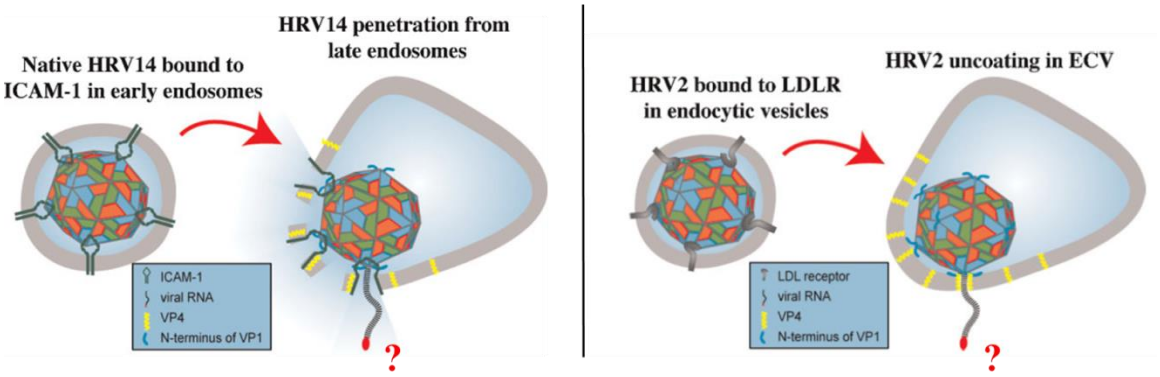


Figure 6: Models for penetration and uncoating of a major and a minor group HRV

Major group viruses (such as HRV14) enter the cytoplasm by endosome disruption. Exposure of the N-terminus of VP1 and VP4 is mainly triggered by binding of the receptor ICAM-1. VP4 inserts into the membrane; it was suggested that shearing forces of the receptor cause membrane disruption. Minor group viruses (such as HRV2) release VP4 and the VP1 N-termini upon acidification of endosomal carrier vesicles (ECV). VP4 forms pores through which the genome is released into the cytoplasm. In this model, the RNA exits with the VPg at the 5´first, however, recently it was demonstrated that it exits tail first (i.e. beginning with the poly-(A)). Furthermore, there is evidence that the RNA exits at the twofold axis rather than at the fivefold vertex. Picture adapted from *Fuchs & Blaas, 2010*.

### 2.3.3 Uncoating

Uncoating denotes the process of RNA release from the capsid, ideally into the cytoplasm. In the case of rhinoviruses, uncoating is associated with entry. Conformational changes described above that expose membrane active peptides also prime the virus for release of its genome. The structures of native and empty particles of representatives of major and minor viruses have been studied by cryo-electron microscopy and X-ray crystallography. Comparison of those structures hints at putative exit points for the membrane-active peptides as well as for the RNA.

Conformational changes of minor group viruses are independent of the receptor (*Brabec et al., 2003*). Comparing the crystal structures of native and empty particles of HRV2, the diameter of the empty particle is enlarged and pores have opened. Reorganization of the VP1 units around the fivefold axes in combination with a coordinated shift of VP2 and VP3 exerts strain on the protomer interfaces, and pores open at the canyon floor and at the two-fold axes. The pores at the canyon floor are located along a line connecting the three-fold and five-fold axes; they are suggested to allow temporal exposure of the N-termini of VP1. The RNA was proposed to exit at one of the pores opened at the twofold axes; first, these are large enough to accommodate an RNA strand; second, the inner surface of this channel is lined with electronegative atoms, which would facilitate extrusion of the RNA genome (*Verdaguer et al., 2000, Garriga et al., 2012*). If RNA egress is aborted, residual RNA organizes into a rod- like structure which is contacting the inner surface of the capsid at a twofold axis (*Harutyunyan et al., 2013*). Further, picturing the closely related poliovirus during the process of RNA release via cryo-electron microscopy indicates that the RNA leaves the capsid through a hole near one of the viral 2-fold axes (*Bostina et al., 2011*).

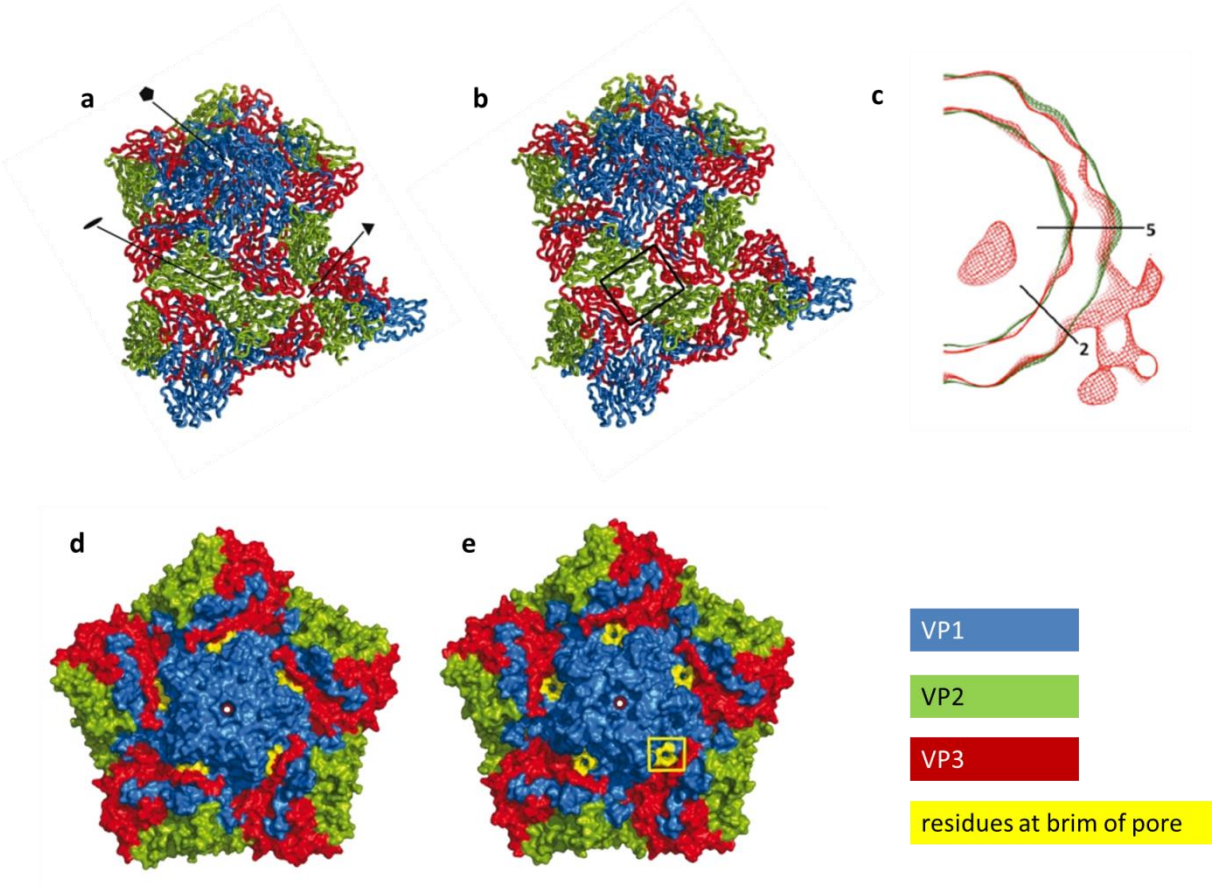


Figure 7: comparison of native and empty structures of HRV2

Conformational changes of VP1 around the fivefold axes together with alterations in VP2 and VP3 induce strain at the twofold axes and pores open both at the twofold axes as well as at the floor of the canyon

a+b: Ribbon diagrams reconstructed from X-ray crystallography focusing on contacts between pentamers in the native (a) and empty (b) HRV2 particle. Shown is one pentamer that interacts with units of neighboring pentamers at a twofold and a threefold axis. The fivefold (pentagon), threefold (triangle) and twofold (oval) axes are indicated. In the empty capsid, a pore has opened at the twofold axis that was suggested as the exit point for the RNA genome. Figure taken from *Garriga et al., 2012*
c: Poliovirus caught in the act of uncoating. Cryo-EM data picture the RNA to leave at a pore near the 2 fold axis. Picture taken from *Bostina et al., 2011*
d+e: Surface reconstruction of a native (d) and an empty (e) HRV2 particle from X-ray crystallography. Residues at the capsid surface that rearrange to open the pores at the canyon floor are highlighted in yellow. Those pores were proposed as exits for the N-termini of VP1 in the 135S particle. In the empty particle, the N-termini of VP1 are most probably re-internalized, but the pores remain open. Figure taken from *Garriga et al., 2012*

Uncoating of major group viruses is induced by the receptor and aided by low endosomal pH (*Nurani et al., 2003*). Xing et al. proposed the following mechanism for uncoating of major group viruses through ICAM-1: By a mechanism called breathing the interprotomer junctions are opened transiently at physiological temperatures (*Li et al., 1994*, *Lewis et al., 1998*). The receptor inserts into the canyon between two adjacent protomers and thereby locks the virion in the opened conformation. In comparison to the native capsid of HRV3, the structure of the receptor-bound expanded capsid shows significant differences along the interprotomer interfaces in the canyon region and at the twofold axis junctions. The N-terminal regions of

VP1s as well as VP4s are suggested to be externalized through the open canyon region. Expulsion of the RNA and VP4 result in a further conformational change of VP1 and dissociation of the empty capsid from the receptor (*Xing et al., 2003*). Analysis of HRV14 structural changes suggested a more active role of the receptor in uncoating. Comparison of empty particles to native virus indicated that binding of the receptor ICAM-1 expels the pocket factor and induces a hinge-type movement of VP1 to open up channels at the 5 fold axis. However, below the 5 fold axes the N-termini of VP3 are intertwined to form β barrels, which block the channel. Nevertheless, originally, it was hypothesized that a single permissive pore is opened at one of the 5-fold axes by enlargement of one of the VP3 β barrels; such features, would, however, escape detection in symmetrical reconstructions. At the twofold axes, through the rearrangement of VP2 units, a gap is opened. In HRV14 the N-termini of VP1 are suggested to escape at pores formed between neighboring VP1 units on the rim of the canyon, similar to HRV3. VP4 was modeled to only partially exit the empty particle at the 5-fold axes. The 2-fold axes as well as the 5-fold axes were classified as potential exit points for the RNA in HRV14 (*Hewat et al., 2004*).

### 2.3.4 Gene expression

Being of positive polarity, picornaviral RNA can be translated directly upon arrival in the cytoplasm. Picornaviral RNA lacks the 5´-terminal cap structure present in eukaryotic messenger RNAs and translation starts at the internal ribosomal entry site (IRES) located within the 5´UTR (*Golini et al., 1978*). The IRES recruits both canonical as well as non-canonical translation factors from the host cell. Non-canonical translation factors are cellular RNA binding proteins that are not involved in translation; the so- called IRES trans-activating factors (ITAFs) can act as chaperones on the viral RNA, stabilizing the IRES in a functional conformation. Alternatively, they can be involved in recruitment of the translational machinery. Canonical translation initiation factors required for poliovirus translation include eIF4G and eIF4B, which bind to the viral RNA, and eIF3 and eIF2, which must pre-bind the 40S subunit (*reviewed in Lin et al., 2009*).

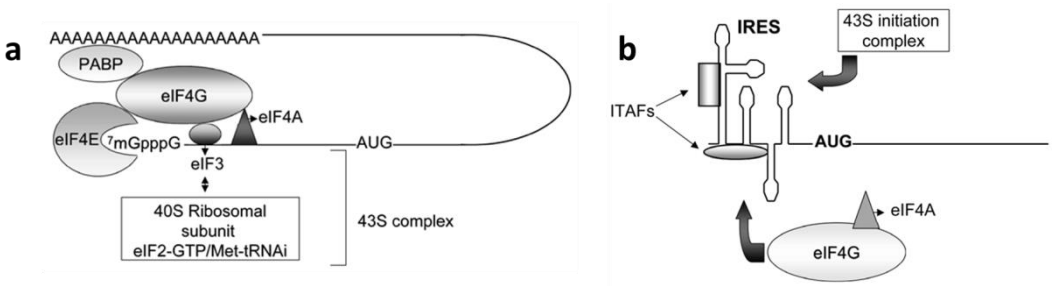


Figure 8: Translation initiation complex assembled at cap-structure and IRES

a: simplified model of assembly of an initiation complex at an eukaryotic RNA. The eIF4F complex is recruited by poly A binding protein (PABP) and eIF4E bound to the methylated cap. eIF4F and eIF3 recruit the 40S ribosomal subunit. eIF: eukaryotic initiation factor
b: cap- independent assembly of the initiation complex. A conserved secondary structure, the IRES, serves as binding platform for both canonical as well as non-canonical translation initiation factors. IRES trans-activating factors (ITAFs) act as chaperones, stabilizing the functional conformation of the IRES and/ or recruit canonical translation initiation factors.
Figures taken from *López-Lastra* et al., 2005

The single open reading frame of picornaviruses encodes one polyprotein, but full-length translation products are not observed. Intramolecular cleavages of the viral proteases during translation generate three primary cleavage products[5]. The polyprotein consists of one region destined to be processed to structural proteins, the P1 region and two regions that are further cleaved to yield proteins involved in gene expression, replication and interference with host cell mechanisms, the P2 and P3 regions. Not only the final products of protein processing have distinct biological functions but also the intermediate products, thus generating a variety of biochemically active proteins plus structural proteins from one precursor. To give an example, 3CD is the precursor of 3C and 3D. 3CD is a multifunctional protein that is involved in polyprotein processing, circularization of the viral genome prior to replication and recruitment of host cell proteins that are required for viral replication. Upon cleavage of 3CD a protease (3C) and a RNA-dependent RNA polymerase (3D) are generated. Viral proteins that modulate host cell functions interfere with cellular gene expression, protein localization, signal transduction and membrane rearrangement to fit them to their needs for replication and exit from the cell (*reviewed in Lin et al., 2009*).

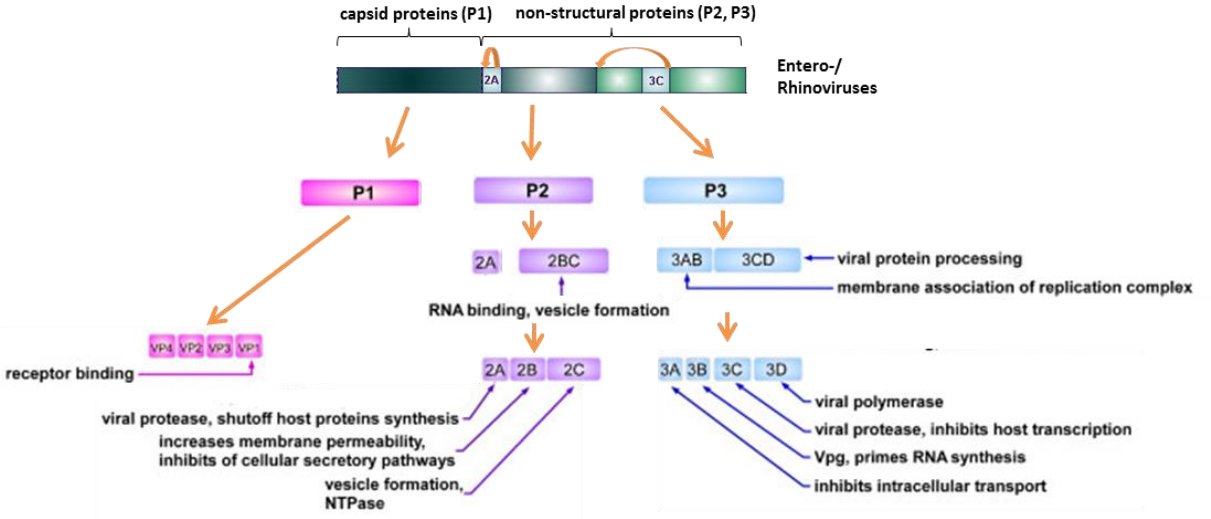


Figure 9: Polyprotein processing of enteroviruses, functions of processing intermediates and products

Intramolecular cleavage during translation generates the precursor for structural proteins (P1) and the nonstructural precursors P2 and P3. Further cleavage generates biologically active precursors that change function upon additional cleavage. Functions of precursors and cleavage products are indicated. Adapted from the webpage of the Ryan´s laboratory at University of St Andrews[6] and *Lin et al., 2009*

### 2.3.5 Replication

Since the template of the polyprotein is the same molecule that needs to be multiplied, translation is turned off to allow replication. Switch from translation to replication is mediated by viral proteases that cleave ITAFs stabilizing the IRES and processing of intermediates to products that bind to the RNA, hindering translation and initiating replication. Viral proteins

[5] http://www.st-andrews.ac.uk/ryanlab/page1.htm [July 2013]

[6] Ryan´s laboratory webpage, Picornavirus Polyprotein Processing: http://www.st-andrews.ac.uk/ryanlab/page1.htm [July 2013]

that insert into membranes induce vesicle formation and recruit viral replicative proteins to the membranes, thereby assembling the membrane-bound viral replication complex (RC). The precursor of the RNA-dependent RNA polymerase circularizes the viral genome and recruits host cell proteins required for replication. The precursor of VPg is involved in unwinding of the secondary structures and is uridylylated by the viral replicase. Uridylylated VPg is utilized as a primer in both positive- and negative-strand RNA synthesis (*reviewed in Lin et al., 2009*).

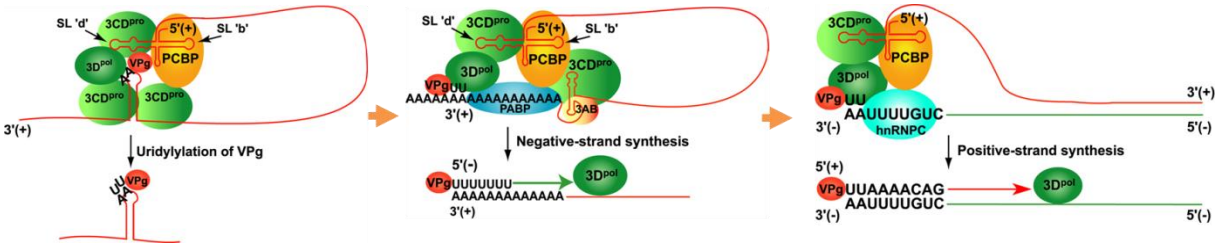


Figure 10: Simplified model of Replication of the Picornavirus genome

3CD binds to both the 3´ and the 5´ end of the RNA, thereby circularizing it. Recruitment of host cell factors, such as poly A binding protein (PABP, in light blue) and poly (rC) binding protein (PCBP, orange) assembles the replication initiation complex. 3AB, the precursor of VPg unwinds secondary structures and is uridylylated by 3CD. A highly conserved hairpin structure (***cre***), located within the coding region is used as the template for VPgpUpU synthesis. Cleavage of 3AB and 3CD frees the RNA dependent RNA polymerase (3D) as well as the primer required for (-) and (+) strand synthesis (3B = VPg). Figures modified from *Ogram & Flanegan, 2011*

### 2.3.6 Assembly, Maturation and Release

The P1 region of the polyprotein is cleaved to VP0, VP1 and VP3, which interact to form the basic protomers. The protomers self- associate into pentameric subunits, 12 of which assemble to an icosahedral capsid. Inclusion of the RNA genome into partially assembled or empty capsids triggers cleavage of VP0 to VP2 and VP4. This cleavage generates a metastable capsid protecting the genome but primed for release when exposed to the trigger (*Rossmann et al., 1985*, *reviewed in Hogle, 2002*). Myristoylation of the future VP4 contributes to its membrane binding activity and is aiding poliovirus assembly (*Moscufo et al., 1991*). Richards & Jackson suggested a non-lytic exit mechanism for picornaviruses. The virally induced vesicles that anchor the replication complex are proposed to invaginate thereby enclosing the replication complex together with assembling capsids in double- membraned vesicles. Fusion of those double-membraned vesicles with the plasma membrane would release a single-membraned vesicle, which is unstable and is disrupted to release virus. Alternatively, the double-membraned vesicles are suggested to mature to single-membraned vesicles that free enclosed virus upon fusion with the plasma membrane (*Richards & Jackson 2013*).

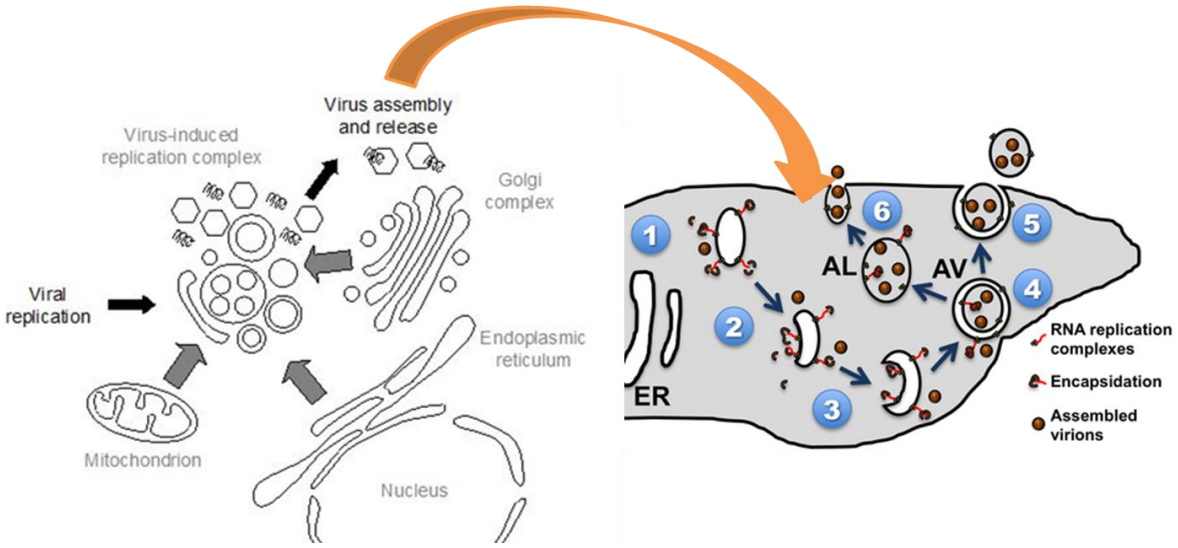


Figure 11: Model of recruitment of membranes for replication and release

1 and left: Viral proteins insert into membranes and induce budding of vesicles from the endoplasmic reticulum (ER). Replicative proteins are recruited to those vesicles; a membrane-bound viral replication complex is assembled
2-4: The virus- induced vesicles begin to invaginate, thereby enclosing the replication complex together with assembling capsids in double- membraned autophagic vesicles (AV).
5, 6: Those double-membraned vesicles could fuse with the plasma membrane to release a single-membraned vesicle filled with virus; alternatively, the double-membraned vesicles are suggested to mature to single-membraned vesicles that free enclosed virus upon fusion with the plasma membrane.
Figures taken from *Martín-Acebes*[7] *et al., 2013* and *Richards & Jackson 2013*

### 2.3.7 Subviral particles

During entry and uncoating distinct entry intermediates are generated. *In vitro*, two different particles were found upon acidification: Intermediate (A) particles do not contain VP4 and have externalized the hydrophobic N-termini of VP1, but they still contain the RNA genome. Empty (B) particles neither contain VP4, nor RNA (*Korant et al., 1972*, *Hewat et al., 2002*). Based on sedimentation rates, the A particles are also referred to as 135S particles, whereas B particles sediment at 80S. A particles are hydrophobic and attach to liposomes, B particles are not; presumably the N-termini of VP1 are re-internalized following egress of RNA (*Lonberg-Holm et al., 1976, Garriga et al., 2012*). Recently, the structure of another intermediate, the 'rod-particle' was determined. The rod-particle has expelled part of its genome and the RNA remaining inside organizes into a rod-like structure spanning the particle between a threefold and a twofold axis (*Harutyunyan et al., 2013*). *In vitro*, conversion of native virus to 135S and 80S particles is mediated by acidification (pH<5.8) or heating (50°C–56°C) (*Korant et al., 1972, Lonberg-Holm & Yin, 1973, Weiss et al., 2012*).

[7] Lipid involvement in viral infections: http://www.intechopen.com/books/lipid-metabolism/lipid-involvement-in-viral-infections-present-and-future-perspectives-for-the-design-of-antiviral-st [July 2013]

## 2.4 Aim

The aim of this study was to find out if the release of the genome of Human Rhinovirus proceeds in an ordered fashion. We wanted to know if a certain end is designed to exit from the particle first. Further, in the empty capsids of rhinoviruses several pores are opened. Is one single pore chosen as exit for the genome, or is the RNA looping out through several pores?

## 2.5 Approach

The question about directionality of RNA release was addressed by two different chemical methods that were focused on either quickly capturing a snapshot of RNA in the act of egress or alternatively, halting egress. Reagents used in SHAPE chemistry (e.g. NMIA[8], 1M7, BzCN (see 2.5.1.1)) modify single stranded RNA (ssRNA); the reaction is complete in between ~1 sec and ~20 min, depending on the chemical (*Mortimer & Weeks, 2007*). Thereby, a snapshot of RNA release might be taken, capturing the protruding part of the genome. Formaldehyde reacts with both amino acids as well as the bases of nucleic acids. Crosslinking of RNA to the capsid would halt RNA egress and allow for characterization of the remaining part of the RNA.

For the following experiments, Human Rhinovirus A2 (HRV2), a representative of minor group HRVs was chosen. Minor group viruses have the advantage that uncoating is independent from the receptor. The serotype HRV2 has been studied since 1972, a cDNA copy of its genome is available in a plasmid and crystal structures of native capsid and empty capsid have been determined (*Yin & Knight,* 1972*, Skern et al., 1985, Duechler et al., 1989, Verdaguer et al.,* 2000, *Garriga et al., 2012*). *In vitro,* uncoating of HRV2 can be induced by acidification to pH<5.8 or by heating to 56°C (*Korant et al., 1972, Lonberg-Holm & Yin, 1973*). We chose acidification, as it is the more physiological trigger.

### 2.5.1 Selective 2´-Hydroxyl Acylation and Primer Extension (SHAPE)

SHAPE is a method designed for analysis of RNA structure. In principle, an electrophile reagent reacts with the 2´hydroxyl (2´OH) group of RNA to form an ester; this bulky adduct is detected via a halt during reverse transcription of the modified RNA. Reverse transcriptase cannot pass the 2´OH adduct, resulting in a transcriptional stop; modifications therefore result in a shorter cDNA (*Merino et al., 2005*).

[8] NMIA: *N*-Methylisatoic anhydride: http://www.sigmaaldrich.com/catalog/product/aldrich/129887?lang=de&region=AT [September 2013] and *Merino et al., 2005*

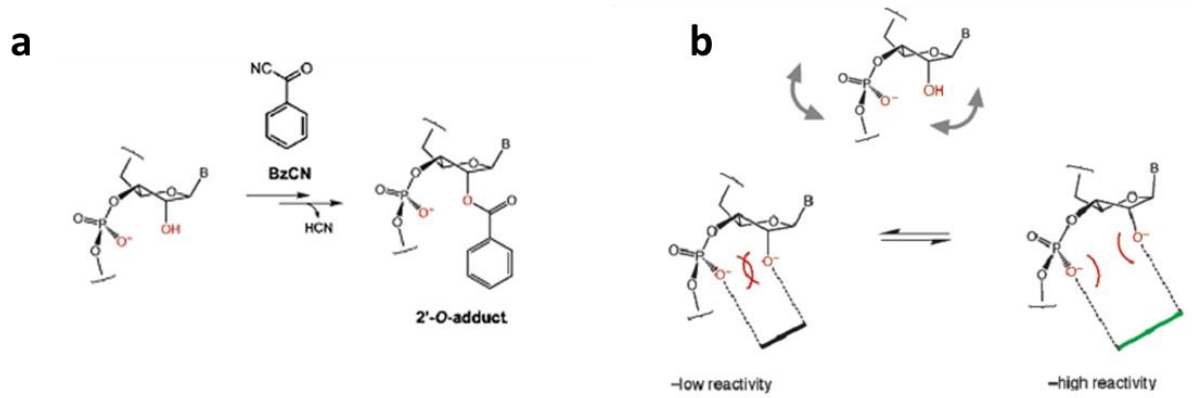


Figure 12: SHAPE chemistry

a) An electrophile reagent (BzCN) reacts with the 2´hydroxyl group of RNA, forming an adduct.
b) Proximity of 3´- phosphodiester to the 2´OH inhibits formation of the deprotonated, nucleophilic oxyanion. Nucleotides involved in base pairing or tertiary interactions are conformationally locked in the low reactivity state. Free (unpaired) nucleotides can adopt both conformations. Pictures adapted from *Merino et al., 2005*

If the 2´OH is deprotonated, a nucleophilic oxyanion is generated, which is far more reactive. The ability of forming the 2´-oxyanion is strongly modulated by the adjacent 3´-phosphodiester anion. If the 3´- phosphodiester is too close, it inhibits formation of the nucleophilic oxyanion from of the 2´- hydroxyl group (see Figure 12). Nucleotides that are involved in base pairing (canonical as well as noncanonical) or even tertiary interactions are conformationally constrained, and are unreactive towards electrophile reagents due to proximity of the 3´- phosphodiester. Only 2´hydroxyl groups of nucleotides that are located in single stranded regions and do not participate in tertiary interactions are reactive because they can adopt a broad range of conformations and are therefore better able to reach a facilitated transition state in which the 3´- phosphodiester becomes appropriately positioned (i.e. displaced) with respect to the 2´- hydroxyl group (*Merino et al., 2005*).

#### 2.5.1.1 Using SHAPE to investigate directionality of egress of the HRV2 genome

Mortimer and Weeks developed two reagents that are highly reactive towards the 2´hydroxyl group of RNA; 1-methyl- 7- nitroisatoic anhydride (1M7) and Benzoyl cyanide (BzCN). In parallel to forming a stable ester with RNA, 1M7 and BzCN are hydrolyzed in aqueous solution, making a quenching step dispensable. Reaction with RNA and hydrolysis is complete in ~70 seconds (1M7, *Mortimer & Weeks, 2007*) or in ~1 second (BzCN, *Mortimer & Weeks, 2008*). Due to the rapid inactivation by hydrolysis of those reagents, it was expected that the extruding end of RNA is preferentially modified, leaving the RNA that lags behind in the capsid unmodified. If RNA inside the capsid is inaccessible to the chemical, modified regions of the RNA allow conclusion about number of chosen exits, directionality of egress and conformation of emitted RNA.

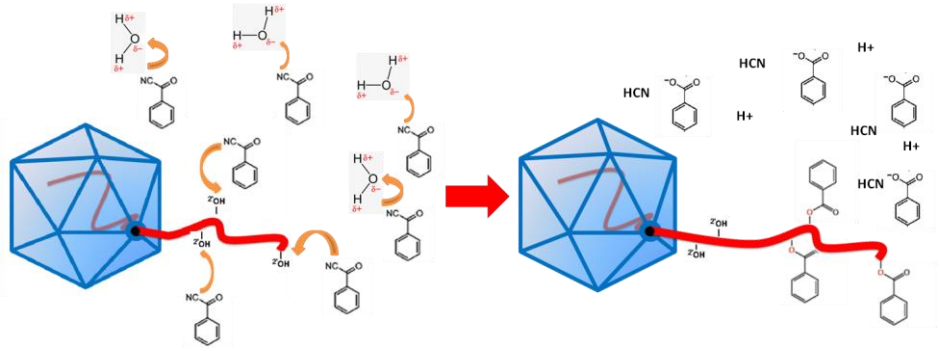


Figure 13: Schema outlining how SHAPE is supposed to identify the leading end of the HRV2 genome

Benzoyl cyanide (BzCN) reacts with 2´OH groups of unpaired nucleotides. The reaction with BzCN is complete within ~1 second. In parallel to reacting with RNA, BzCN is hydrolyzed in aqueous solution. Therefore, it was expected that the extruding end of RNA is preferentially modified, leaving the RNA that lags behind in the capsid unmodified.
Drawing of viral capsid and viral RNA by Gerhard Bilek,
Structural formulae of BzCN adapted from *Mortimer & Weeks, 2008,*
Structural formula of water molecule adapted from http://commons.wikimedia.org/wiki/File:Hydrogen-bonding-in-water-2D.png [June 2013]

### 2.5.2 Formaldehyde crosslinking and digestion of the protruding end of the HRV2 genome

Formaldehyde crosslinking was supposed to freeze egress and 'seal' the capsid. One would thus obtain particles that have part of their RNA extruded but still harbor part of the RNA in a protected form. Given that the RNA inside the crosslinked capsid is inaccessible to RNases, digestion and characterization of the remaining RNA should allow conclusion about the number of points of egress and/ or directionality of release.

#### 2.5.2.1 Formaldehyde crosslinking

Formaldehyde crosslinking was initially used for tanning and preservation of specimen. Its use was then extended to the identification of DNA binding proteins (*Gustavson, 1956*, *Solomon & Varshavsky, 1985*) and characterization of RNA-protein interaction (*Kim et al., 2005*). Crosslinking of proteins occurs as follows:

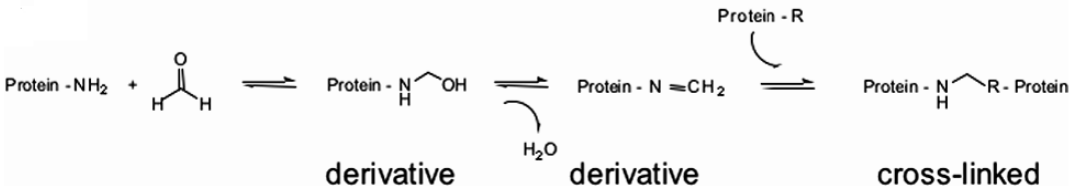


Figure 14: Formaldehyde- crosslinking of proteins.

Formaldehyde crosslinking is a two-step mechanism. In a first step methylol groups and Schiff-bases are formed; the formation of methylol and Schiff-bases is reversible by washing with water or alcohol. In a second step the bound hydroxymethyl group reacts with other nitrogen atoms to form methylene bridges (*Kiernan, 2005*). Figure taken from *Sutherland et al., 2008*.

Crosslinking is caused by formation of stable methylene bridges between nitrogen atoms. In a first step formaldehyde reacts with primary amino and thiol groups of N-terminal amino acid residues and the side-chains of arginine, cysteine, histidine and lysine. In a second step, a linkage is formed to a variety of other amino acid residues, i.e. arginine, asparagine, glutamine, histidine, tryptophan, and tyrosine. In protein crosslinking, no methylene bridges are formed between two primary amino groups (*Metz et al., 2004*). Apart from proteins, also the bases of DNA and RNA react with formaldehyde, preferentially adenine and cytosine (*McGhee & von Hippel, 1975 II*, *McGhee & von Hippel, 1975 I, Masuda et al., 1999*).

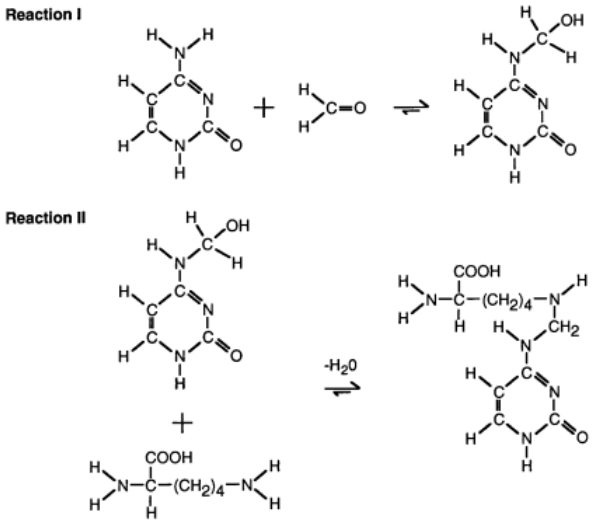


Figure 15: Crosslinking reaction between a base and an amino acid

Also the bases of DNA and RNA react with formaldehyde, preferentially adenine and cytosine. Figure taken from *Orlando et al., 1997*

### 2.5.2.2 Using formaldehyde crosslinking to halt egress of the HRV2 genome

Schmiedeberg et al. report that the crosslinking reaction that traps the DNA binding protein MeCP2 on the DNA requires a minimum of about 5 seconds to complete (*Schmiedeberg et al., 2009*). Gerhard Bilek and Angela Pickl-Herk monitored temporal progress of HRV2 genome transfer into receptor-decorated liposomes upon lowering of pH using transmission electron microscopy. Release of RNA from HRV2 into receptor-decorated liposomes is complete after 15 minutes of incubation at pH ~5.4 (*Bilek, 2009*). It was thus assumed that the crosslinking reaction with formaldehyde is quick enough to freeze the exit of the HRV2 genome mid-release.

Initially, it was planned to freeze the release of the genome and to identify the protruding part of the RNA using reverse transcription. This idea was rejected because it was reported that the crosslinks induced by formaldehyde hinder reverse transcription. Crosslinks can be reversed by heating in TE buffer to 70°C for one hour, but this would also cause disassembly of the capsid (*Masuda et al., 1999*, *von Ahlfen et al., 2007*). Therefore, the approach was reversed: Digestion of the protruding part and characterization of RNA protected inside the capsid was supposed to reveal directionality of genome release. Bovine pancreatic ribonuclease A (RNase A; EC 3.1.27.5) is a small, extremely stable enzyme that depolymerizes RNA. RNase A catalyzes the cleavage of the P-O5´bond of an RNA strand. This enzyme contains three subsites that contact

the bases of RNA (B1, B2, and B3) and three subsites that contact the phosphoryl groups (P0, P1, and P2). RNase A preferentially binds to a pyrimidine followed by two purines in single stranded RNA (*reviewed in Raines, 1998*).

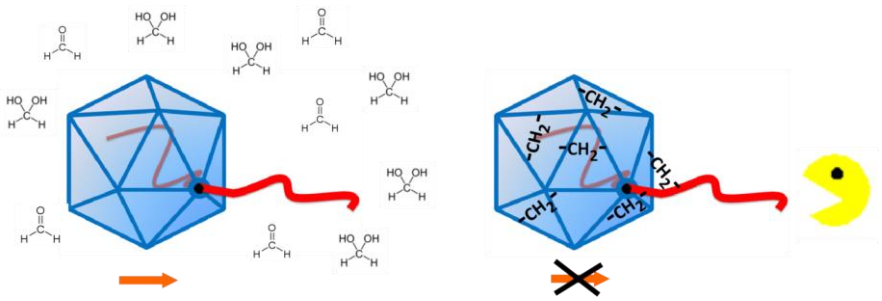

Figure 16: Schema outlining interruption of RNA egress followed by degradation of protruding RNA

Addition of formaldehyde to virus undergoing the process of release is supposed to either crosslink the RNA to the capsid or to trap the RNA in the crosslinked pore and thereby halt its egress. Subsequent digestion with RNase A should remove protruding RNA and leave the remaining RNA inside the capsid.
Drawing of viral capsid and viral RNA by Gerhard Bilek,
Formaldehyde in aqueous solution reacts with water to form methylene glycol: structural formulae taken from *Kiernan, 2005*

# 3 Materials and Methods

## 3.1 Materials

### 3.1.1 Chemicals

All chemicals were purchased from Sigma Aldrich, if not indicated otherwise.

Nuclease-Free Water ($H_2O_{NF}$): Qiagen, Catalog N° 129114 (10 x 50 ml), prepared without the use of DEPC (diethylpyrocarbonate). Nuclease-Free Water was purchased because distilled water and MilliQ water were highly variable in pH, and residual DEPC can interfere with reverse transcription (see 3.1.3).

1-methyl- 7- nitroisatoic anhydride (1M7): 1M7 was a generous gift from the Weeks laboratory[9]

Benzoyl cyanide (BzCN), 98%: Sigma Aldrich, product # 115959

Dimethyl sulfoxide (DMSO): Sigma Aldrich, product # 41640. Since 1M7 and BzCN are hydrolyzed in water, the solvent for this chemicals needs to be water- free, like DMSO.

1M7, BzCN and DMSO were stored in an exsiccator.

Formamide: Hi-Di™ Formamide, Applied Biosystems, Catalog N° 4311320. Aliquoted, stored at -20°C

Formalin = solution containing 37% w/w (= 40% w/v) formaldehyde in water

Dry milk powder: Maresi

### 3.1.2 Enzymes

Restriction enzymes and corresponding buffer solutions were purchased from NewEngland BioLabs

rRNasin plus: Promega, #N2611

RNase A: Roche, CatN° 10 109 169 001 suspended to a stock concentration of 1mg/ml, later: life technologies, CatN° 04390278CT

DNase: Fermentas #EN 0521, c= 1u/µl

[9] Kevin Weeks, Department of Chemistry, CB-3290, University of North Carolina, Chapel Hill, NC 27599-3290
919-962-7486; 919-962-2184 - Laboratory
weeks@unc.edu

### 3.1.3 Buffers, Media, Solutions

**Acidification of HRV2**

100mM Boratpuffer pH 8.3: Boric acid was adjusted with 3M NaOH and 100mM NaOH to pH 8.3
50mM Sodiumacetate (NaAc) pH 5.2: NaAc was adjusted with 100mM AcOH (acetic acid) to pH 5.2

**Bacterial Culture**

LB medium: 1% Bacto-Trypton, 0.5% Yeast-Extract, 10mM Tris/HCl pH 7.5, 170mM NaCl
LB-Amp Agar-Agar plates ($LB^{amp}$ plates): 1.5% Agar-Agar was added to LB-Medium, the mixture was autoclaved at 120°C for 20 min. When cooled to room temperature, ampicillin (100mg/L) was added and LB-Amp Agar-Agar was poured into plates.

**Agarose gel electrophoresis (both DNA as well as RNA)**

Tris-acetate-EDTA (TAE) Buffer, 50× stock, pH 8.2: 1M Tris base, 250mM NaAc, 50mM EDTA, diluted 1:100
Loading Buffer (LB): 6xLoading Dye Solution #R0619, Lot701 (Fermentas)
Alternatively: Loading Buffer, 10×: 1mM EDTA, 0.1% Orange G, 10% Ficoll in 0.5x TAE-Buffer
Ethidiumbromide: $10^{-4}$ % Ethidiumbromide in 0.5x TAE-Buffer
Coomassie staining solution: 0.4% (w/v) Coomassie R250, 45% MetOH, 10% Acetic acid.

**Purification methods**

Denaturing solution (sol D): 4M guanidinium thiocyanate, 25mM sodium citrate, 0.5% (w/v) sarkosyl, 0,1M 2-mercaptoethanol

**Selective 2´-Hydroxyl Acylation and Primer Extension (SHAPE)**

Folding buffer +/- $Mg^{2+}$, 3×: 333mM NaCl, 333mM HEPES, (33,3mM $MgCl_2$), adjusted to pH 8 using 3M NaOH
Hybridization buffer, 5×: 250mM K-HEPES pH7.0 (pH adjusted with KOH), 500mM KCl

**Formaldehyde crosslinking**

Saturated glycine solution: glycine was added to 0.5x hybridization buffer to obtain a saturated solution (solubility in water at 25 °C: 25.0 g/100 ml)

**SDS-PAGE**

4× LGS (Lower Gel Buffer): 1.5M Tris/HCl (pH 8.8), 0.4% SDS
4× UGS (Upper Gel Buffer): 0.5M Tris/HCl (pH 6.8), 0.4% SDS
10x Running Buffer: 500mM Tris, 3.85M Glycine, 1% SDS
5× reducing sample buffer: 0.4M Tris/HCl (pH 6.8), 10% SDS, 50% glycerol, 4% β-mercaptoethanol, 0,25mg/ml bromphenolblue

**Western Blot**

Blotting Buffer: 25 mM Tris-HCl pH 8.0, 30 % methanol, 194 mM glycine
Phosphate-buffered saline (PBS), 10×: 1.37M NaCl, 27mM KCl, 100mM $Na_2HPO_4$, 18mM $KH_2PO_4$. The pH is adjusted to pH 7.4 with HCl, if necessary

#### 3.1.3.1 DEPC treatment of solutions used for manipulation of RNA

To all solutions that were used for manipulating RNA, except those containing primary amines or which were purchased RNase-free, 0.1% v/v diethylpyrocarbonate (DEPC) were added. DEPC-treated solutions were incubated at 37°C for 2-3 hours. DEPC not only inactivates RNases, but also reacts with N7 of adenine, thereby interfering with reverse transcription reactions (*Ehresmann et al., 1987*). Therefore, DEPC-treated buffers and solutions were autoclaved to convert DEPC to ethanol and $CO_2$.

### 3.1.4 HRV2 sequence

The complete sequence of HRV2 is available under the GenBank accession N° X02316. The plasmid HRV2_bluescript contains a complete cDNA copy of HRV2 under control of a T7 promoter. The backbone sequence encodes an ampicillin resistance. Cloning of the vector is described in *Duechler et al., 1989.* A *Kpn*I/ *Acc*65I restriction site at the end of the poly-(A) encoding sequence allows linearization of the plasmid prior to *in vitro* transcription to yield full length viral RNA including a poly-(A) tail of about 50 nucleotides. According to a very helpful e-mail conversation with Dr. Severine Schröder[10], the backbone is most probably pBluescript KS+.

### 3.1.5 Oligonucleotides

For sequences and binding sites see Table 1. HRV2_5´bis468rev was designed specifically for SHAPE; therefore part of the HRV2 genome (following replacement of T by U[11]) was folded using the RNAfold Webserver[12] and the primer was chosen to bind to a loop region of the RNA. Care was taken to minimize homodimer formation, hairpin formation and multiple binding sites throughout the genome using the Oligo Analyzer tools of INTEGRATED DNA TECHNOLOGIES[13]. The corresponding forward primer, HRV2_5´ab125fwd was chosen because of similar melting temperature and minimal heterodimer formation. Oligonucleotides were obtained from VBC-Biotech, Vienna, Austria. Reverse primers were ordered both labeled and not labeled, non-labeled primers were used for PCR. To the labeled version of HRV2_5´bis468rev an additional adenine was added to lessen quenching effects of the guanines next to the fluorophore.

[10] Genomics Technical Support Scientist (Agilent Technologies /Stratagene Products Division)
[11] T → U http://www.fr33.net/seqedit.php (August 2013)
[12] RNAfold Webserver: http://rna.tbi.univie.ac.at/cgi-bin/RNAfold.cgi (August 2013)
[13] Oligo Analyzer Tools, IDT: http://eu.idtdna.com/analyzer/Applications/OligoAnalyzer/ (August 2013)

| name | primer sequence | orientation | binds to nt | Tm | usage | label |
|---|---|---|---|---|---|---|
| HRV2_5´ab125fwd | 5´-GAC CAA TAG CCG GTA ATC AG- 3´ | fwd | 125-144 | 60.1°C | PCR | none |
| HRV2_5´bis468rev | 5'- (A)A GGG TTA AGG TTA GCC ACA TTC AG -3' | rev | 445-468 | 56.1°C | RT, PCR | 5´- ABI-FAM<br>5´- ABI-HEX |
| HRV2_5´end | 5´- GTC ACC ATA AGC AAA TAT AAA CC-3´ | rev | 561-583 | 49.9°C | RT, PCR | 5´- ABI-FAM |
| HRV2_7A | 5´- GAG TTG ACT TAC CTA TGG TCA CC-3´ | fwd | 6126- 6148 | 48.9°C | PCR | none |
| PR5 | 5´-CTC TGG ATC ACA TCC AAC TGC TGA TCC AG-3 | rev | 6304- 6325 | 61.9°C | PCR | none |
| HRV2_3´end | 5´-CCA CTC ATG CAA AAG CAA ATC-3´ | rev | 7028 – 7048 | 52.4°C | RT, PCR | 5´- ABI-FAM |

Table 1: List of primers

Note that labeled HRV_5´bis468rev contains an extra adenine; this is because guanine is acting as quencher and should be avoided next to a fluorescent label;
Abbreviations: RT: reverse transcription/ fwd: forward/ rev: reverse/ FAM is 6-FAM

### 3.1.6 Cells

For propagation of the plasmid HRV2_bluescript the bacteria *Escherichia coli* of the strain TOP 10F' were used.

### 3.1.7 Virus

Human rhinovirus serotype 2 (HRV2) was originally obtained from the American Type Culture Collection (ATCC). Its identity is routinely confirmed with guinea pig anti-HRV2 antibodies from ATCC.

## 3.2 Methods

### 3.2.1 Virus growth and purification

HRV2 samples were prepared by Irene Gösler. HRV2 was grown in a suspension culture of HeLa Ohio cells and purified as described elsewhere (*Skern et al., 1984*, *Hewat et al., 2000*). Purified HRV2 was suspended in 50 mM borate buffer pH 7.4 and concentration was determined using capillary electrophoresis as described in *Okun et al., 1999* and *Weiss, 2009*. Both first fraction (bottom band) as well as second fraction (top band) virus was used. Concentration of 1$^{st}$ fraction virus ranged from 1 to 7mg/ml with a mean concentration of 6.5mg/ml. Concentration of 2$^{nd}$ fraction virus ranged from 2 to 8.5mg/ml with a mean concentration of 5.8mg/ml.

### 3.2.2 Acidification of HRV2

Per final sample virus calculated to contain ~1.5µg RNA was used. Because dilution of virus was reported to promote formation of empty particles (*Weiss et al., 2012*), purified virus was diluted 1:5 in borate buffer (100mM, pH 8.3) or in $H_2O_{NF}$. The minimal volumes required for acidification and re-neutralization of diluted virus samples were tested in large scale and verified with a pH electrode. In those preliminary tests borate buffer (50mM, pH 7.4) without virus was used.

Acidification → $V_{sample}$: $V_{NaAc}$ = 1:0.25 → pH= 5.1 (virus diluted in water) or pH 5.4 (diluted in borate buffer)

Reneutralization → $V_{NaAc}$: $V_{b.b}$ = 1:1.2 → pH= 7.5 (both)

NaAc (50mM, pH 5.2, DEPC-treated); b.b.= borate buffer (100mM, pH 8.3, DEPC-treated)

If not indicated otherwise, acidified samples were incubated at 37°C (incubator) for 15 min. Following re-neutralization samples were kept on ice.

Acidification prior to dilution and addition of minimal volumes NaAc/ borate buffer: 1.5µl virus + 2µl NaAc→ 15 min 34°C → + 4µl borate buffer

### 3.2.3 Capillary electrophoresis (CE) of virus and subviral particles

CE was performed by Xavier Subirats as described in *Weiss, 2009*. Analysis was performed on a 3D CE instrument (Agilent, Waldbronn, Germany), using a fused silica capillary of 50 µm inner diameter, 375 µm outer diameter, 60.1 cm total and 51.6 cm effective length (Polymicro, Phoenic, US). Because HRV2 in borate buffer forms aggregates when analyzed by CE, detergents are added to sample buffer (SB) and Background electrolyte (BGE). If SDS is added, native virus can be separated from the contaminant (a so far unknown component found in all virus preparations); in heated samples the individual viral proteins and the viral RNA can be detected. In presence of Thesit, native virus can no longer be separated from the contaminant, but in heated samples 135S particles or empty capsids can be analyzed instead of the individual viral proteins.

### 3.2.4 Bacterial Culture

#### 3.2.4.1 Preparation of competent cells

An aliquot of competent bacteria (stored at -80°C) was thawed and an overnight (o/n) culture was inoculated in 3ml LB medium; the o/n culture was incubated at 37°C and 229rpm. The following day the o/n culture was transferred to 200ml liquid LB. The cells were grown at 37°C, 229rpm until an $OD_{600}$ of 0.4- 0.5 was reached. Cells were pelleted by centrifugation at 4°C, 4000rpm for 10 min in an Haereus Varifuge 3.0R, the supernatant was discarded, and cells were resuspended in 25ml ice cold 0,1M $CaCl_2$. After incubation on ice for 25 min cells were pelleted by centrifugation at 4°C, 4000rpm for 10 min. The supernatant was discarded and cells were resuspended in 10ml of ice cold $CaCl_2$ and incubated o/n at 4°C. Sterile 80% glycerol (2ml) was added and aliquots of 200µl were snap frozen in liquid nitrogen. Cells were stored at -80°C.

Competence of bacteria was checked by transformation with ~10ng and ~100ng of a control plasmid (HRV14 in psp72).

#### 3.2.4.2 Transformation via heat shock

Competent bacteria were thawed on ice, 20-100ng plasmid DNA was added to an aliquot of 100µl, the remaining 100µl of competent bacteria served as negative control. Following 20 min incubation on ice, bacteria were heated to 42°C for 2 min in a water bath. Bacteria were returned to ice, after 10 min incubation on ice 0.8ml of LB medium was added. Bacteria were incubated at 37°C for one hour without shaking and spun down to concentrate. 100µl of

supernatant and 100µl concentrated bacteria were plated on LB plates containing ampicillin. $LB^{amp}$ plates were incubated in an incubator at 37°C over night.

#### 3.2.4.3 MIDI preparation

Midipreparation was conducted using the NucleoBond$^{R}$ plasmid purification kit (Qiagen, Catalog N° 12143). Single colonies of freshly transformed cells were inoculated in 50ml liquid LB supplied with 50µl ampicillin (100mg/ml) and grown at 37°C, 215rpm over night. The cultures were transferred to 50ml falcon tubes and cells were collected by centrifugation at 4000rpm (Heraeus Sepatech Megafuge 1.0). The supernatant was discarded; cells were resuspended in 4ml buffer S1 and decanted to Sorvall tubes. 4ml buffer S2 was added, the tubes were inverted thoroughly and cells were incubated ~5 min at room temperature. 4ml buffer S3 was added, the suspension was inverted, kept on ice for 5 min and centrifuged at 15.000rpm, 4°C for 30 min (SS34 Rotor, Sorvall RC5Cplus). Columns were equilibrated with 2.5ml buffer N2 prior to loading the supernatant. Columns were washed with 5ml buffer N3, DNA was eluted with 5ml buffer N5 and collected in 3.5ml isopropanol. The eluate was aliquoted into 6 1.5ml Eppendorf tubes and DNA was pelleted via centrifugation at 4°C, 14.000rmp for 30 min (Eppendorf Zentrifuge 5415C in cold store). Pellets were collected and combined by centrifugation at room temperature, 14.000rpm for 3 min. The supernatant was discarded; the pellet was washed with 1ml 70% ethanol and following centrifugation at room temperature, 14.680 rpm (Eppendorf 5424), the pellet was air dried for ~ 20 min and resuspended in 40-50µl $H_2O_{NF}$, depending on the size of the pellet. Buffers were included in the kit.

To verify identity of the plasmid, a digestion control using the enzyme combinations *Pst*I/ *Acc*65I and *Pst*I/ *Bsa*I was performed.

### 3.2.5 DNA Methods

#### 3.2.5.1 DNA restriction reactions

**Control digestions:**

*Pst*I/ *Acc*65I: 2.5µg plasmid DNA was digested with 7.5units *Pst*I and *Acc*65I each in a final volume of 25µl over night at 37°C. Both enzymes require NeBuffer 3 and BSA.
*Pst*I/ *Bsa*I: 2.5µg plasmid DNA was digested first with 7.5 units *Pst*I in NeBuffer 3 + BSA in a final volume of 25µl at 37°C over night, then *Bsa*I was added, the temperature was raised to 50°C and digestion was continued for 3.5 hours.
Double digestion with *Pst*I and *Bsa*I should result in fragmentation into two pieces of 2kb and one piece of 6kb. Double digestion with *Pst*I and *Acc*65I is supposed to yield fragments of about 2kb, 3.4kb and 4.7kb in length. Samples were directly loaded onto a 0.7% agarose gel without purification.

**Linearization of the plasmid HRV2_bluescript prior to *in vitro* transcription**

Prior to *in vitro* transcription plasmid DNA needs to be linearized. A circular template DNA would yield extremely long, heterogeneous RNA transcripts[14]. HRV2_bluescript contains a

[14] Instruction manual, AppliedBiosystems MEGAscript®T7 Kit #AM1333

unique restriction site recognized by *Acc*65I or *Kpn*I just after the poly(A) tail to allow transcription of a complete HRV2 RNA copy.

15µg plasmid was digested with 30 units *Acc*65I in NeBuffer3 + BSA in a final volume of 50µl. The reaction was incubated for 105 min at 37°C (incubator). The linearized plasmid was purified using phenol-chloroform extraction and resuspended in 20µl $H_2O_{NF}$. (Yield: 13.6µg, A260/280 ~ 1.85, A260/230 ~ 1.97)

#### 3.2.5.2 Generation of the template for a short RNA

**Enzymatic digestion:**

The enzyme *Pst*I cuts within the HRV2 sequence at nucleotides 472 and 2423; digestion of the plasmid HRV2_bluescript with *Pst*I fragments the plasmid into pieces of 8kb and 2kb; the 8kb piece contains the T7 promoter and the first 472 nucleotides of the HRV2 cDNA. 15µg of plasmid DNA were digested with 45units of *Pst*I in a final volume of 50µl for 5 hours at 37°C. *Pst*I requires NeBuffer 3 and BSA. Digestion with *Pst*I was partial, resulting in heterogeneous RNA which is not adequate for SHAPE.

**PCR:**

The exact sequence of the bluescript vector backbone was unknown (pBluescript SK and pBluescript KS differ in the orientation of the MCS. From both vector types there are (+) and (-) versions differing in the orientation of f1 origin[15]. Therefore, the forward primer was to bind within the 3´ region of the HRV2 sequence (HRV2_7A). As reverse primer, HRV2_bis468rev was used, the same primer that is used for reverse transcription. This approach generates a ~4,4kb fragment that contains the vector backbone, the last 1000nt and the first 468nt of the HRV2 cDNA. Only the first 468nt of the HRV2 cDNA are under control of the T7 promoter, so upon *in vitro* transcription exactly the piece of RNA that is desired is produced (see Figure 17, primers see Table 1).

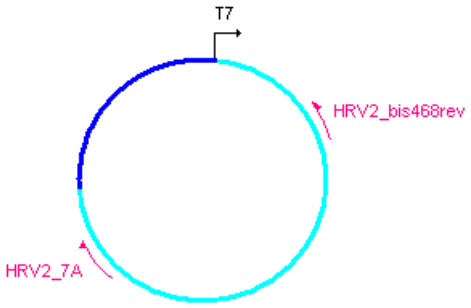


Figure 17: Sketch outlining the PCR strategy

The forward primer was designed to bind in the 3´ region of the HRV2 sequence (HRV2_7A). As reverse primer, HRV2_bis468rev was used. This approach generates a ~4,4kb fragment that contains the vector backbone, the last 1000nt and the first 468nt of the HRV2 cDNA. Only the first 468nt of the HRV2 cDNA are under control of the T7 promoter, so upon *in vitro* transcription exactly the piece of RNA that is desired is produced.
Blue: vector backbone, most probably pBluescript KS+, Cyan: HRV2 cDNA, Pink arrows: primer

[15] Genomics Technical Support Scientist (Agilent Technologies /Stratagene Products Division)

PCR was carried out using Promega *Pfu* DNA polymerase Cat#M7741; according to the usage information, the thermocycling conditions were as well according to the Promega recommendations, with an annealing temperature of 50°C and 35 cycles. Lowering of template amount to 0.22µg/50µl and enzyme amount to 0.9u/50µl increased the yield 2.5 fold. PCR products were analyzed in a 1% agarose gel. Prior to *in vitro* transcription the PCR product was Phenol/ Chloroform purified.

#### 3.2.5.3 Agarose gel electrophoresis (both DNA as well as RNA)

Depending on the size of the respective fragments, DNA and RNA was separated in TAE gels containing different concentrations of agarose, ranging from 0.7% for large fragments to 1.5% for small fragments. Briefly, agarose was boiled in 0.5× TAE and gels were poured. To RNA gels SDS or DEPC (see 3.1.3.1) was added to a final concentration of 0.1%. Since DEPC needs to be autoclaved, usually a 250ml bottle of DEPC-agarose was prepared. Gels were submerged in 0.5× TAE buffer, and DNA or RNA was separated at a constant voltage of 80V for 30 to 45 min. RNA samples were usually heated to 70°C for 2 min in a thermoblock and immediately transferred to ice prior to addition of loading buffer in order to melt secondary structures. In parallel, a size marker was loaded onto the gel. For assignment of small fragments a 100bp DNA ladder (new England Biolabs, #NO467G) was used, for large fragments a 1kb DNA Ladder (Fermentas, #SM0311) or λ/*Hind*III (home made by David Neubauer) was used. To detect RNA or DNA, agarose gels were submerged in a $10^{-4}$ % EtBr bath for 5-10 min and a picture was taken using a UV trans-illuminator. Gels that contained SDS were washed 3× 10 min in distilled water prior to EtBr-staining. To detect proteins, agarose gels were submerged in Coomassie brilliant blue solution for 5 minutes and destained in $H2O_{dd}$ over night.

### 3.2.6 RNA Methods

#### 3.2.6.1 RNA transcription

RNA was transcribed using the Applied Biosystems MEGAscript®T7 Kit #AM1333, according to the instruction manual. 1µg of linearized plasmid DNA or 0.2- 1µg of PCR product was set in as template for full length RNA or 468nt RNA synthesis respectively. The DNA solution was adjusted with $H_2O_{NF}$ to a volume of 8µl and 2µl each of ATP, CTP, GTP, UTP- solution, 10× reaction buffer and enzyme mix (all reagents supplied with the kit) were added. Following incubation at 37°C (incubator) for 4 hours, 1µl of TURBO DNase (supplied with the kit) was added and the reaction was incubated at 37°C for 15 min to digest template DNA. RNA was recovered by Phenol/Chloroform extraction. The concentration of RNA as well as the ratios $A_{260/280}$ and $A_{260/230}$ were determined using a nanodrop 1000. $A_{260/280}$ should be above 1.7 (reflecting residual proteins,) $A_{260/230}$ should be above 2 (aromatic compounds).

**Quality control of *in vitro* transcribed RNA:**

To check debris of DNA template and contamination with RNases 4µg of freshly transcribed RNA was incubated with either 1µl of DNase (Fermentas #EN 0521, c= 1u/µl, reaction supplied with 10× reaction buffer containing $MgCl_2$) or 1µl of RNase (c= 1mg/ml) in a final volume of 10µl at 37°C for 20 min. In parallel, two samples containing solely RNA were either incubated at 37°C for 20 min or kept on ice for the same time. 2µl of RNase free loading dye were added, and samples were analyzed in an agarose gel.

### 3.2.6.2 Purification methods (both DNA and RNA)

**Phenol/ chloroform extraction:**

The sample was adjusted with $H_2O_{NF}$ to 500µl, 500µl Phenol: Chloroform: Isoamyl alcohol 25:24:1 (Fluka) was added and the solution was vortexed thoroughly. Following centrifugation at 14,000rpm for 2 min (Eppendorf centrifuge 5415C) the upper, aqueous phase was transferred to 1ml of 96% ethanol, 50µl 3M NaAc pH5.2 were added and the solution was inverted utterly. The sample was kept at -80°C for 30 min and RNA or DNA was pelleted via centrifugation at 4°C, 14000rpm for 10 min (eppendorf centrifuge 5415C). The supernatant was discarded and the pellet was washed with 0.75ml of 70% ethanol (EtOH). Following centrifugation at room temperature, 14,680rpm for 5 min (Eppendorf centrifuge 5424) the supernatant was discarded and residual ethanol was either sucked off using a water-jet pump or spun down and pipetted off. The pellet was air dried for about 5 minutes and resuspended in $H_2O_{NF}$. *In vitro* transcribed RNA was solubilized in 50µl $H_2O_{NF}$. Concentration was determined using the nanodrop 1000. RNA was stored at -80°C, DNA at -20°C.

**Guanidine Method for RNA extraction:**

Adapted from: Wiley, Current Protocols in Molecular Biology, ISBN: 978-0-471-50338-5/ Volume 1, Unit 4.2: Guanidine Methods for Total RNA Preparation, 1996

The sample was filled up to 500µl with sol D and mixed well. Following 15 min incubation on ice, 500µl Phenol: Chloroform: Isoamyl alcohol 25:24:1 was added, and the mixture was vortexed thoroughly. It was continued as described in “Phenol/ chloroform extraction”. The pellet was air-dried and resuspended in 0.5 × hybridization buffer (here: 39µl).

**Phenol /chloroform /SDS precipitation**

Adapted from: Wiley, Current Protocols in Molecular Biology, ISBN: 978-0-471-50338-5/ Volume 1, Unit 4.1: Preparation of Cytoplasmic RNA from tissue Culture Cells, 1990

The Sample was filled up to 500µl with 0.2% SDS (w/v, in $H_2O_{NF}$) and mixed immediately by vortexing. 400µl of 25:24:1 phenol: chlorophorm: isoamyl alcohol (RT) was added, the solution was vortexed for at least 1 min and the sample was centrifuged in for 5 min at 14000rpm at RT. The upper, aqueous phase was transferred to a new tube (carefully omitting precipitated material) and 400µl 24:1 chlorophorm: isoamyl alcohol (4°C) was added. The mixture was vortexed for 30 seconds and centrifuged for 1 min at 14000rpm, RT. The upper, aqueous phase was transferred into 1ml of 96% EtOH, 40µl NaAc (3M, pH5.2; DEPC-treated) was added and the sample was mixed by inversion. The following steps are identical as described in “Phenol/ chloroform extraction”. The pellet was air-dried and resuspended in 0.5 × hybridization buffer (here: 39µl).

Here: RT= room temperature

### 3.2.6.3 Selective 2´-Hydroxyl Acylation and Primer Extension (SHAPE)

The procedure has been adapted from *Wilkinson et al., 2006* and *Mortimer & Weeks, 2008* and is still to be adapted to full length (fL) RNA and conditions essential for triggering RNA release from virus particles.

**Structure- selective RNA modification:**

8µl 468nt RNA (*in vitro* transcribed, c=2.5µg/µl) was adjusted with $H_2O_{NF}$ to 60µl, the sample was incubated at 95°C for 2 min, and 30µl of folding buffer (+$MgCl_2$) was added. Folding of RNA was allowed by incubation at 37°C for 20 min, then the sample was spun down briefly, an aliquot of 22µl (containing ~5µg RNA) was analyzed in an agarose gel (1% agarose, 0.1% DEPC), and the remaining sample was split into two aliquots of 34µl each. To one aliquot 5µl of BzCN (3.6M in DMSO) was added, the other sample received 5µl of plain DMSO. The reaction was allowed to proceed for 70 seconds at room temperature, and 466µl of EtOH-precipitation mastermix was added. The samples were inverted and incubated at -80°C for 30 minutes and centrifuged at 14000rpm, 4°C for 10 minutes (centrifuge in the cold room). The supernatant was discarded and pellets were resuspended in 8.5µl 1 × hybridization buffer.

**Primer extension (reverse transcription):**

Samples from above were heated to 95°C for 3 min in a heat block without shaking and spun down. To the modified samples 4.5µl of FAM-labeled primer (10pmol/µl) were added, to the negative control 4.5µl of the same primer, labeled with HEX (10pmol/µl) were added (no vortexing). For primer annealing the samples were incubated at 65°C for 6 min (heat block, not shaking, protected from light) and transferred to ice. Samples were spun down and 7µl of reverse transcription master mix and 1µl of superscript III reverse transcriptase was added. The reverse transcription reaction was allowed to proceed for 25 min at 55°C (heatblock, no shaking, protected from light) and the samples were incubated for further 15 min at 70°C (other heatblock, preheated, no shaking, protected from light).
To 14µl aliquots of each sample 3µl loading dye was added and the aliquots were analyzed in an 2% agarose gel, the remaining 6µl were split into aliquots of 2µl and 4µl containing calculated 5pg and 10pg of 468nt RNA for CE analysis. Samples for CE analysis were filled up to 10µl with $H_2O_{NF}$ and 466µl of EtOH-precipitation mastermix were added. EtOH-precipitation was performed as described above, with an additional washing step using 70% EtOH. To each sample destined for CE analysis 10µl of formamide/size standard mix was added and the pellets were resuspended by shaking in the cold room. Samples were sent in to VBC-Biotech Service GmbH (VBC) for fragment length analysis.

Later, both the modified sample as well the negative control were converted to cDNA using the FAM- labeled primer and the (+) and (-) reagent samples were analyzed separately.

EtOH-precipitation mastermix: 60µl $H_2O_{NF}$, 400µl EtOH (96%), 5µl NaCl (5M, in $H_2O_{NF}$), 1µl glycogen (20mg/ml in $H_2O_{NF}$) per sample. The mastermix was prepared for the respective number of samples, plus one additional sample.

Reverse transcription master mix: 4µl 5× RT buffer, 1µl dNTPs, 1µl DTT, 1µl RNasin plus per sample – the mastermix was prepared with one sample in excess. (All reagents included in the superscript III RT kit, Invitrogen, 18080-044, rRNasin plus: Promega, #N2611)

Formamide/ size standard mix: 9.75µl Hi-Di™ Formamide, 0.25µl GeneScan™-500 ROX™ STANDARD (Product N° 401734E).

#### 3.2.6.4 RNase A treatment

RNase A was added to the samples to obtain a final concentration of ~ 0.1mg/ml. Samples were incubated at 37°C (incubator) for 15-20 minutes and returned to ice.

### 3.2.7 Formaldehyde crosslinking, preliminary experiments

#### 3.2.7.1 What is the appropriate concentration of formaldehyde for extensive crosslinking?

0.7µl of second fraction virus (c ~2.2mg/ml) was treated with different concentrations of formaldehyde in a final volume of 10µl in 0,5x hybridization buffer. Formalin (37%) was added to obtain concentrations of 1%, 5% and 10% and samples were incubated at RT for 5 minutes. To quench excess reactive groups, 10µl saturated glycine solution was added, the reaction with glycine was allowed by 10 min incubation at RT. 5µl 5x reducing sample buffer was added, the sample was heated to 56°C for 10min and loaded to a 15% polyacrylamide gel.

#### 3.2.7.2 Is proteinase K inhibited by formaldehyde?

8µl virus (~2µg/µl) was filled up with 0.5x hybridization buffer to 15µl and 5µl formalin (37%) was added. The crosslinking reaction was allowed to proceed for 5 min at RT, then the sample was split; in one sample the reaction was quenched by addition of 30µl saturated glycine, to the other sample 30µl 0.5x hybridization buffer was added. The samples were incubated at RT for 10minutes, then the samples were split again, and to 20µl of quenched or not-quenched sample 10µl proteinase K (10mg/ml) was added. The samples were incubated at RT for 30 minutes. Then the samples were split again, to one set of samples 3µl of 5x reducing sample buffer was added, the samples were heated to 95°C for 5 minutes and loaded to a 15% polyacrylamide gel. The other set of samples was incubated at 70°C for one hour (Eppendorf Mastercycler Gradient) to reverse crosslinks, RNA was phenol-chloroform purified and analyzed in a 1% agarose gel (results not shown).

The amount of virus sample in the following experiments was chosen by means of RNA content; 1µl viral RNA is usually well discernible in agarose gel electrophoresis. The Mw of HRV2 was calculated to be 8 084 661 Da (*Bacher et al., 2001*), the Mw of the HRV2 genome was calculated to be 2 184 017.61 Da (EnCor Biotechnology webtool[16]). The amount of virus required to obtain 1.5µl RNA varied with the preparations, as they varied in concentration.

#### 3.2.7.3 Does formaldehyde inhibit RNase?

3.5µl of virus preparation was filled up with 0.5x hybridisation buffer to a Volume of 7.5µl, and 2.5µl formalin (37%) was added. The sample was incubated at RT for 5 minutes. The sample was split; to one sample 15µl saturated glycine solution was added, to the other sample 15µl plain 0.5x hybridisation buffer. Samples were incubated for 10 minutes at RT. To each of the samples 10µl *in vitro* transcribed RNA (i.v.t. RNA) (0.7µg/µl) was added. Again, samples were split and to 15µl of each (+) and (-) glycine sample 1.5µl RNase A (1mg/ml) or 1.5 µl $H_2O_{NF}$ was added. Samples were incubated at 37°C for 20min (incubator). 3µl loading dye was added to the samples, and they were loaded to a 1% agarose, 0.1%SDS gel.

[16] EnCor Biotechnology webtool to calculate the Mw of a sequence: http://www.encorbio.com/protocols/Nuc-MW.htm [August 2013]

Controls: 3µl i.v.t RNA (0.7µg/µl) was filled up to 10µl with $H_2O_{NF}$ or saturated glycine solution or 0,5x hybridization buffer. The two positive controls contained 3µl i.v.t RNA filled up to 10µl with $H_2O_{NF}$ or saturated glycine and 1µl of RNase A (1mg/ml). The controls containing RNase A were incubated at 37°C for 20minutes. To the control samples 2µl loading dye was added, and the samples were applied to a 1% agarose, 0.1%SDS gel.

**Are RNA-RNA or RNA-protein crosslinks an impediment to RNase A?**

RNA added after the crosslinking reaction was quenched (should not be crosslinked):

4.5µl 2$^{nd}$ fraction virus (~2µg/µl) was filled up to a volume of 12µl with 0,5x hybridization buffer and 4µl formalin (37%) was added. The sample was incubated at RT for 5 min and 34µl saturated glycine solution was added. Samples were incubated at RT for 10minutes. 10µl i.v.t RNA (2.6µg/µl) was added, and the sample was split to 4 aliquots of 15µl each. To the samples 0/ 0.75µl/ 1.5µl and 3µl of RNase A (1mg/ml) was added, and the samples were incubated at 37°C for 20 minutes.

RNA and proteins subjected to crosslinking reaction

10µl i.v.t RNA (2.6µg/µl) was added to 4.5µl virus, the sample was filled up to a volume of 19.5µl with 0,5x hybridization buffer and 6.5µl formalin (37%) was added. The sample was incubated at RT for 5 min and 34µl saturated glycine solution was added. Following incubation at RT for 10minutes, the sample was split to 4 aliquots of 15µl each. To the samples 0/ 0.75µl/ 1.5µl and 3µl of RNase A (1mg/ml) was added, and the samples were incubated at 37°C for 20 minutes. To all samples 2µl loading dye was added and they were applied to a 1%agarose, 0.1%SDS gel. One additional sample contained 2.5µl i.v.t RNA (2.6µg/µl), 7.5µl $H_2O_{NF}$ and 2µl loading dye.

**Is emerging RNA crosslinked to the capsid? If so, is RNA accessible to RNase A?**

6µl virus (2.1µg/µl) was acidified with 8µl NaAc (50mM, pH 5.2, DEPC-treated); the sample was incubated at 34°C for 15 minutes and reneutralized with 16µl borate buffer (100mM, pH 8.3). The sample was split; to one aliquot 5µl formalin (37%), to the other aliquot 5µl 0,5x hybridization buffer was added. Crosslinking was allowed to proceed for 5minutes at RT and the reaction was quenched by addition of 20µl saturated glycine solution. Again, samples were split into 20µl aliquots, and to one sample that was crosslinked and one sample that was not crosslinked 2µl RNase A (1mg/ml) was added. Samples were incubated at 37°C for 20 minutes. To each sample 4µl loading dye was added and they were applied to a 0.7%agarose, 0.1%DEPC gel. One additional sample contained 2.5µl i.v.t RNA (2.6µg/µl), 7.5µl $H_2O_{NF}$ and 2µl loading dye

#### 3.2.7.4 Is RNA of acidified virus protected by a protein?

6µl virus (2.1µg/µl) was acidified with 8µl NaAc, the sample was incubated at 34°C for 15 minutes and reneutralized with 16µl borate buffer. The sample was split to two aliquots of 15µl each. To one sample 20µl proteinase K (10mg/ml) was added, to the other sample 20µl 0,5x hybridization buffer. Samples were incubated at RT for 30 minutes and split again to 17.5µl aliquots. To one sample that was subjected to proteinase K digestion and one sample that remained untreated 1.75ml RNase A (1mg/ml) was added. All samples were incubated at 37°C for 20 min (incubator). 3µl loading dye was added to each sample and they were applied

to a 0.7%agarose, 0.1%DEPC gel. Control samples consisted of 1.5µl virus filled up with borate buffer (100mM, pH 8.3) to 10µl and 1µl of i.v.t. RNA (2.6µg/µl) plus 9µl $H_2O_{NF}$.

## 3.2.8 Protein methods

### 3.2.8.1 SDS-PAGE

To analyze the protein content of EtBr-stained bands, bands from several agarose gels were excised and collected. They were stored at -20°C.

For analysis of viral proteins, gels containing 15% acrylamide were prepared. Usually two gels were prepared; one was stored in the refrigerator until use. To prepare the separation gel, 2.5ml $H2O_d$, 2.5ml LGS (4× resolving gel buffer) and 5ml Acrylamide solution (30% acrylamide, 0.8% Bis-acrylamide) were mixed well, 50µl APS was added and the gel was poured quickly. The gel was overlaid with $H_2O_d$ and allowed to polymerize for ~ 30 min, then the water was removed. The stacking gel was composed of 4ml 4.5% stacking gel solution plus 50µl APS, the gel was poured, combs were inserted and polymerization was allowed for ~15 min. To the gel slices 10µl of 5× reducing sample buffer was added, samples were heated to 95°C for ~ 20 min whilst shaking on a thermoblock and the samples were loaded quickly onto the polyacrylamide gel. As positive control, 2µl of 2$^{nd}$ fraction HRV2 (10.07.09) was mixed with 14µl $H_2O_d$ and 4µl 5× reducing sample buffer was added, the sample was heated to 95°C for 3-5 min. To load dissolved agarose gel slices to the SDS gel, it is advisable to load the samples onto the gel AFTER disassembly of the gel-pouring-station and BEFORE inserting the gel to gel chamber and addition of running buffer. Take only two samples at a time out of thermoblock, spin down and load directly without loitering. The gel was inserted into the gel chamber and covered with 1× running buffer. Then the positive control and 6µl molecular weight marker (Bio- Rad #161-0373 all blue) were loaded. To one gel a constant current of 25mA (300V) was applied for ~ 1h, to two gels a constant current of 50mA (300V), ~ 1h. If the gel was not used for western blotting, it was covered with coomassie solution for 5-10 min after disassembly and de- stained in $H2O_d$ over night.

4.5% stacking gel solution: 12.5ml UGS + 7.5ml acrylamide (30% acrylamide, 0.8% Bis-acrylamide), filled up to 50ml with $H_2O_d$, stock stored in refrigerator

### 3.2.8.2 Western Blot

Proteins were transferred to an Immobilon transfer membrane (Millipore) using a BIORAD trans-blot SD semi-dry transfer cell. Viral proteins were detected using rabbit αHRV2 serum and HRP-conjugated α rabbit antibody, total proteins were visualized via Coomassie brilliant blue staining of the acrylamide gel following western blotting.

Whatman papers were cut to 7.5cm × 9.5cm, the membrane was cut to 7×9cm. Whatman papers were prewet in blotting buffer, the membrane was first prewet in MetOH and then in blotting buffer. A sandwich of 3× whatman paper → PVDF membrane → gel → 3 × whatman paper was assembled, bubbles were removed and the sandwich was wet additionally with blotting buffer. Excess buffer surrounding the sandwich was removed, the lid was closed and 400mA were applied for ~ 1.5h to transfer the proteins to the membrane. Following transfer, the side to which proteins stick was marked, and the membrane was incubated in blocking

solution (~5 % dry milk powder in 1× PBS) over night at 4°C. Rabbit αHRV2 serum was diluted 1:500 in blocking solution; the membrane was incubated for 1.5h with the primary antibodies. To remove unbound antibodies, the membrane was washed with PBS (3× 10min). The secondary antibody (goat α rabbit, HRP conjugated, purified) was diluted 1: 10.000 in blocking solution, and the membrane was incubated for 1h. Excess 2$^{nd}$ antibody and proteins were removed by washing with PBS (3× 10min), and immune-complexes were detected using the SuperSignal West Pico Chemiluminescence Detection Kit: solution a and b were mixed in a ratio 1:1, one gel was overlaid with a total volume of 1.5ml and incubated for ~5 min. The membrane was covered with plastic foil, and an X-ray film (AGFA) was exposed for ~5 seconds, depending on signal intensity. The film was developed in a CURIX 60 developing machine (AGFA, Mortsel, BE).

The polyacrylamide gel was not discarded but submerged into Coomassie brilliant blue for 10 min and destained in $H_2O_d$ over night.

Solution a: Super Signal West Pico Luminol/ Enhancer solution: ThermoFisher, prod # 1856136
Solution b: Super Signal West Pico Stable Peroxide solution: ThermoFisher, prod # 1856135

### 3.2.9 RT-PCR of RNase A treated HRV2 135S particles

**Generation of 135S particles:**

28µl 2$^{nd}$ fraction virus (c ~2.2mg/ml) was filled up to a volume of 140µl with $H_2O_{NF}$. 35µl NaAc was added and the sample was incubated at 37°C for 15 minutes. 43µl borate buffer was added and the sample was split. To one of the aliquots 10µl RNase A (1mg/ml) was added, and both samples were incubated at 37°C for 20 minutes. 9µl aliquots from both samples were applied to an agarose gel. The remaining material was again divided into two aliquots and RNA was purified either by using the 'guanidine method' or by the 'phenol/ chloroform/ SDS precipitation'. RNA was resuspended in 39µl 0.5 × hybridization buffer. The sample was split to three aliquots, 13µl were applied to an agarose gel, 13µl were used as template for reverse transcription using the 3´ end primer and 13µl were used as template for reverse transcription using the 5´ end primer.

NaAc (50mM, pH5.2, DEPC-treated)
Borate buffer (100mM, pH 8.3, DEPC-treated)

**Reverse transcription:**

In half of the samples reverse transcription was primed with HRV2_5´bis468rev, in the other half with the primer HRV2_3´end. Reverse transcription was conducted using the superscript III RT kit, according to the manual. Briefly, secondary structures were melted by heating to 95°C for 3 min, 2µl primer was added (1pmol/µl, non-labeled) and annealing was allowed at 65°C for 6 min, samples were returned on ice and spun down. To each sample 7µl of reverse transcription master mix and 2µl of superscript III reverse transcriptase was added. The reverse transcription reaction was allowed to proceed for 60 min at 55°C; the reaction was inactivated by incubation at 70°C for further 15 min. An aliquot of cDNA was applied to an agarose gel; the remaining sample was set in for PCR.

Reverse transcription master mix: 4µl 5× RT buffer, 1µl dNTPs, 1µl DTT, 1µl RNasin plus per sample – plus one. (All reagents included in the superscript III RT kit, Invitrogen, 18080-044, rRNasin plus: Promega, #N2611)
Incubations at 95°C, 65°C, 55°C, 70°C: Heatblock, no shaking. Two heatblocks were used alternating to allow preheating/ cooling to correct temperature.

**PCR:**

For amplification of a fragment at the 5´end, the primer pair HRV2_5´ab125fwd + HRV2_5´bis468rev was chosen, for amplification of a fragment near the 3´end the primer pair HRV2_7A + PR5 (see Table 1). PCR was carried out using *Pfu* DNA polymerase, according to the manual. Briefly, the cDNA was filled up to 50µl with $H_2O_{NF}$ and 0.5µl of the two primers (10pmol/µl), 1µl dNTPs (10mM), 5µl 10× buffer (with MgSO4) and 1µl *Pfu* DNA polymerase (30U/µl) was added. PCR was performed using a Eppendorf Mastercycler Gradient. The thermal program was chosen as follows: 2min 95°C, (45 sek 95°C, 45 sek 52°C, 2min 72°C) × 50, 10 min 72°C, ∞: 4°C. As positive control, the plasmid HRV2_bluescript was used.

*Pfu* DNA polymerase: Promega, Cat#M7741

# 4 Results

This chapter is subdivided in two parts, presenting the two approaches separately.

## 4.1 Selective 2´-Hydroxyl Acylation and Primer Extension (SHAPE)

The following section describes adaptions of the method and their implications.

### 4.1.1 Software

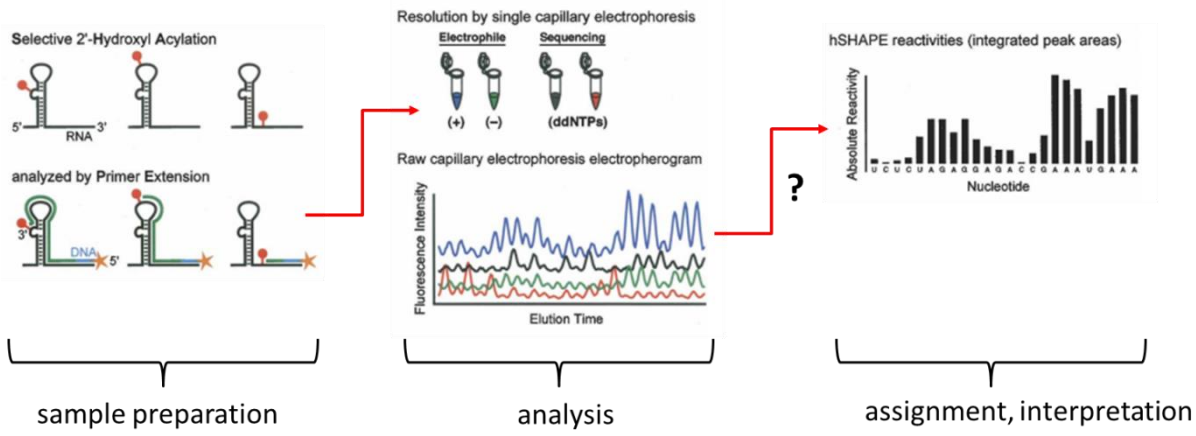


Figure 18: Outline of a SHAPE experiment

Sample preparation: Nucleotides that are not involved in pairing interactions are modified. The reverse transcriptase cannot pass the modifications, thus elongation is stopped at sites of acylation. If every RNA molecule is statistically modified once, different length of cDNA fragments reflect sites of modification. In the case of HRV2 uncoating, modifications would further reflect accessibility of the genome to the reagent.
Analysis: The no- reagent control, the sample and two sequencing reactions, each labeled with a different dye, are combined. Fragments of different length are resolved by capillary electrophoresis. CE generates raw data, plotting intensity of the four dyes versus elution time.
Assignment, interpretation: Peaks in the (-) reagent trace are subtracted from (+) reagent peaks to eliminate signals derived from stable secondary structures and degradation. The resulting SHAPE relativities are assigned to the nucleotides by comparison to the sequencing lanes.
ShapeFinder was designed to use two sequencing lanes to correlate the SHAPE fragments with positions in the input RNA sequence. However, the analysis setup by VBC rather required a size standard (i.e. labeled cDNA fragments of defined length) instead of the two sequencing lanes. Therefore, assignment of fragments to the RNA sequence and calculation of individual reactivity for each nucleotide was not possible with the program ShapeFinder. Picture adapted from Vasa et al., 2008.

Briefly, in SHAPE analysis, unpaired nucleotides of an RNA molecule are modified, modifications cause the reverse transcriptase to fall off, and thereby (given, the RNA is modified statistically once per molecule) cDNA fragments of different length are generated. The fragments are mapped to the sequence of the input RNA by comparison to two sequencing lanes. The amount of a given fragment reflects the degree of modification of the corresponding nucleotide. The elongation of cDNA is not only aborted at sites of modification, but is also influenced by stable secondary structures and degradation of the RNA. Therefore, a (-) reagent control is included. Fragments of the (+), (-) reagent samples, and the two sequencing reactions, each labeled with a different dye, are combined and resolved by capillary electrophoresis (CE). The output of an electrophoresis instrument is raw data that

plots intensity of fluorescence of the four dyes versus elution time in an electropherogram (also trace). The customized software ShapeFinder converts raw data into information about SHAPE reactivity for the distinct nucleotides (*Mortimer & Weeks, 2007, Mortimer & Weeks, 2008, Vasa et al., 2008*).

Resolution of cDNA fragments was outsourced to VBC-Biotech Service GmbH (VBC); VBC offers run-only service, leaving analysis of the data to the customer. Analysis by VBC required addition of a size standard (i.e. labeled cDNA fragments of defined length) instead of the two sequencing lanes. This precluded processing of raw data by ShapeFinder that was not designed to compare fragments to a size standard. So the first task was to find a computer program for analysis of the data. VBC sequencing service performs fragment length analysis using an ABI Prism 310 Genetic Analyzer; this instrument generates fragment analysis sample files (.fsa). Two computer programs that process .fsa files using a size standard for assignment of cDNA fragments were tested. To test the software, *in vitro* transcribed HRV2 RNA was modified; cDNA was generated using two primers hybridizing near the 5´end as well as near the 3´end (HRV2_5´end and HRV2_3´end, see Table 1). cDNA was sent to VBC for analysis.

#### 4.1.1.1 Peak Scanner™

Applied Biosystems offers the program Peak Scanner™ for download[17]. This free software was designed for DNA fragment length analysis in genotyping, such as amplified fragment length polymorphism (AFLP), loss of heterozygosity (LOH), microsatellite- and SNP genotyping (*Applied Biosystems, 2000*). Several test samples were analyzed by VBC sequencing service; all of them contained enormous peaks at the onset of the electropherogram. In several samples, this initial signal was so huge, that the program could not calculate any downstream peaks at all and therefore did not even display the traces. In the manual of Peak Scanner™ those peaks are referred to as off-scale peaks; the fluorescence signal of an off-scale peak is greater than the maximum readable signal on the Genetic Analyzer.

In the protocol describing SHAPE it is mentioned, that the first 10-20 nucleotides next to the primer binding site cannot be analyzed, because pausing of the reverse transcriptase during the initiation process generates short cDNA fragments that are not distinguishable from termination of cDNA synthesis caused by modification (*Wilkinson et al., 2006*). Peaks stemming from short fragments are neither shown in *Mortimer & Weeks, 2007,* nor in *Mortimer & Weeks, 2008.* In both publications, the traces shown start from nucleotide position 90. Hence, there must be a way of excluding perturbing short fragments at the beginning of a trace. The manual of the program designed for SHAPE analysis- ShapeFinder- provides a tool for excluding peaks that exceed the sensitivity limits of the detection equipment, in particular intense primer peaks. Regions at the beginning and end of a trace are simply deleted to improve analysis of the data (*Giddings et al 1998*, *Vasa et al 2008*). Since Peak Scanner™ would not even display many of the test traces there was no way of trimming the electropherograms.

[17] http://www.appliedbiosystems.com/absite/us/en/home/support/software-community/free-ab-software.html May 2013

#### 4.1.1.2 STRand

STRand is an open-source program provided by Davis' Veterinary Genetics Lab at the University of California[18]. This program was designed for analysis of DNA fragment length polymorphism samples. This software can read .fsa files, uses a size standard to assign fragment lengths and provides a tool to exclude short fragments at the beginning of a trace. The disadvantage of STRand is that it did not recognize the size standard peaks, so the lengths of cDNA fragments could not be calculated. Since this program could at least display all of the samples, it was chosen for further testing.

### 4.1.2 Sample preparation

Conditions for modification of the HRV2 genome were set up using *in vitro* transcribed HRV2 RNA. The reagent BzCN was chosen because of its fast reactivity. In a SHAPE experiment, the (+) reagent reaction is designed such that, on average, every RNA molecule is modified once. The recommended concentration of the reagent varies with RNA length (*Wilkinson et al., 2006*). The required concentration of the reagents may differ between reagents, because they undergo hydrolysis (i.e. inactivation) with different half-lifes. E.g. 1M7 undergoes hydrolysis with a half-life of 14 s (*Mortimer & Weeks, 2007*), whereas BzCN undergoes hydrolysis with a half-life of 0.25 s (*Mortimer & Weeks, 2008*). Stefanie A. Mortimer and Kevin M. Weeks introduce the two fast reacting reagents 1M7 and BzCN assessing the secondary and tertiary structure of the specificity domain of *Bacillus subtilis* ribonuclease P. *B. subtilis* RNase P RNA is 154 nucleotides in length (*Krasilnikov et al., 2003*), whereas the HRV2 genome devoid of the poly A tract comprises 7102 nucleotides ( *Skern et al., 1985*). *In vitro* transcribed RNA includes a poly A tract of about 50 nucleotides and therefore is 7152nt in length (*Duechler et al., 1988*) – that is ~46 times more hydroxyl groups to be modified.

5 to 10µg *in vitro* transcribed HRV2 RNA, an amount that corresponds to ~2 to ~5 pmol, was subjected to folding conditions and was treated with BzCN in different final concentrations, ranging from 100mM to 500mM. No-reagent-controls were treated with plain solvent (DMSO). Two ABI-FAM labeled primers were chosen for cDNA synthesis to report modifications at both the 3´and the 5´end (HRV2_3end and HRV2_5end, see Table 1). In initial test samples, the (+) and (-) reagent samples were elongated from equally labeled primers and thus were analyzed separately. In order to ascertain that the RNA had not been degraded during the folding step, a PCR was performed on an aliquot of the cDNA prior to turning the samples in for CE analysis. The primer HRV2_7A binds 922 nucleotides upstream from the primer HRV2_3end; PCR yields products if cDNA of sufficient length is present.

The PCR control (Figure 19) indicates absence of RNases in the unmodified as well as in the BzCN-modified sample; both samples show a strong band. Figure 20 shows two of the corresponding electropherograms; they contain the above mentioned huge peaks at the onset of the trace, hardly any fragments are visible. In the electropherograms shown in Figure 21 all fragments shorter than 35nt (the size of the first size standard peak) were excluded. In the trimmed electropherograms, peaks stemming from cDNA fragments are substantially better perceptible. Still, the concentration of fragments is very low, when fragment peaks (blue) are

[18] http://www.vgl.ucdavis.edu/informatics/strand.php , May 2013 , Version 2.2.30

compared to size standard peaks (red). Further, cDNA fragments of different length are not equally distributed, short fragments are prevalent. Prevalence of short fragments can indicate degradation of RNA or multiple modifications per RNA molecule. If the concentration of reagent is too high, RNAs contain multiple modifications- since reverse transcription stops at the first modification, elongation of long cDNAs is prevented and short cDNAs are favored. This is contradicted by the PCR control. At the other hand, absence of evenly distributed fragments and low concentration of short fragments could also imply that the concentration of reagent was too low. If the concentration of the reagent is too low, the majority of the RNA is transcribed to full length cDNA. Further, low concentration of fragments could implicate that cDNA was lost in subsequent purification steps. Since the full length cDNA is not visible in this setup, it is unclear whether RNA was degraded, if material was lost in subsequent purification steps, or if the concentration of the reagent was too high or too low.

In the article initially describing SHAPE it is mentioned that depletion of the peak presenting the full length cDNAs in comparison to the no-reagent-control allows conclusion about the degree of modification (*Merino et al., 2005*). Neither the primer binding proximal to the 3´ end, nor the one binding close to the 5´ end gives a cDNA that can be displayed by this setup. Analysis at VBC sequencing service stops after elution of the last size standard peak which is 500nt in length (personal communication with Barbara Moesl, head of sequencing service). cDNA elongated from the 5´ located primer is just not visible, as it is 583 nucleotides in length. The absence of a full length cDNA peak denotes lack of important information. Therefore it was decided to become familiar with the method by using a shorter RNA to gain a full length peak as additional control.

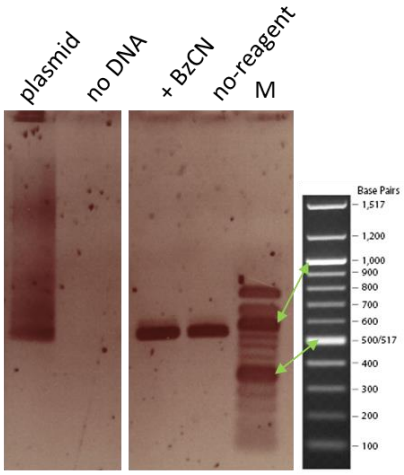


Figure 19: PCR control of cDNA prior to resolving fragments per capillary electrophoresis

An aliquot of cDNA was tested via PCR to see if template RNA was degraded by contaminating RNases. The primer HRV2_7A binds 922 nucleotides upstream from the primer HRV2_3´end; PCR yields a product only if cDNA of sufficient length is present. All samples, except the negative control show a band.
Lanes showing samples not related to BzCN-modified samples were removed computationally from this picture.
M: Marker: new England biolabs 100 bp DNA Ladder
Plasmid: positive control: HRV2 cDNA in the plasmid bluescript
1% agarose, 80V, 45´

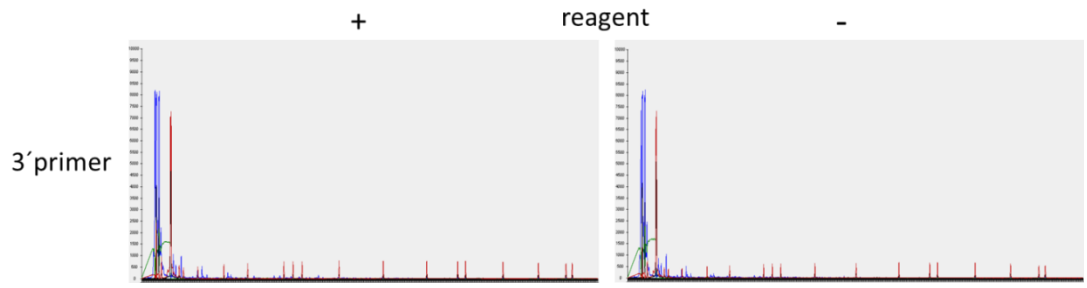


Figure 20: Two electropherograms shown in Figure 21, total length

Samples contain an enormous initial peak. Hardly any fragments are visible.

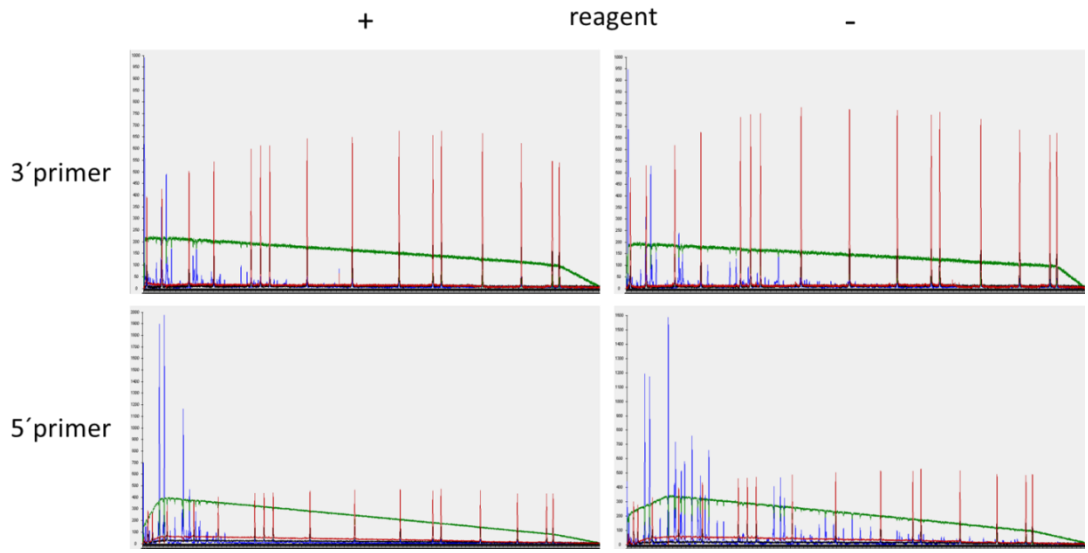


Figure 21: test samples modified with BzCN; fragments < 35 nucleotides were computationally removed.

Left column: cDNA of HRV2 RNA modified with BzCN at 550mM. Right column: cDNA of unmodified HRV2 RNA. Blue: fragment peaks, red: size standard peaks. The primer used for cDNA synthesis is indicated at the left border. Peaks are shown starting from the first size standard peak (35nt).
When compared with the size standard peaks, the concentration of the cDNA fragments is low. Further, cDNA fragments of different length are not equally distributed, short fragments are prevalent. Prevalence of short fragments could indicate that RNA was degraded, or that the concentration of reagent was too high. The low concentration of fragments could also imply that most of the RNA was transcribed to full length RNA (concentration of reagent too low) or that cDNA was lost in subsequent purification steps. Since the peak representing full length cDNA is not visible in this setup, it is not clear which of those possibilities is applicable.

Size standard: GeneScan™ -500 ROX™ STANDARD (35, 50, 75, 100, 139, 150, 160, 200, 250, 300, 340, 350, 400, 450, 490, and 500 nt in length)

### 4.1.3 Problem analysis using a short RNA

Reverse transcription of an RNA that is shorter than 500nt should yield a peak for full length cDNA derived from unmodified RNA strands, and it should show a decrease of full length product in parallel to an increase of short fragments upon modification. A primer was designed that binds 468nt downstream from the 5´end. An *in vitro* transcribed fragment of the HRV2 genome 468nt in length was used in the following experiments.

#### 4.1.3.1 Off-scale peaks

The identity of the short fragments at the onset of the trace was not clear. Such short fragments could be caused by several conditions. They could be composed of unbound primer and/ or short fragments generated during initiation of reverse transcription. In the course of the initiation process the reverse transcriptase pauses and thereby produces short fragments (*Wilkinson et al., 2006*). Short fragments could also hint at an overdose of reagent. If the concentration of reagent is too high, RNAs contain multiple modifications- since reverse transcription stops at the first modification, short cDNAs are favored.

To assess the nature of the very intense peaks in the beginning of the trace, 468nt RNA was transcribed to cDNA using different amounts of primer without any preceding modifications or treatments. 5pmol of RNA was primed with 0.05, 1, 5 and 10pmol of FAM labeled primer for reverse transcription, and subjected to capillary electrophoresis. In parallel, two blanks were analyzed. One blank consisted of the solvent formamide and the size standard, the other blank contained plain solvent. Figure 22 presents the electropherograms of the blanks; interestingly they show very high initial peaks composed of not only a ROX (label of the size standard) signal, but also intense FAM and HEX peaks. Those fluorophores were not added. This indicates that the prominent, low molecular weight peak is at least partially caused by the system. Low molecular weight contaminations can cause a change in the refractive index of the solvent and cause such peaks. Further, if the conductivity of the sample buffer differs significantly from the conductivity of the background electrolyte, the electric field at the injection point might not be amplified properly, causing system peaks (*Chien & Burgi, 1991*).

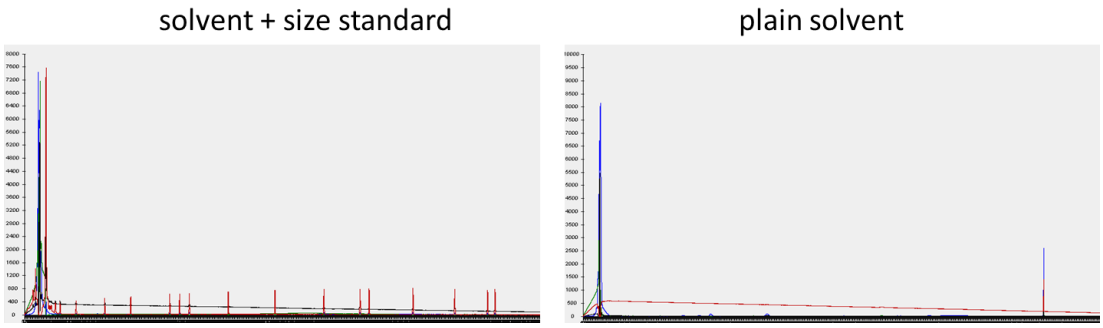


Figure 22: Blanks: solvent (formamide) plus size standard and plain solvent

Two blanks, one consisting of formamide and ROX GeneScan™ -500 ROX™ STANDARD (shown in red), the other consisting of plain formamide, were sent in for analysis. No HEX (depicted in green) or FAM (depicted in blue) labeled cDNA was added; still a pronounced peak is visible at the start of the traces.

In Figure 23 different template: primer ratios are compared. All samples show a pronounced peak between 450 and 490nt, representing the full length product. Hardly any fragments are visible, indicating good quality of RNA and optimal reverse transcription (RT) conditions. Most electropherograms show 3 peaks at identical positions between 350 and 400nt. Those peaks might be caused by an extensively folded region in the RNA, hindering elongation by reverse transcriptase. It is observable, that if the ratio of template: primer exceeds 1:0.2 enormous primer peaks arise that may influence analysis. So, unbound primer also contributes to the huge initial peak. Employing 0.05 pmol primer for 5 pmol RNA, reverse transcription yields a reduced peak for full length product, and also the “characteristic” peaks between 350 and

400nt are not observable. Using 1pmol primer for 5pmol RNA yields sufficient cDNA signals and no exuberant primer peaks.

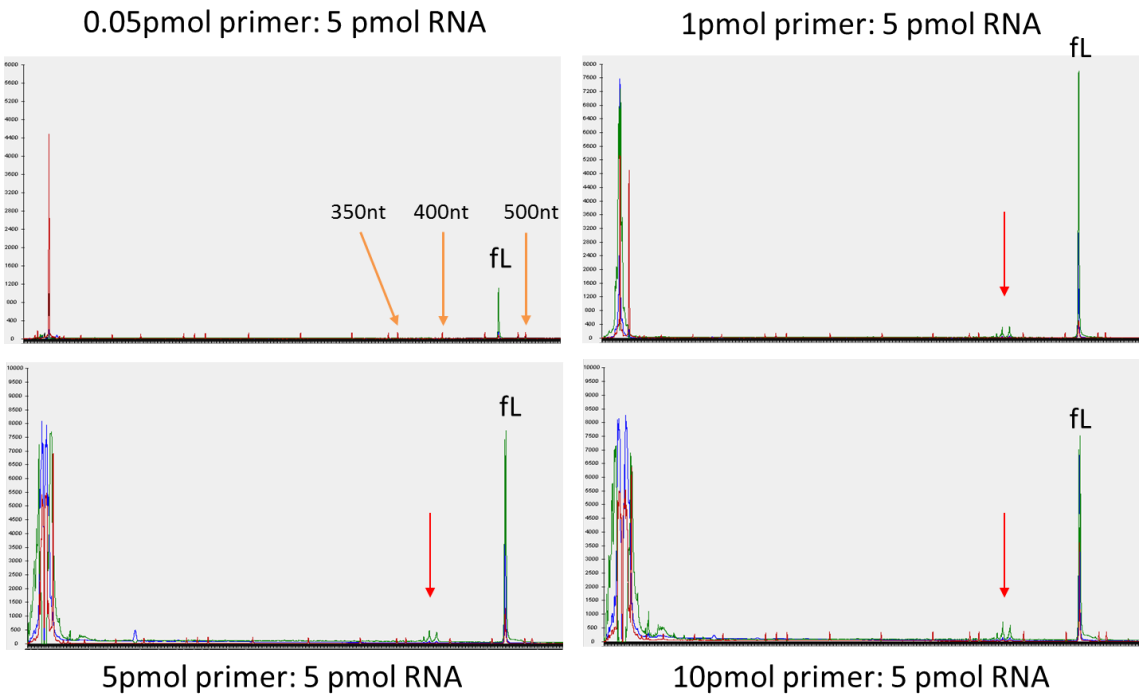


Figure 23: comparison of different amounts of primer, implication on the initial peak

5 pmol 468nt RNA was transcribed to cDNA with different amount of primer (HEX labeled, shown in green) without prior modification. Amount of primer is indicated above/ below traces. All samples display intense full length peaks (fL). Reduction of amount of primer reduces primer peaks but also fragment peaks. Most electropherograms show 3 peaks at identical positions between 350 and 400nt (red arrow). Fragments in unmodified samples are due to stable secondary structures.

Size standard: GeneScan™ -500 ROX™ STANDARD (35, 50, 75, 100, 139, 150, 160, 200, 250, 300, 340, 350, 400, 450, 490, and 500 nt in length), depicted in red.

#### 4.1.3.2 Spectral overlap

In a SHAPE experiment, the values for the (-) reagent profile are subtracted from the (+) reagent profiles to yield the absolute nucleotide- reactivity for every position of the RNA (*Vasa et al., 2008*). Therefore, the primer for cDNA synthesis was labeled with two different fluorophores, FAM and HEX, to allow parallel analysis of the (+) and (-) reagent samples. cDNA synthesis of the (+) reagent sample was primed with the FAM-labeled version, cDNA synthesis of the (-) reagent sample was primed with the HEX-labeled version of the primer.

5 pmol 468nt RNA was incubated under folding conditions and modified with BzCN (200mM). No-reagent-controls were treated with DMSO only. An example of obtained traces is shown in Figure 24. At first appearance, fragments of different length are present and a pronounced full length peak indicates that the RNA was not contaminated with RNases. Upon closer examination, the peak patterns of the (+) reagent trace and the no-reagent-control are identical. Fragments in the (-) reagent sample usually arise from termination of the reverse transcriptase at stable secondary structures and/ or degradation. The (+) reagent trace should contain additional peaks stemming from termination at sites of modification. So, peaks in the

(+) and the (-) reagent sample should not be identical. However, the HEX trace seems like a faint copy of the FAM trace. Further, the peak representing full length cDNA is higher in the (+) reagent trace than in the untreated sample. This is contrary to the assumption that untreated RNA is converted to cDNA to a far higher extent as modified RNA.

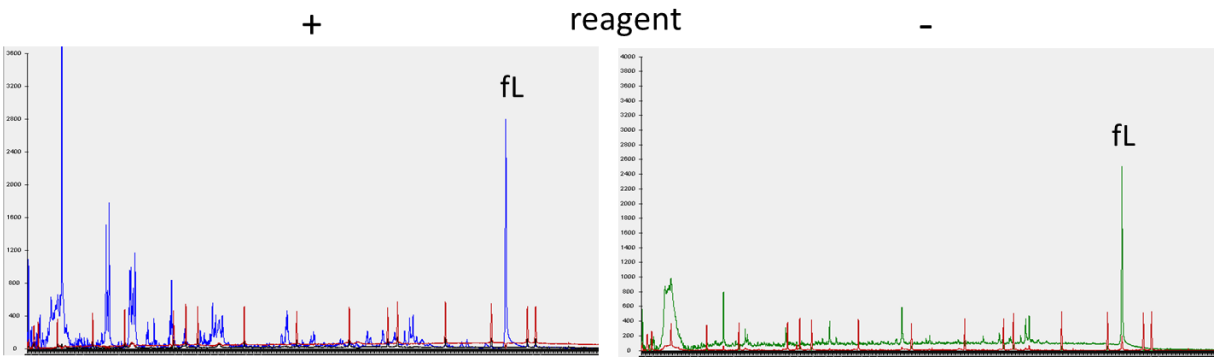


Figure 24: Identical peak patterns in the (+) and (-) reagent trace

468nt RNA modified with BzCN. Associated (+) and (-) reagent samples were combined prior to capillary electrophoresis. The (+) reagent cDNA was labeled with FAM (blue, left); the (-) reagent cDNA was labeled with HEX (green, right).

Fragments in the (-) reagent sample are due to stable secondary structures. The (+) reagent trace should contain fragments due to secondary structures plus additional peaks stemming from termination at sites of modification. Although peaks in the (+) reagent trace are more pronounced, peaks in the (+) and (-) reagent traces are at identical positions. Further, the peak representing the full length (fL) cDNA is more pronounced in the (+) reagent electropherogram than in the no-reagent-control. Modifications prevent elongation of full length cDNA, therefore the no-reagent-sample should contain a more pronounced fL peak than the (+) reagent sample.

Size standard: GeneScan™ -500 ROX™ STANDARD (35, 50, 75, 100, 139, 150, 160, 200, 250, 300, 340, 350, 400, 450, 490, and 500 nt in length), depicted in red

Presence of extenuated peaks at identical positions in different channels of a trace indicate occurrence of spectral overlap between the fluorescent channels. The fluorescent dyes used to distinguish the (+) and the (-) reagent trace have overlapping emission spectra, and are detected in several fluorescent channels by the instrument detector. According to the manual, the detector of the ABI PRISM 310 Genetic Analyzer records light intensity in different regions of the spectrum, depending on the combination of dyes. Those “windows” are chosen in a way, that they record wavelength close to the emission maxima of the respective dye, but with maximum possible separation among the emission maxima of different dyes. Certain combinations of “windows” are referred to as “virtual filter set” (see Figure 25). However, since emission spectra of dyes show overlap, it is not possible to eliminate spectral overlap completely. Following detection a multicomponent matrix is applied to the fluorescence intensity data to correct for spectral overlap between the dyes (*Applied Biosystems, 2000*).

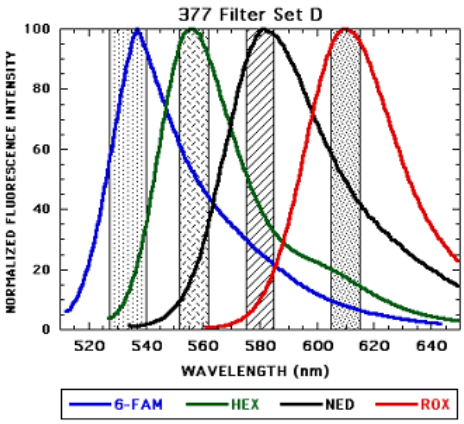


Figure 25: Virtual Filter Set D, the filter set used for analysis of cDNA fragments generated by SHAPE

The graph plots emission spectra of the dyes 6-FAM, HEX, NED and ROX and the respective detection windows (shaded areas). At the wavelengths where HEX-emission is detected, FAM still shows relatively high intensity of fluorescence. Also NED emission interferes with ROX detection.

Picture taken from the ABI PRISM 310 reference guide, *Applied Biosystems, 2000*

Although the fluorophores HEX and 6- FAM belong to the same "virtual filter set", and STRand was designed for analyzing files from instruments including the ABI PRISM®310 Genetic Analyzer, it was tested if spectral overlap is corrected sufficiently, or if signals of one dye are displayed by another channel. 5 pmol of 468ntRNA were treated with BzCN or plain solvent and transcribed into cDNA using 1pmol of primer. As mentioned above, the (+) reagent sample was primed for reverse transcription using FAM labeled primer, the (-) reagent sample with HEX labeled primer. To see if detection of one dye interferes with detection of the other dye, the FAM and the HEX labeled cDNA was analyzed separately. Samples, which contain only HEX-labeled primer (Figure 26), also show peaks in the FAM channel, so fluorescent overlap does happen in multifluor runs and dye separation is unsatisfactory. Therefore, it is not clear how much of the intensity of a signal is caused by the actual dye. Therefore, the two fluorophores cannot be used simultaneously in this setup. None of the (+) reagent samples contains fragments, probably the aliquot of the reagent was hydrolyzed. In further experiments, the (+) and (-) reagent samples were analyzed separately.

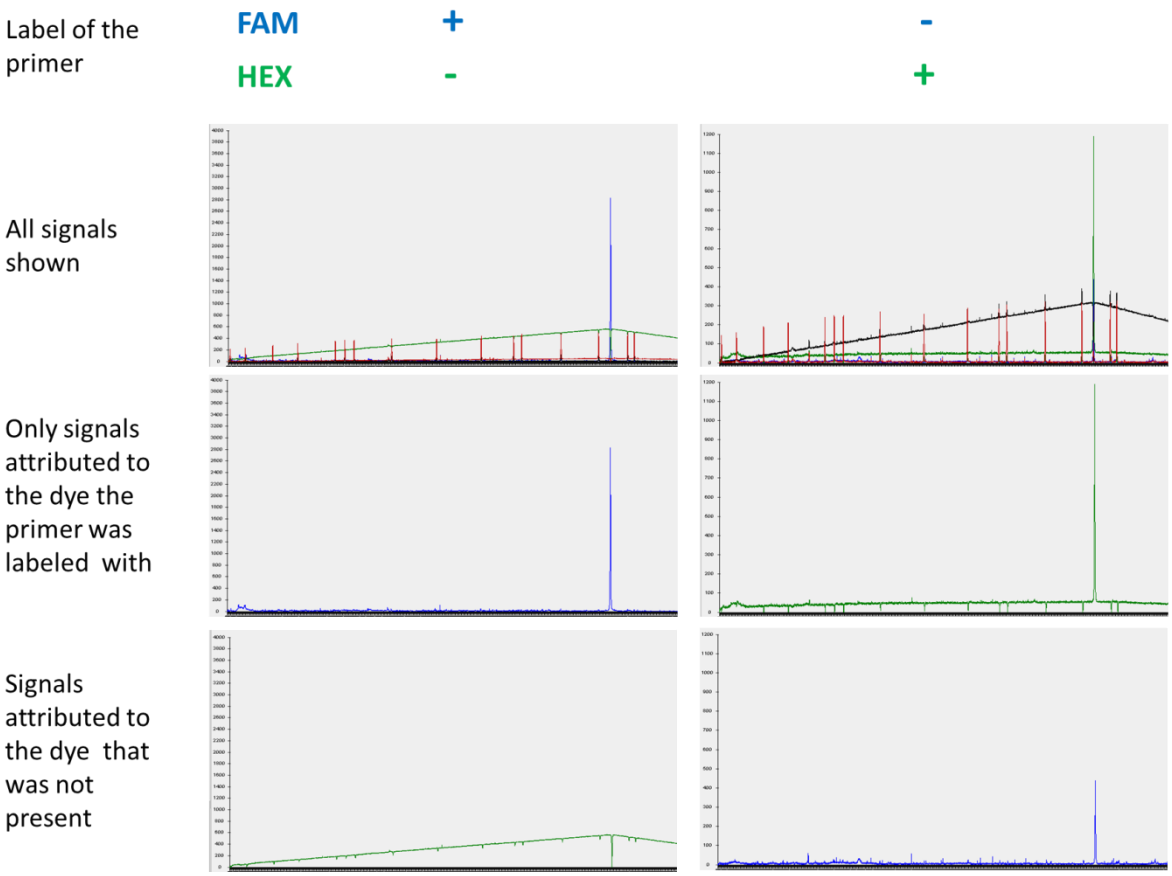


Figure 26: Testing the instrument/ software combination for correction of fluorescent overlap

To see if detection of one dye interferes with detection of the other dye, the differently labeled cDNA was analyzed separately. cDNA derived from modified RNA was labeled with FAM (shown in blue), cDNA derived from unmodified RNA was labeled with HEX (depicted in green). Presence of the fluorophore FAM or HEX is indicated above. Signals of a dye are displayed by a respective channel; it is possible to selectively show and hide signals attributed to an individual dye. In the sample containing HEX only, there is a peak in the FAM channel at the same position as the HEX peak. So, dye separation is not calculated automatically, neither by the instrument nor by the program STRand. None of the (+) reagent samples contains fragments, probably the aliquot of the reagent was hydrolyzed.

Size standard: GeneScan™ -500 ROX™ STANDARD (35, 50, 75, 100, 139, 150, 160, 200, 250, 300, 340, 350, 400, 450, 490, and 500 nt in length), depicted in red

#### 4.1.3.3 Upscaling of RNA

Peaks in the (+) reagent sample were rather small in all previous experiments. Therefore, it was tested if increasing the concentration of the starting material produces more distinct signals. CE analysis of different amounts of material was compared. It was started with 20µg of 468nt RNA, Following cDNA synthesis, aliquots containing calculated 5pmoles and 10pmoles cDNA were sent in for CE analysis. This time, the (+) and (-) reagent samples were resolved separately. Increase from 5pmol to 10pmol DNA already yielded more pronounced peaks (Figure 27). The (+) reagent samples show identical fragment patterns, divergent from the fragment pattern of the no-reagent-control, therefore fragments can be considered as being caused by stops at specific sites of modification rather than being randomized fragments caused by degradation.

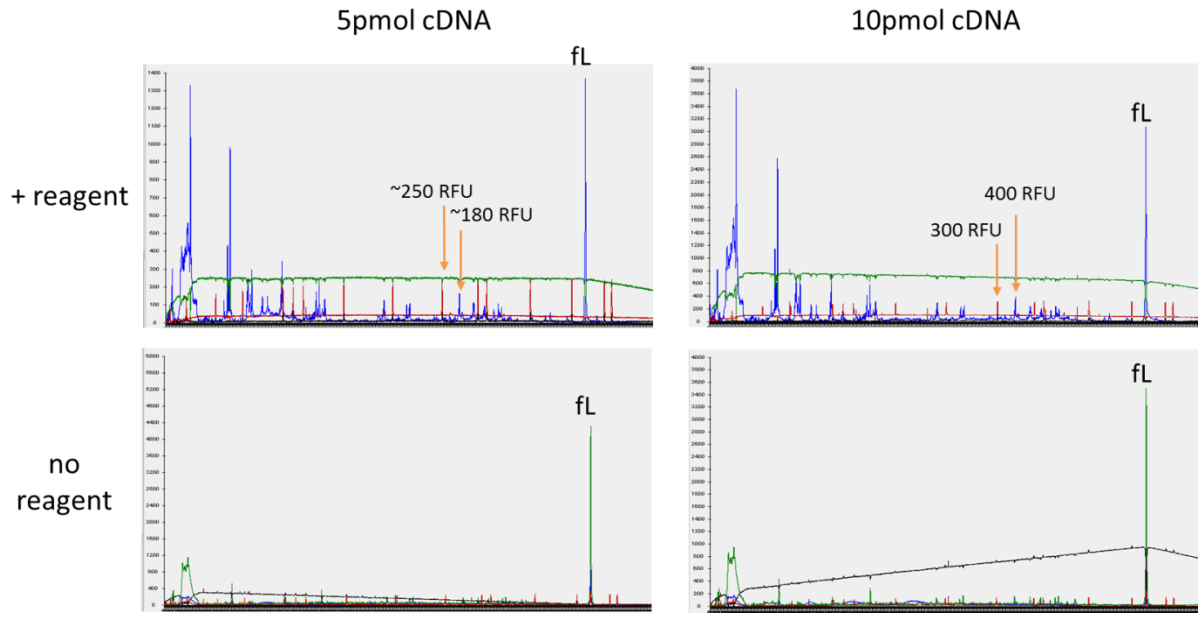


Figure 27: Comparison of different sample concentrations

Samples contained 5 and 10pmol cDNA, derived from 468nt RNA modified with BzCN and corresponding negative controls. cDNA of (+) reagent samples are shown in the upper row (blue), corresponding negative controls are shown below (green). (+) and (-) reagent samples were analyzed separately to avoid fluorescent overlap. From each sample cDNA corresponding to calculated 5pmol and 10pmol were aliquoted and sent in for CE analysis. Higher amount of material clearly gives more distinctive fragment peaks (in comparison to the size standard peaks). Interestingly, the full length (fL) peaks in the (+) reagent samples are comparable to the no-reagent-control; the more fragments are present; the less full length product should remain.

Size standard: GeneScan™ -500 ROX™ STANDARD (35, 50, 75, 100, 139, 150, 160, 200, 250, 300, 340, 350, 400, 450, 490, and 500 nt in length), depicted in red.

fL: full length product peak, RFU: relative fluorescence units

#### 4.1.3.4 No correction for diverging emission intensity

Interestingly, peaks representing full length (fL) cDNA in (+) reagent samples are often more intense as in (-) reagent controls (e.g. Figure 24). Upon excitement by the laser of the ABI PRISM 310 Genetic Analyzer, different fluorophores show different intensity of fluorescence. The fluorophores can be sorted in order of increasing emission intensity as follows: ROX < HEX < NED < FAM; compared to ROX, the intensity of emitted fluorescence of FAM is about eight times higher (*Applied Biosystems, 2000*). Given that neither the instrument nor the analysis program could eliminate spectral overlap, it was tested if deviation in signal strength of the different dyes is corrected.

Two samples were prepared; in one of them labeling with FAM and HEX was switched. Indeed, both fragment peaks and full length product peaks are weaker in the HEX labeled (+) reagent sample than in the FAM labeled (+) reagent sample, indicating that emission intensity of FAM is higher than intensity of HEX (Figure 28). If signal intensity is not converted to the actual amount of dye, deducing the degree of modification from signal intensity and comparison of peaks in the (+) and (-) reagent trace is not legitimate.

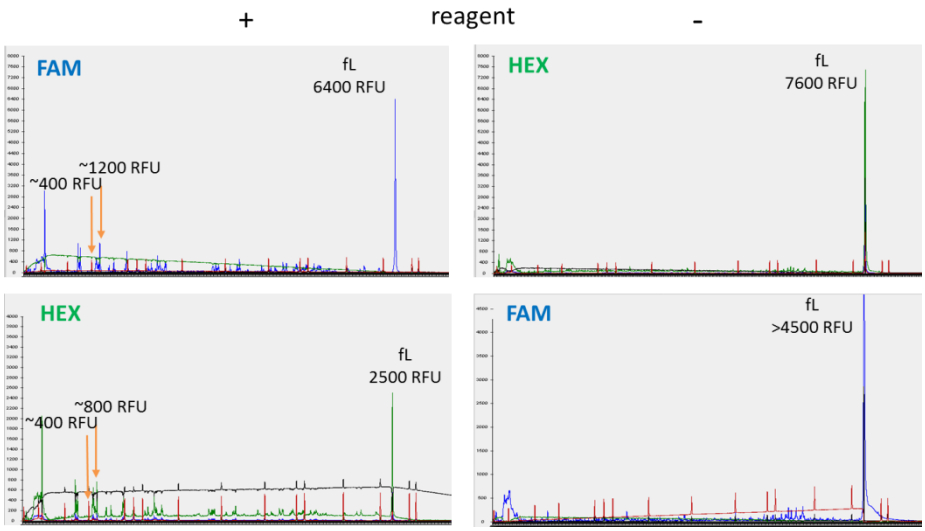


Figure 28: comparing signal intensity of FAM and HEX

Upper row: the (+) reagent cDNA is FAM labeled, cDNA of the no-reagent-control is HEX labeled. Beneath the labeling had been switched. Fragment peaks as well as full length product peaks are weaker in the HEX labeled (+) reagent sample than in the FAM labeled (+) reagent sample. Further, when the (+) reagent sample is labeled with FAM and the no-reagent-sample is labeled with HEX, the intensities of the full length peaks are comparable, if the fluorophores are switched, the intensity of the full length peak in the no-reagent-control is about double. This indicates, that diverging emission intensities of FAM and HEX are not corrected.
Size standard: GeneScan™ -500 ROX™ STANDARD (35, 50, 75, 100, 139, 150, 160, 200, 250, 300, 340, 350, 400, 450, 490, and 500 nt in length), depicted in red.
fL: full length product peak, RFU: relative fluorescence units

To compare fragments in the (+) and (-) reagent samples without distortion of the results caused by different emission intensity of the two dyes, FAM and HEX, fragments of both the (+) reagent and the no-reagent-samples were labeled with FAM. Using the same dye for both samples, differences in fragment patterns of the (+) and (-) reagent traces becomes more explicit (see Figure 29). In the (+) reagent sample the peak representing full length cDNA is reduced, whereas signals of short cDNAs are abundant. The (-) reagent trace shows few peaks, among them the characteristic peaks between 350 and 400nt as already found in Figure 23.

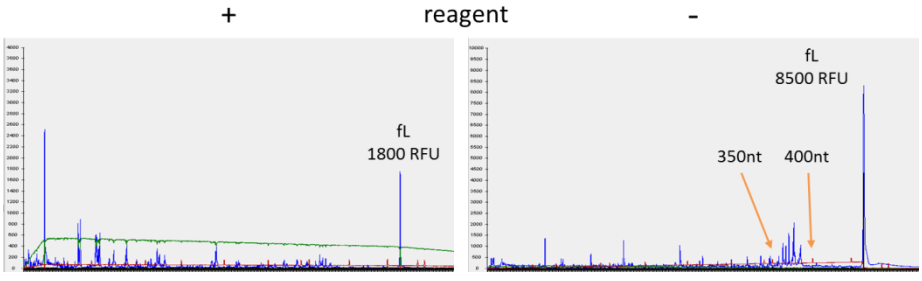


Figure 29: Using the same dye for (+) and (-) reagent samples, the difference becomes clear

cDNA in both the (+) and (-) reagent sample were labeled with FAM. Modification of RNA results in emergence of short cDNAs and reduction of the full length peak in relation to the (-) reagent control. The no-reagent-control trace shows few peaks, amongst them the peaks between 350 and 400nt also seen in Figure 23. fL: full length product peak, RFU: relative fluorescence units

Figure 30 compares different traces obtained by modification of the 468nt *in vitro* transcribed fragment of the HRV2 genome. Fragment patterns are reproducible. Using the same label for the modified sample as well as for the negative control and separate resolution shows a significant difference in peak distribution and intensity. Therefore, fragments can be considered as being caused by stops at specific sites of modification rather than being randomized fragments caused by degradation.

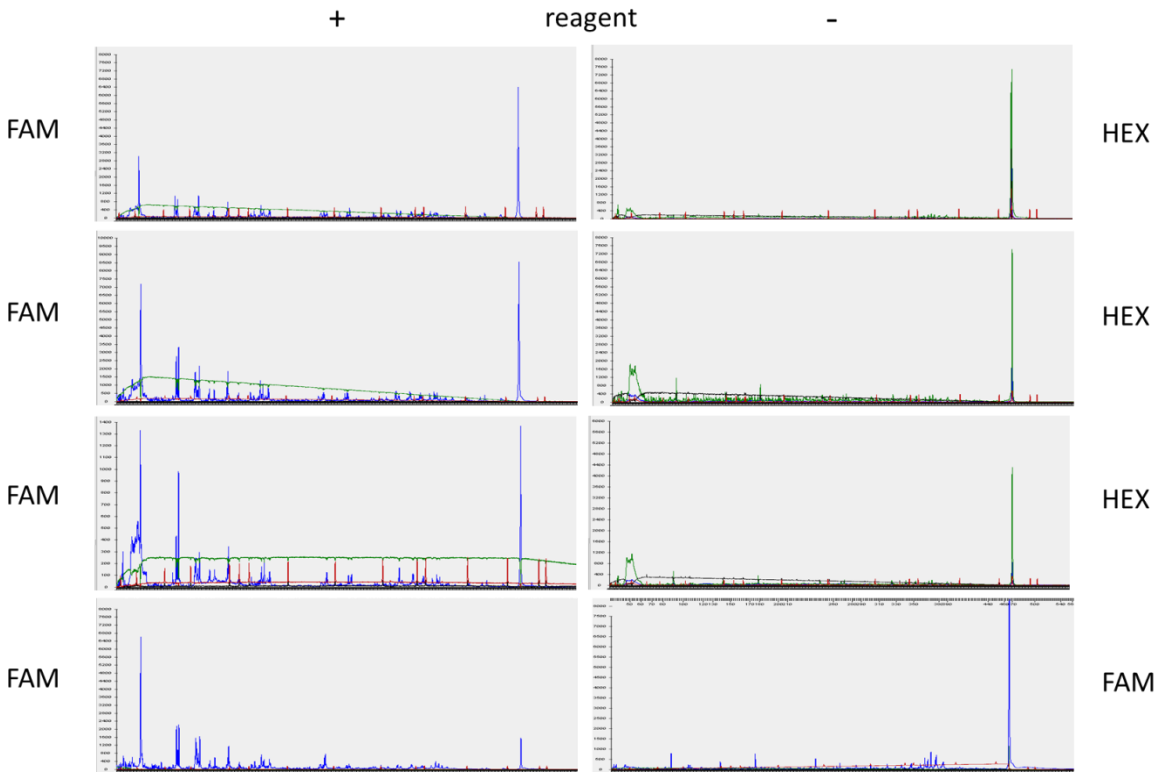


Figure 30: The fragment pattern of modified 468nt RNA is reproducible

Modified samples (left column) show the same peak pattern. Using FAM (depicted in blue) for both the (+) and the (-) reagent sample (last row), and analyzing the samples separately, difference of peak frequency and distribution becomes apparent.

In all (+) reagent traces, peaks at the left of the trace are far more intense than those at the right (Figure 29, Figure 27 Figure 24). If signal intensity allows conclusion about the amount of dye, short fragments are more numerous than long fragments. Excess of short fragments could be caused by too high concentration of the reagent or degradation. At high concentration of reagent multiple modification are introduced in the RNAs favoring short fragments. At the other hand, if RNA is modified statistically more than once or contaminated with ribonucleases, the full length peak should be missing. Another explanation for this phenomenon would be signal decay. *Vasa et al.,* (*2008*) describe signal decay of raw data such that peaks at the start of a trace are four times more intense than those towards the end. Considering that fluorescent overlap and differing emission intensities cannot be corrected with this setup, it is possible that the attenuation of the signal with increasing length of fragments is rather due to signal decay than to multiple modifications or degradation.

The only program available that could visualize all data sets could not correct for fluorescent overlap, divergence in emission intensity of different dyes, and signal decay. This aggravated interpretation of obtained traces and made results unreliable. For this reason, we sought another method to detect which end leaves the capsid first.

## 4.2 Halting egress and digesting protruding RNA

The workflow of the experiment was planned as follows; following triggering the release of the RNA by lowering the pH, addition of formaldehyde was supposed to halt the egress either by inducing crosslinks between exiting RNA and the capsid or by trapping the leaving RNA by extensively crosslinking the site of egress. Addition of bovine pancreatic ribonuclease A (RNase A) removes the protruding part. If the capsid is impermeable to RNase A and if it is possible to remove RNase A and get access to the RNA that was left behind in the sealed capsid, characterization of the remaining RNA would allow conclusion about directionality of egress.

RNase A is a very stable enzyme, once added it is difficult to remove. *Jackson et al.* (*1990*) compared different extraction methods to retrieve high quality DNA and RNA from formalin fixed samples and fresh tissue. Best protection from tissue-derived RNases was achieved by incubation with proteinase K for 1 h followed by phenol-chloroform extraction.

### 4.2.1 Preliminary experiments to halting egress by formaldehyde crosslinking

In preliminary experiments it was tested

- Which is the appropriate percentage of formaldehyde for quickly halting RNA egress
- If formaldehyde at a high concentration abolishes RNase A and/ or proteinase K activity, and if so, if quenching the crosslinking reaction is sufficient to restore activity.
- If proteinase K digestion followed by phenol-chloroform extraction is adequate to remove RNase A and retrieve high quality RNA

#### 4.2.1.1 What is the appropriate percentage of formaldehyde for sufficient and quick crosslinking?

Young-Chan Kim et al. report that 5 min incubation in a 0.1% solution of formaldehyde yields 1% of cross-linked products between a short RNA and the respective RNA binding protein (*Kim et al., 2005*). The goal of formaldehyde crosslinking was to halt the release of RNA during its egress and to seal the capsid; 1% of cross-linked product was considered insufficient. Different final percentages of formaldehyde and the effect on integrity of the viral capsid under denaturing conditions were compared. Heating of HRV2 in the presence of SDS for 10 min to 56°C leads to disassembly of the viral capsid into individual monomers of VP1, 2, 3 and 4 (*Weiss, 2009*) but should not reverse the crosslinks induced by formaldehyde. Sufficient crosslinking was interpreted as lack of bands for the individual viral proteins in SDS-polyacrylamide gel electrophoresis following heat denaturation.

About 1.5µg of virus was incubated with 0, 1, 5, and 10% formaldehyde for 5 min. The crosslinking reaction was quenched with excess of saturated glycine solution. Reducing sample

buffer was added and the samples were heated to 56°C for 10 min prior to separation in a 15% polyacrylamide gel. The non-crosslinked sample in Figure 31 shows three bands, running at 37, ~28 and 25kDa, matching VP1, 2 and 3 (32, 29 and 26kDa), VP4 is not visible on this gel (*Rossmann et al., 1985*). In the sample treated with 1% formaldehyde final concentration, no difference to the untreated sample is perceptible; crosslinking, which is supposed to prevent disassembly into the individual viral proteins is negligible at this concentration of reagent. 5% formaldehyde final concentration appears to be already sufficient to cause exhaustive crosslinking; no bands representing the separate viral proteins VP1-3 are visible. However, 10% final concentration of formaldehyde was chosen to proceed with, because of the demand to halt the process of RNA release as fast as possible. The faint bands in the lanes where the samples treated with 5% and 10% formaldehyde running at about 40kD probably represent crosslinked VP4; larger aggregates or whole crosslinked virus presumably was not capable of entering the separating gel, the stacking gel was removed.

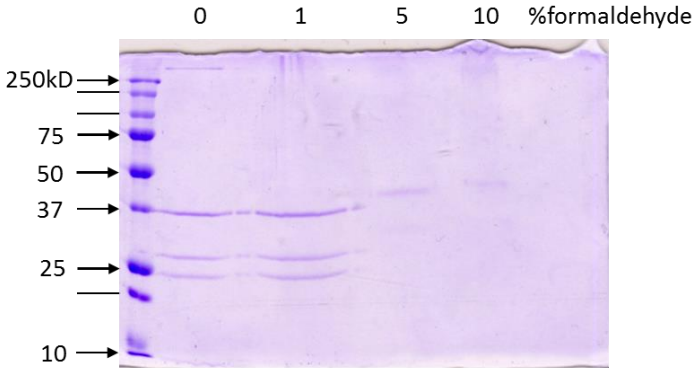


Figure 31: Effect of different concentrations of formaldehyde on heat denaturation of HRV2

Virus was incubated with different concentrations of formaldehyde, percentage is indicated on top. The reaction was quenched by addition of glycine and the sample was heated to 56°C in reducing sample buffer for 10 min. Proteins were separated in a 15% polyacrylamide gel (25mA, 300V, ~1h). 5% formaldehyde induced enough crosslinks that the viral capsid withstands denaturing conditions.
Marker: BIORAD precision plus protein standard all blue #161-0373.

#### 4.2.1.2 The effect of formaldehyde on RNase A and proteinase K

Glycine is the commonly used quenching agent in chromatin immunoprecipitation (*Orlando et al., 1997*), but Sutherland et al. report that not even 12-fold molar excess of glycine is sufficient to stop the crosslinking reaction immediately (*Sutherland et al., 2008*). Therefore, it was tested if formaldehyde would inhibit RNase A and/or proteinase K, the enzymes used in subsequent steps. Does formaldehyde need to be removed (e.g. by dialysis) prior to enzymatic digestion, or is it sufficient to add glycine?

To test whether RNase A is functional under crosslinking conditions, *in vitro* transcribed HRV2 RNA was added to native virus in a 10% formaldehyde solution and subjected to RNase A digestion. Virus was included in this pretrial, because in the actual experiment, when RNA is released from the capsid, also both proteins and RNA will be present. To one sample excess of saturated glycine was added prior to addition of RNA and RNase A, in the other sample the reaction was allowed to proceed during RNase A digestion. Digestion of RNA was assessed in an agarose gel. In the sample where RNA was subjected to RNase digestion without addition of

glycine, RNA is only partially degraded (Figure 32). When the crosslinking reaction was quenched prior to addition of RNA and RNase, RNA is completely digested. RNA in the controls that contain glycine and/ or the protein background but no RNase (left) is as intact as plain *in vitro* transcribed RNA; therefore the absence of RNA in the sample that was treated with RNase after addition of glycine can be attributed uniquely to RNase A digestion.

Reduced degradation of the RNA could either be due to a direct effect of formaldehyde on RNase A, or by RNA-RNA or RNA-protein crosslinks, that hinder degradation. In short: removal of formaldehyde is not necessary if glycine is added, but it had to be evaluated if RNA-RNA and/ or RNA-protein crosslinks are an impediment to RNase A digestion (see 4.2.1.3).

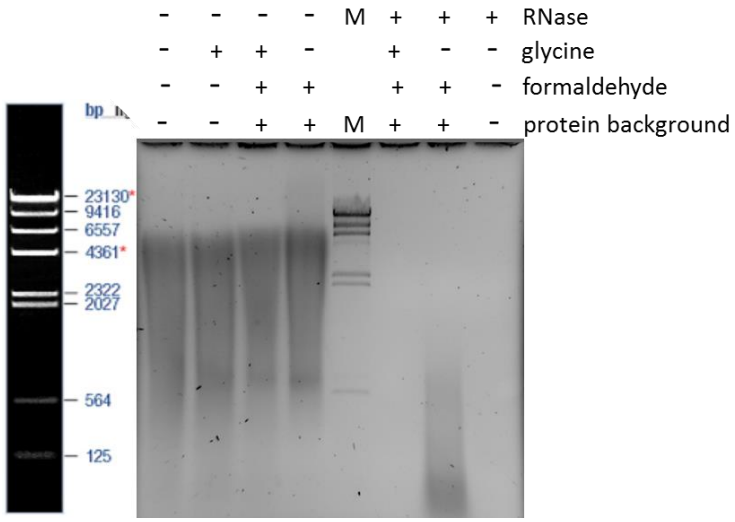


Figure 32: Does formaldehyde inhibit RNase A?

*In vitro* transcribed RNA was digested in a 10% formaldehyde solution containing 2nd fraction virus with or without addition of glycine. Addition of 2nd fraction virus (protein background), formaldehyde, glycine and RNase A is indicated on top. If the crosslinking reaction is allowed to proceed, digestion of RNA by RNase A is reduced, but not prevented. If the crosslinking reaction is quenched by addition of glycine, RNA is degraded completely.
Control samples (left, far right) indicate, that none of the used solutions was contaminated with RNases, digestion of RNA is solely attributable to RNase A.
M: marker, λ DNA digested with *Hind*III, 1% agarose 0.1% SDS gel, 80V, 45 min

To examine the influence of formaldehyde on proteinase K, 2nd fraction virus was treated with formaldehyde in a final concentration of 10%, the crosslinking reaction was quenched by addition of saturated glycine in excess or allowed to proceed, and proteinase K was added. Following incubation at room temperature for 30 minutes, reducing sample buffer was added and the samples were heated to 95°C for 5min. Degradation of viral proteins was surveyed by running the samples in a 15% polyacrylamide gel. In samples where the crosslinking reaction was quenched by addition of glycine, significantly more low molecular weight products are visible than in samples where the crosslinking reaction was allowed to proceed (Figure 33). In all samples bands are visible that just entered the separating gel. The size of whole virus particles was calculated to be 8.1MDa (*Bacher et al., 2001*). It is not likely that a ~8MDa particle enters a 15% separating gel; it is thus rather likely that some proteins are crosslinked preferentially; the bands just beneath the stacking gel stemming from crosslinked neighboring

viral proteins. Comparing the samples without proteinase K, virus in the quenched sample is disintegrating into individual monomers to a certain extent, in contrast to virus that was subjected to prolonged crosslinking. Formaldehyde inhibits proteinase K but addition of glycine restores proteinase K activity; it is thus not necessary to remove formaldehyde prior to protease digestion.

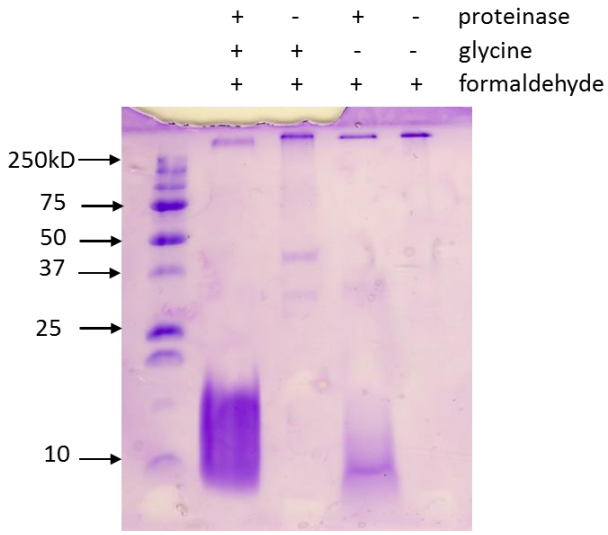


Figure 33: Does formaldehyde inhibit proteinase K?

HRV2 was crosslinked with formaldehyde (10% final concentration) for 5 minutes. In one set of samples, an excess of saturated glycine was added, in the other set of samples, the reaction was allowed to proceed. Presence of glycine and proteinase K is indicated on top. Following incubation with or without proteinase K for 30 minutes at room temperature, samples were heated to 95°C with reducing sample buffer for 5 min. Formaldehyde has an inhibitory effect on proteinase K. Addition of glycine sufficiently quenches the crosslinking reaction to allow proteinase K digestion.
Proteins were separated in a 15% polyacrylamide gel (25mA, 300V, ~1h). Marker: BIORAD precision plus protein standard all blue #161-0373.

#### 4.2.1.3 RNA-RNA, RNA-protein crosslinks and RNase A

In Figure 32 it is shown, that digestion of RNA by RNase A is reduced in the presence of formaldehyde and proteins. It was not clear whether the reduced RNase A activity was due to a direct effect of formaldehyde on RNase A, or by induction of RNA-RNA or RNA-protein crosslinks.

*In vitro* transcribed RNA was added to native virus and submitted to crosslinking. To preclude an inhibitory effect of formaldehyde on RNase A, the crosslinking reaction was quenched prior to addition of RNase A. Different final concentrations of RNase ranging from 0.05mg/ml to 0.2mg/ml were used for digestion. *In vitro* transcribed RNA was added to a virus-formaldehyde-solution either prior to quenching or after addition of glycine. RNA incubated along with proteins (virus) in a formaldehyde-containing solution shows a band shift in comparison to RNA that was added to proteins after stopping the crosslinking reaction or plain RNA, suggesting that RNA-RNA or even RNA-protein crosslinks do occur (see Figure 34, to the left of the marker). RNA added to the protein-RNA mixture after quenching the reaction is entirely degraded in contrast to crosslinked RNA (Figure 34, to the right of the marker). In

summary, it can be stated, that RNA-RNA and maybe even RNA-protein crosslinks do occur. They hinder RNase A digestion, but only to a minor extend.

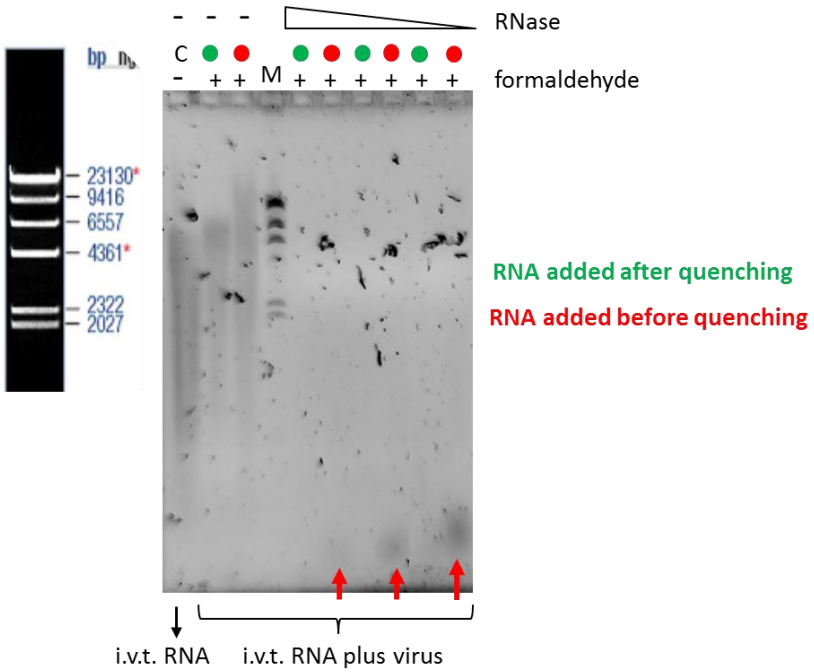


Figure 34: Are RNA-RNA or RNA-protein crosslinks hindering digestion by RNase A?

*In vitro* transcribed RNA was added to 2nd fraction virus in formaldehyde solution. RNA was added to the virus-formaldehyde mixture either after quenching the crosslinking reaction (no RNA-RNA or RNA-protein crosslinks) or before quenching (crosslinking of RNA). Aliquots of each sample were digested with RNase A at concentrations of 0.05, 0.1 and 0.2mg/ml. RNA that was submitted to formaldehyde crosslinking in presence of virus shows a band shift in comparison to RNA that was added to virus after quenching the reaction (left to the marker). Crosslinked RNA is only partially degraded, in contrast to RNA that was added to virus after quenching the crosslinking reaction (right to the marker).
C: in vitro transcribed RNA in $H_2O_{NF}$, M: marker, λ DNA digested with *Hind*III
1% agarose, 0.1%SDS, 80V, 40min.

To assess whether exiting RNA gets crosslinked to the capsid and possibly is protected from degradation by RNase, virus was triggered to release its genome, crosslinked and submitted to RNase A digestion. Conditions for triggering release of the RNA genome were chosen based on conditions that trigger genome transfer into liposomes (*Bilek, 2009*). Virus samples were acidified with sodium acetate (NaAc, 50mM, pH 5.2) to a pH of ~5.4 and were incubated at 34°C for 15 min. Samples were reneutralized with borate buffer (pH 8.3, 100mM).

Following reneutralisation, one aliquot was crosslinked, the other aliquot remained untreated. An aliquot of both crosslinked and non-crosslinked virus was incubated with RNase A; all samples were applied to an agarose gel without purification. Only samples that were not crosslinked show bands; regardless, if RNase A was added or not (Figure 35). The absence of a band in the crosslinked, non-digested sample could be explained by aggregation of viral particles by crosslinking, the aggregates being too bulky to enter the gel. Finding a band in the sample that was not crosslinked but subjected to RNase digestion was surprising. Even more so, as the band migrates with exactly the same mobility as full length *in vitro* transcribed RNA; this pattern proved to be reproducible. It has to be mentioned, that the gels used for resolving

RNA bands were treated with diethyl pyrocarbonate (DEPC) and did not contain SDS. Therefore, viral proteins should not be denatured upon electrophoresis.

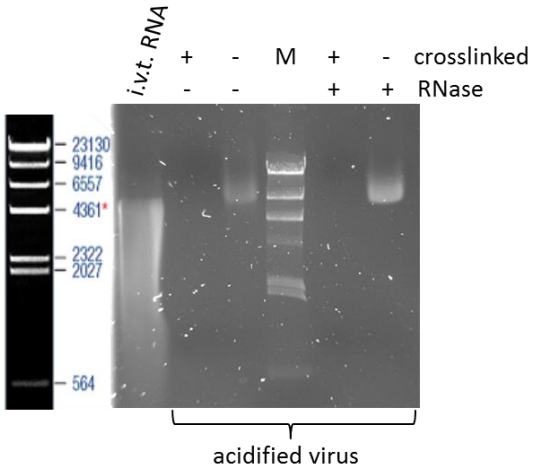


Figure 35: Does crosslinking of exiting RNA to its capsid affect RNase A degradation?

HRV2 samples were acidified to pH 5.4 using 50mM NaAc, incubated at 34°C for 15 min and reneutralized with borate buffer (pH 8.3, 100mM). To one set of samples formaldehyde was added (10% final concentration), samples were incubated at room temperature for 5 min and the reaction was quenched by addition of glycine, the other set of samples was left untreated. An aliquot of both crosslinked and non-crosslinked virus was digested with RNase A (0.1mg/ml) for 20 minutes at 37°C. The samples were loaded onto an agarose gel without purification. Crosslinking and addition of RNase A is indicated on top.
Only samples that were not crosslinked show bands. Interestingly, the sample that was treated with RNase A shows a band that migrates exactly at the size of the full length HRV2 genome.
i.v.t. RNA: *in vitro* transcribed HRV2 RNA in $H_2O_{NF}$, M: marker, λ DNA digested with *Hind*III, 1% agarose, 0.1% DEPC, 80V, ~ 30´- 45

## 4.2.2 RNA obtained from acidified HRV2 is not naked

Reproducibly, incubation of HRV2 under conditions that were shown to trigger transfer of the RNA genome into liposomes yielded material that was stained by ethidium bromide (EtBr), migrated to exactly the same position as *in vitro* transcribed full length HRV2 RNA and was resistant to RNase A digestion. Is there an inhibitory effect of a viral protein on RNase A?

### 4.2.2.1 Testing formation of ribonucleoprotein

In 1967 Sandy McGregor and Heather D. Mayor suggested that heating to 50°C of poliovirus and HRV (HRV1B and HRV14) leads to formation of ribonucleoprotein (RNP). Enzymatic probing of RNPs showed that they were resistant to RNase digestion unless pepsin, a proteinase was added. They concluded that viral proteins reorganize to coat the viral genome (*McGregor & Mayor, 1968*). The only viral protein that is lost upon acidification is VP4 (*Korant et al., 1972*). VP4 is a small protein of ~7kDa that lines the inner surface of the virion, per virion there are 60 copies of VP4 (*Korant et al., 1972*, *Rossmann et al., 1985*). That such a low number of a small protein could cover the HRV2 genome which is ~7kb in length appears highly unlikely. Nevertheless, this was investigated.

In a first attempt to see if HRV2 RNA is released in association with proteins, the agarose gels showing RNA bands in the presence of RNase A were stained with Coomassie brilliant blue. Coomassie brilliant blue stains proteins unspecifically by complexing with basic side chains and aromatic residues (*Compton & Jones 1985*). Lambda DNA (marker) is stained by Ethidium Bromide, but not by Coomassie brilliant blue, indicating that Coomassie brilliant blue interacts with proteins, but not with nucleic acids (Figure 36). Bands that appeared upon Ethidium Bromide staining are also stained by Coomassie brilliant blue. This suggests that HRV2 RNA is associated with a protein (or proteins) that protect it from RNase digestion. Though, it is peculiar that a ribonucleoprotein would migrate at exactly the same size as the naked 7.1kb HRV2 RNA.

The notion that RNA of crosslinked virus does not give any bands because of retention of aggregates in the slots is backed up by the remarkably darker stain of the slots where crosslinked samples were applied (red arrows in Figure 36).

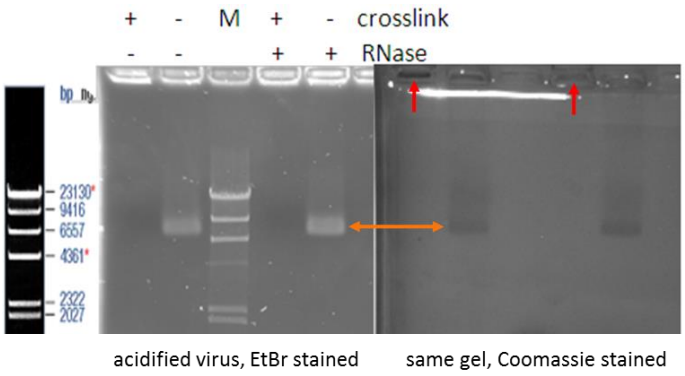


Figure 36: Ethidium bromide and coomassie brilliant blue staining of a gel presenting acidified HRV2

HRV2 was subjected to formaldehyde crosslinking or not, acidified and incubated along with RNase A (conditions see Figure 35). Left: bands stained with ethidium bromide. Right: the same gel, bands stained by coomassie brilliant blue. This is the same gel as shown in Figure 35. Bands stained with coomassie brilliant blue are at the same position as bands stained by ethidium bromide (orange arrow). Since coomassie brilliant blue does not stain nucleic acids (there are no bands visible where the marker was applied) it can be stated that RNA "released" by HRV2 is associated with proteins. Crosslinked virus is retained in the slots (red arrows).

To confirm association of proteins with the RNA, digestion with RNase was preceded by proteolysis. Virus was acidified, putative RNPs were incubated with proteinase K or in plain buffer and an aliquot of each sample was exposed to RNase A. Samples were run in a DEPC-treated agarose gel without purification. Following ethidium bromide staining, the gels were stained with Coomassie brilliant blue to validate removal of proteins by proteinase K. Although the putative RNPs migrate differently as observed in Figure 36, the protective function of proteins is verified. Only when RNase A digestion was preceded by incubation with proteinase K, RNA is digested (no EtBr signal, Figure 37).

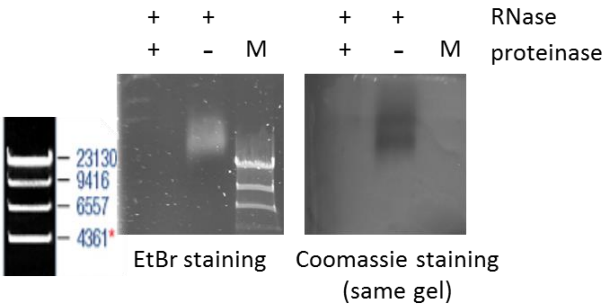


Figure 37: acidified HRV2 incubated with proteinase K and RNase A

Virus was acidified, putative RNPs were incubated with proteinase K (0.6mg/ml) or in plain buffer for 30 minutes at room temperature and an aliquot of each sample was exposed to RNase A (0.1mg/ml, 20 min, 37°C). Following EtBr staining (visualization of RNA) the gel was stained with coomassie brilliant blue (visualization of proteins). Only when the samples are incubated with both proteinase K and RNase A, RNA is digested. In samples were proteinase K digestion was omitted, RNA bands colocalize with protein bands.
M: marker, λ DNA digested with *Hind*III, 1 % agarose, 0.1% DEPC, 80V, ~ 40´

Sandy McGregor and Heather D. Mayor further observed that rhinovirus (HRV1B and HRV14) and poliovirus RNA were sensitive to RNase digestion, if the enzyme is present during denaturation by heat. They suggested that the protein involved in RNP formation is capsid-derived; in the time window between disassembly of the capsid and assembly of this putative RNP, the RNA would be RNase sensitive. They stated that naked RNA is released from within the particle. It unfolds and associates with a protein; only after formation of RNP the RNA would be protected from RNase digestion (*McGregor & Mayor, 1968*, *McGregor & Mayor, 1971*).

To see, if the same stepwise mechanism is true for RNA release from HRV2 when triggered by acidification, 1µg RNase A was added to the samples either during or after 15 min incubation at pH 5.4, 34°C. Degradation of RNA was monitored by agarose gel electrophoresis. When RNase is present during acidification, the RNA was not degraded. In contrast, RNA bands of samples that had been incubated at low pH along with RNase were reproducibly even brighter than bands of samples where RNase was added after reneutralization or not at all (Figure 38). The structural changes of HRV2 upon incubation at low pH must be different to the reorganization of capsid proteins to RNA binding proteins caused by heat degradation described by McGregor and D. Mayor.

Frequently samples that have not been incubated with RNase, including untriggered virus, show a smear of shorter RNA. This short RNA is not associated with proteins (results not shown), it could stem from broken virus present in some preparations and/ or remains from cell culture. Further, the solely acidified sample migrates differently to the RNase treated sample. Probably part of the RNA is loose and can interact between different RPNs, thereby forming aggregates. If RNase is added, junctions are clipped.

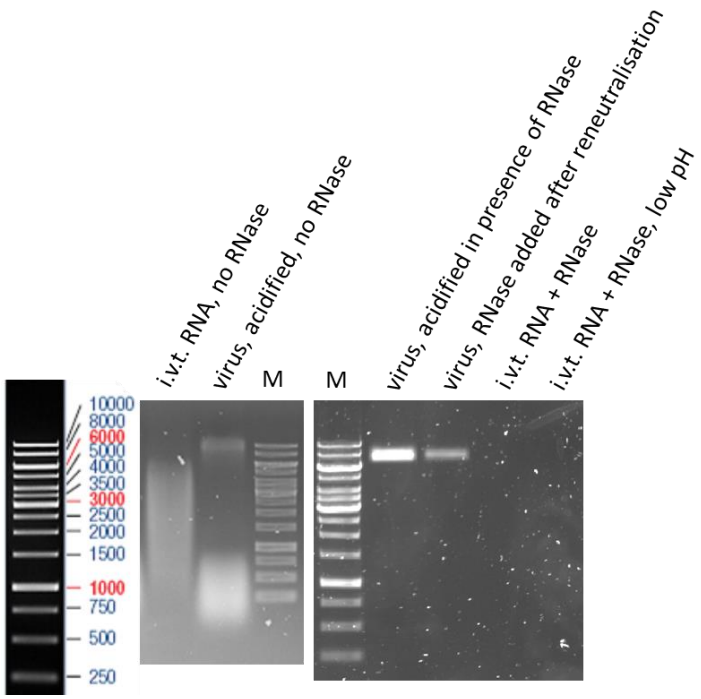


Figure 38: RNase A added to virus during or following acidification

McGregor and Mayor observed RNase sensitivity of HRV1B and HRV14 RNA during the process of uncoating triggered by heat, but resistance to RNase if the enzyme was added subsequently. This is not true for acidified HRV2 which is insensitive to RNase A digestion both during and after incubation at low pH.
i.v.t. RNA: *in vitro* transcribed HRV2 RNA
acidification: incubation at pH ~5.4, 34°C, 15min
M: marker: Fermentas 1kb DNA Ladder #SM0311, 1 % agarose, 0.1% DEPC, 80V, ~ 40´

#### 4.2.2.2 Comparison of acidification and 56°C as trigger for conformational change analyzed via agarose gel electrophoresis

McGregor and Mayor produced RNPs from rhinovirus and poliovirus by heating to 50°C in 0.01 M phosphate buffer (pH 8.0) for times ranging from 10 to 30 min. Korant et al. report that acidification of HRV2 yields two kinds of subviral particles: an A particle, that lacks VP4 but still contains the RNA, sedimenting at 135S in sucrose gradient centrifugation and B particles, which have lost both VP4 and the RNA genome, sedimenting at 75S (*Korant et al., 1972*). Lonberg-Holm and Yin report that acidification of concentrated HRV2 mainly produces 135S particles, whereas heating to 56°C mainly yields empty particles (*Lonberg-Holm & Yin, 1973*). In contrast, Gerhard Bilek reported that acidification is the more efficient trigger to stimulate transfer of the HRV2 genome into receptor-decorated liposomes (*Bilek, 2009*). It is possible that the mechanism of release is different when triggered by elevated temperature and low pH.

Therefore, the effects of heating and acidification on completion of RNA release were compared. Virus samples were either heated to 56°C for 10 minutes or acidified for 15 minutes by addition of 50mM sodium acetate pH 5.4. Heated samples were returned to ice, acidified samples were reneutralized, loading buffer was added and the samples were analyzed in a 1% agarose, 0.1% DEPC gel in parallel to untreated virus. To asses association with proteins, gels were stained with Coomassie brilliant blue following EtBr staining. Both heating and

acidification of HRV2 lead to appearance of EtBr signals on the agarose gel (Figure 39). EtBr bands stimulated by heating are well defined, sharp bands that migrate at about the same distance as *in vitro* transcribed RNA. EtBr stained bands triggered by acidification are more heterogeneous. Comparison of EtBr staining to Coomassie brilliant blue staining reveals that RNA in both acidified as well as heated samples is associated with proteins. Release of RNA does not proceed to completion; neither in acidified nor in heated samples.

Interestingly, untreated virus shows two bands in Coomassie staining. The ratio of upper and lower species differs between preparations (not shown). If virus is heated or acidified, preferentially the lower band is altered to a form that is stained by EtBr. The upper band remains unaltered by heating, but is converted upon acidification.

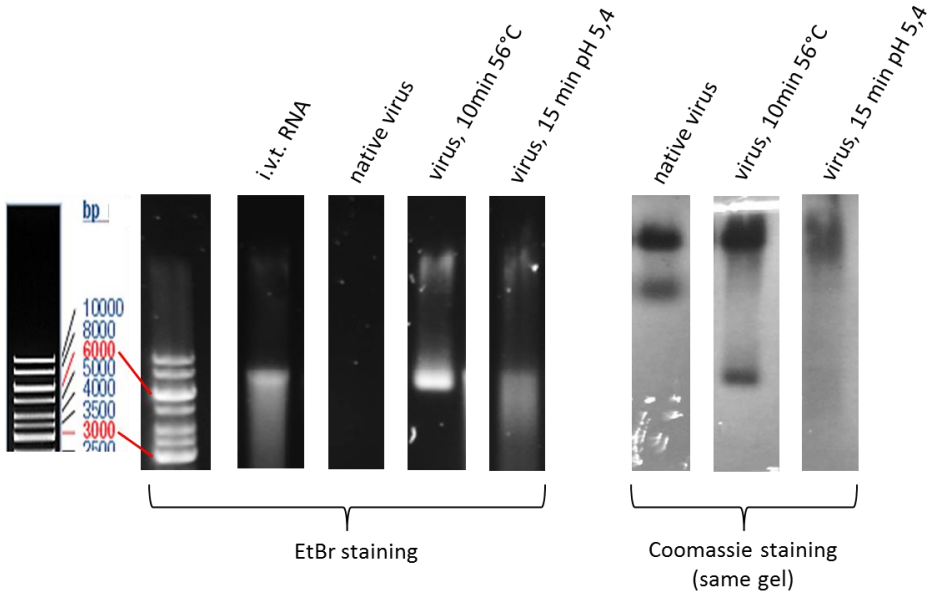


Figure 39: Comparison of heating and acidification of HRV2

EtBr staining: Heated samples show a defined band, migrating at the same position as *in vitro* transcribed HRV2 RNA. Bands obtained by acidification are less homogenous. Native virus gives EtBr signals only upon prolonged incubation in the EtBr bath (see Figure 43).
Coomassie staining: Native virus shows two bands, the lower band is converted to a species that is easily stained by EtBr; the upper band stays unaltered by heating but is influenced by incubation at low pH.
For clarity, only relevant samples are shown.
Acidification: pH 5.4, 34°C, 15min. Heating: 56°C, 10 min. Native virus: kept on ice during acidification or heating of other samples. i.v.t. RNA: *in vitro* transcribed HRV2 RNA in $H_2O_{NF}$
M: Fermentas 1kb DNA Ladder #SM0311, gel: 1% agarose, 0.1% DEPC, 80V, 40-60min

#### 4.2.2.3 Comparison of acidification and 56°C as trigger for conformational change analyzed via CE

To further characterize this RNA-protein complex, samples were analyzed by capillary electrophoresis. Using capillary electrophoresis (CE) with UV-Vis detection the distinct viral proteins and the viral RNA as well as native virus and subviral particles can be separated. Both proteins and the RNA show absorption maxima at 200nm, RNA further absorbs light of 260nm. Since HRV2 has a tendency to aggregate during CE, it is necessary to add detergents. When analyzed in presence of Thesit, native virions can be distinguished from 135S particles and

empty capsids; if SDS is added, native virions, individual viral proteins, and the viral RNA can be detected (*Weiss, 2009*).

Acidified virus (15 min pH 5.4 incubated at 34°C, reneutralized with borate buffer) was compared to heat denatured (10 min heated to 56°C in borate buffer) and native virus (borate buffer) to get an idea if there is a different mechanism of uncoating, and if there is an interaction with a particular viral protein in acidified samples. CE analysis was kindly performed by Xavier Subirats. Sample buffer containing SDS or Thesit was added after returning heated samples to ice or re-neutralization of acidified samples. Samples were run in either SDS or Thesit-containing background electrolyte.

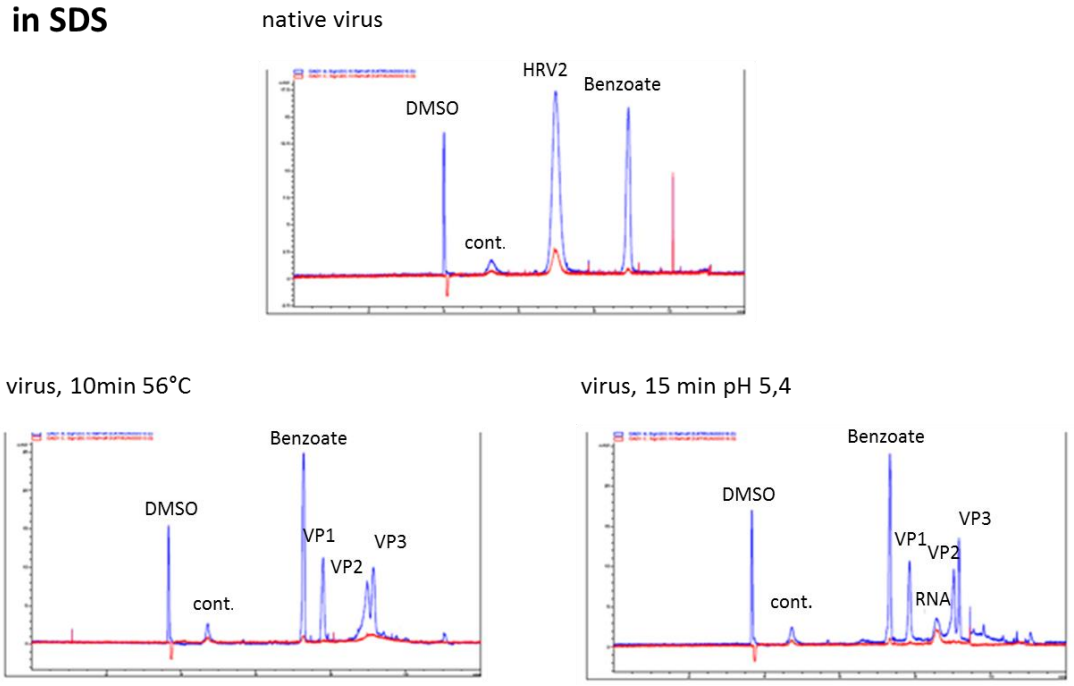


Figure 40: untreated, heated and acidified samples analyzed with CE, SB and BGE containing SDS

Virus samples analyzed on an Agilent 3D CE; UV-Vis-detection. Samples were acidified (15 min pH 5.4 in NaAc, 34°C, reneutralized with borate buffer, 100mM, pH 8.3) or heat denatured (10 min heated to 56°C in borate buffer, 100mM, pH 8.3), untreated virus is suspended in borate buffer.
Heating as well as acidification destabilizes viral particles to an extent that they disintegrate into the individual viral proteins upon subjection to CE analysis in presence of SDS.
DMSO: neutral marker, benzoate: internal standard. Operator: Xavier Subirats
blue: 200nm, red: 260nm

When samples were analyzed in presence of SDS, native virus showed two peaks for intact HRV2 virions and for a contaminant (cont) present in all HRV2 preparations. Heated as well as acidified samples did not show a peak corresponding to native virus, but several peaks depicting the individual viral proteins and –in the case of the acidified sample- the RNA (Figure 40). Heating as well as acidification destabilized viral particles to an extent that they fell apart upon subjection to CE analysis in presence of SDS. In presence of Thesit native virus (plus the contaminant) shows one peak with both 260nm and 200nm absorbance (Figure 41). The contaminant cannot be separated from native virus when the detergent Thesit is added. The heated sample shows a peak with absorbance at 200nm but without absorbance at 260nm,

most probably representing empty 80S particles. The association of RNA with proteins in heated samples is not observed when the sample is analyzed by CE. Acidified virus migrates as a broad peak. EtBr bands visualized in agarose gel electrophoresis also showed rather a smear than a band if the sample was acidified without addition of RNase A, this is in accordance with the broad peak of in CE.

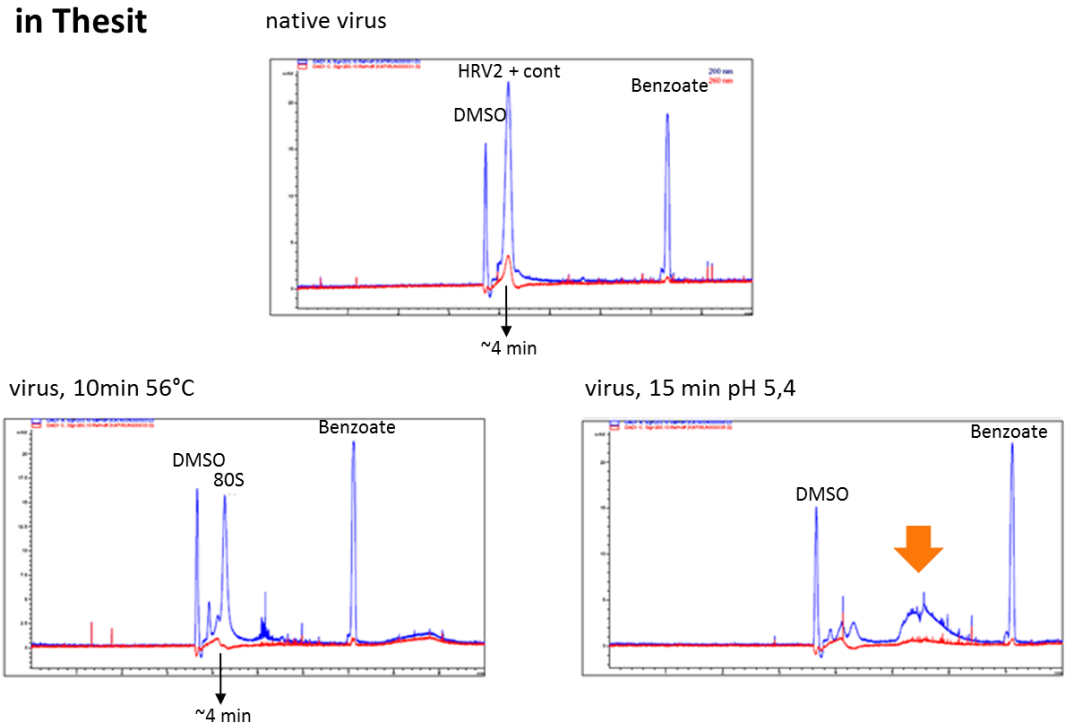


Figure 41: untreated, heated and acidified samples analyzed with CE, SB and BGE containing Thesit

Samples are the same as in Figure 40, analyzed with the same instrument, only the detergent is different. Native virus shows one peak with both 260nm and 200nm absorbance. Native virus cannot be separated from the contaminant in the presence of Thesit. The heated sample shows a peak with absorbance at 200nm but without absorbance at 260nm, most probably representing empty 80S particles. Acidified virus migrates as a broad peak. Native and empty virus migrate with a similar retention time.
DMSO: neutral marker, benzoate: internal standard. Operator: Xavier Subirats
blue: 200nm, red: 260nm

Samples were analyzed immediately after preparation and at time points 20min/ 40min/ and 60min after preparation. During this time period the samples were kept in the tray of the CE instrument at ~28°C. The acidified sample analyzed in presence of Thesit is quite interesting. In contrast to untreated virus and temperature triggered virus (other time points not shown), the virus species in the acidified sample changes over time- a broad peak changes into a sharp peak with absorbance at both 200nm as well as 260nm (Figure 42). This peak migrates dissimilarly to the peak obtained from native virions. According to the retention time, most probably this peak is derived from 135S particles, which have lost VP4, but still contain RNA. Detection of 135S particles in the acidified sample indicates that protection from RNase A digestion is rather due to insufficient triggering of release than to association with a specific protein forming RNPs.

**acidified samples, in Thesit**

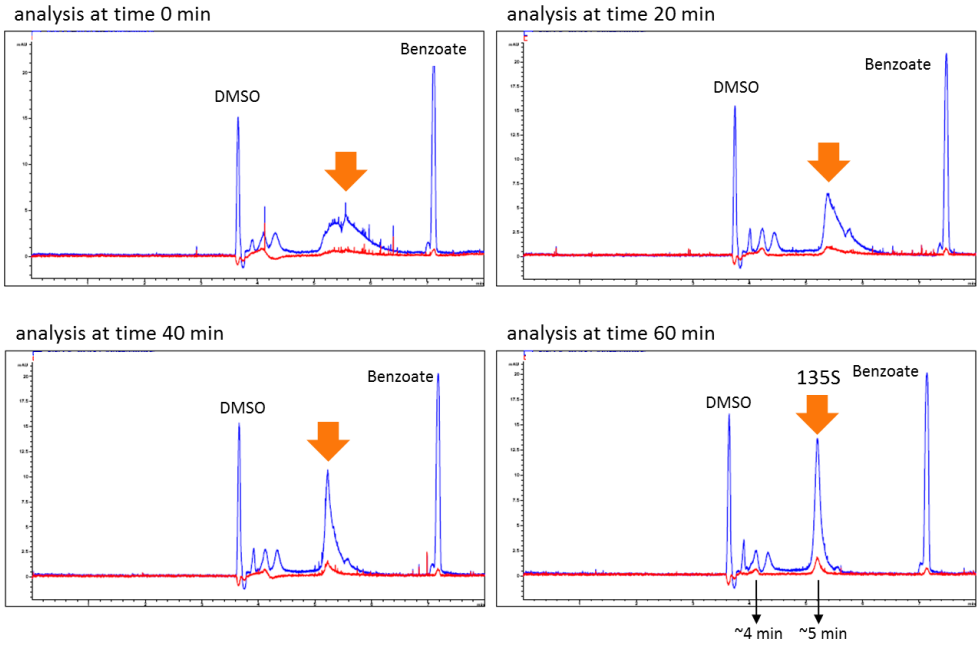


Figure 42: acidified samples, analyzed in Thesit at different time points

Acidified samples (preparation and analysis see Figure 41) were analyzed immediately after preparation and at time points 20min/ 40min/ and 60min after preparation. During this time period the samples were kept in the tray of the CE instrument at ~28°C. The broad peak changes into a sharp peak with absorbance at both 200nm as well as 260nm which migrates with a retention time of about 5 min, native virus migrates at a retention time of about 4 min.

#### 4.2.2.4 Dilution has no effect on uncoating upon acidification

Lonberg-Holm & Yin noticed, that acidification of more concentrated samples yields exclusively 135S particles, whereas acidification of diluted samples results in conversion to both 135S particles as well as 80S particles (*Lonberg-Holm & Yin, 1973*). The effect of virus concentration on the species of subviral particle was confirmed by Victor Weiss using CE. If virus stock is diluted 3:4 in 100mM boric acid prior to incubation at 56°C for 10 min preferentially 135S particles are formed, if virus stock is diluted 1:2 prior to heat denaturation, mainly 80S particles are formed. Interestingly, dilution of virus stocks with different initial virus concentration showed that formation of empty particles is rather due to the level of dilution than to the concentration of virus. Thus, it was hypothesized, that the viral preparations contain a component that stabilizes the native virus at higher concentrations but is ineffective when diluted (*Weiss et al., 2012*). Moreover, cations may have a stabilizing effect on the viral capsid. Zhao et al. indicated that complexation of divalent cations may regulate virus stability and uncoating (*Zhao et al., 1997*).

Up to this moment, virus stock was diluted 3:7 into 50mM sodium acetate pH 5.2 for acidification. To exclude stabilizing effects of a high salt concentration, virus was either diluted 1:5 in the solution virus stocks are kept in (50mM borate buffer, pH 7.4) or in nuclease- free water ($H_2O_{NF}$) prior to acidification. The minimum volumes of NaAc (50mM pH 5.2) and borate buffer (100mM pH 8.3) required for acidification to pH 5.2 (virus diluted in water) or pH 5.4 (virus diluted in borate buffer) and for reneutralization to pH 7.4 were added. Further, the

incubation temperature during acidification was raised from 34°C to 37°C to generate conditions more similar to human body temperature. Following acidification and reneutralization an aliquot of each sample was treated with RNase A, to see if dilution shifted the equilibrium towards formation of 80S particles and naked RNA. Samples were applied to an agarose gel without purification. Dilution of virus samples prior to acidification had no effect on formation of 135S particles. Regardless if virus stock was diluted in borate buffer of water, RNA "released" from HRV2 is RNase resistant (Figure 43). Samples shown in the left and the right gel picture belong to the same set of samples; aliquots for treatment with RNase were drawn after reneutralization; samples that were not subjected to RNase treatment were kept on ice. Untreated virus is visible as a band that migrates quite distinct from bands obtained from triggered samples, indicating that EtBr can enter the capsid, and "shine through the capsid". There are no bands perceptible in lanes where acidified virus with no further treatment was applied, whilst samples that were exposed to RNase A show very sharp and bright RNA bands. Probably incubation with RNase A enhances homogenization of an initially inhomogeneous population of 135S particles.

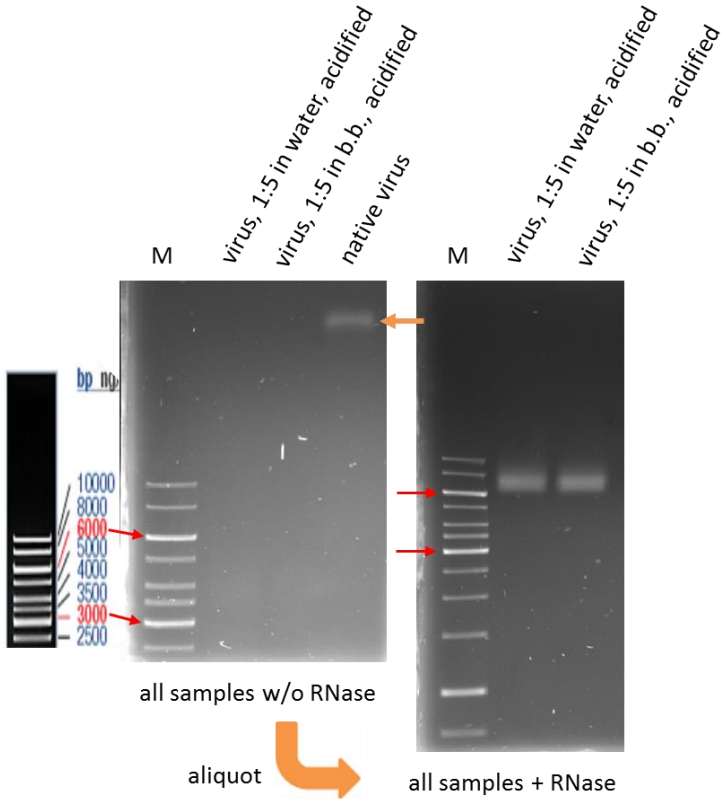


Figure 43: testing the effect of concentration on formation of 135S or 80S particles upon acidification

Virus stock (~2mg/ml) was diluted 1:5 in borate buffer (50mM, pH 7.4) or nuclease- free water ($H_2O_{NF}$). The minimum volume required for acidification to pH 5.2 (virus diluted in $H_2O_{NF}$) or pH 5.4 (virus diluted in b.b) was added. Samples were incubated at 37°C for 15 min and reneutralized by addition of borate buffer. Samples were split, and one aliquot each was incubated for further 20 minutes at 37°C along with RNaseA (~0.1mg/ml). Even though diluted, virus is still converted mainly to the putative 135S particles- following acidification RNA is still resistant to RNase A digestion. It is peculiar that the putative 135S particle is migrating at exactly 7kb, the length of the full length HRV2 genome.
i.v.t. RNA: *in vitro* transcribed HRV2 RNA in $H_2O_{NF}$
M: Fermentas 1kb DNA Ladder #SM0311, gel: 1% agarose, 0.1% DEPC, 80V, 1h

#### 4.2.2.5 RNase A has an accelerating effect on homogenization of the 135S population

Reproducibly, samples that have been treated with RNase following acidification show sharper and clearer bands than samples, which have been triggered for release without further RNase treatment (see e.g. Figure 38). Capillary electrophoresis showed that acidified samples evolve over time; a broad peak condenses into a sharp, distinct peak. Probably acidification generates an initially heterogenic population of converting particles that finally, when all particles finished conversion form a homogenous population of 135S particles. The appearance of much brighter and sharper bands of the sample treated with RNase could be either caused by the action of RNase A, somehow accelerating homogenization of the sample or by the prolonged incubation at 37°C. Therefore, in one set of samples the incubation time at pH 5.2 and 37°C was doubled, and aliquots were subjected to either RNase or DNase treatment. DNase was added to see if the condensing effect is specifically caused by RNase. Formation of sharp bands interpreted as homogenous population of 135S particles clearly is due to presence of RNase A and not to the prolonged incubation at 37°C. Exclusively samples treated with RNase show very well discernible bands (see Figure 44); Comparison of samples that have been acidified for 15 or 30 minutes shows that conversion is complete after 15 minutes; both samples show a smear of the same intensity.

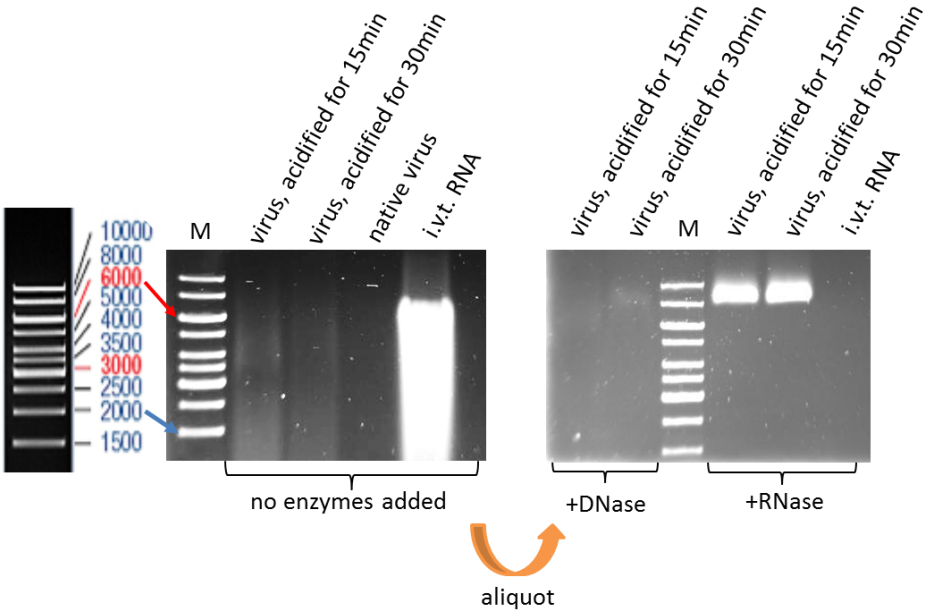


Figure 44: Testing the effect of RNase A and prolonged incubation at 37°C on homogenization of the 135S population

Virus stock (~2mg/ml) was diluted 1:5 in $H_2O_{NF}$ and acidified by adding the minimum volume of NaAc (50mM, pH 5.2) required for acidification to pH 5.2. The sample was incubated at 37°C for 15 or 30 min. Then the sample was split to four aliquots. One aliquot was reneutralized and kept on ice whilst the other samples were incubated for further 15 minutes at 37°C- one sample contained RNase A (final c ~0.1mg/ml) and another contained DNase (final c ~0.1u/µl). Following reneutralization, loading buffer was added and the samples were analyzed in an agarose gel. Solely samples that were incubated along with RNase A show sharp, bright bands.
native virus: 1µl virus stock was filled up with borate buffer (50mM, pH 7.4, DEPC treated) to a final volume of 10µl, and kept on ice during acidification and digestion of other samples.
i.v.t. RNA: *in vitro* transcribed HRV2 RNA
M: Fermentas 1kb DNA Ladder #SM0311, gel: 1% agarose, 0.1% DEPC, 80V, 40-70min

To further characterize the effect of acidification and RNase digestion on diluted virus samples, aliquots were analyzed by Xavier Subirats in CE. HRV2 stock was diluted 1:5 in water and acidified for 15min at 37°C. Following re-neutralization one aliquot was treated with RNase A, the other aliquot was kept on ice. Samples were split, half of the samples was applied to an agarose gel, half of the samples was analyzed by CE. The detergent Thesit was added, to enable detection of 135S particles. Samples were injected directly after preparation and after incubation at 4°C over night.

In gel electrophoresis (GE) only the sample that was incubated along with RNase A shows a well-defined EtBr stained band (see Figure 45). Plain *in vitro* transcribed RNA (left to the marker) is already degraded to some extent; nevertheless it was included to illustrate activity of RNase A (right to the marker). CE directly after preparation shows a broad peak for the sample that was solely acidified and a sharp peak for the sample that was additionally treated with RNase A. The sharp peak most probably represents 135S particles, as it shows absorbance at both 200nm and 260nm and migrates dissimilarly from the native particle. Presumably the heterogeneous population obtained by acidification is dispersed in the agarose gel, and therefore below the detection limit of EtBr staining. In both samples residual native particles and/ or the contaminant is visible. Upon incubation over night, the broad peak of the solely acidified sample evolves into a well-defined peak identical to the peak obtained by RNase A treatment. The RNase A treated sample does not change over night. Seemingly RNase A accelerates homogenization of the putative 135S population.

Curiously, the sample that was treated with RNase A shows 5 distinct peaks due to 200nm and 260nm absorbance with no additional absorbance at 200nm- seemingly this is RNA with no apparent protein content. Given, that RNase is present it is unclear if those peaks represent plain RNA.

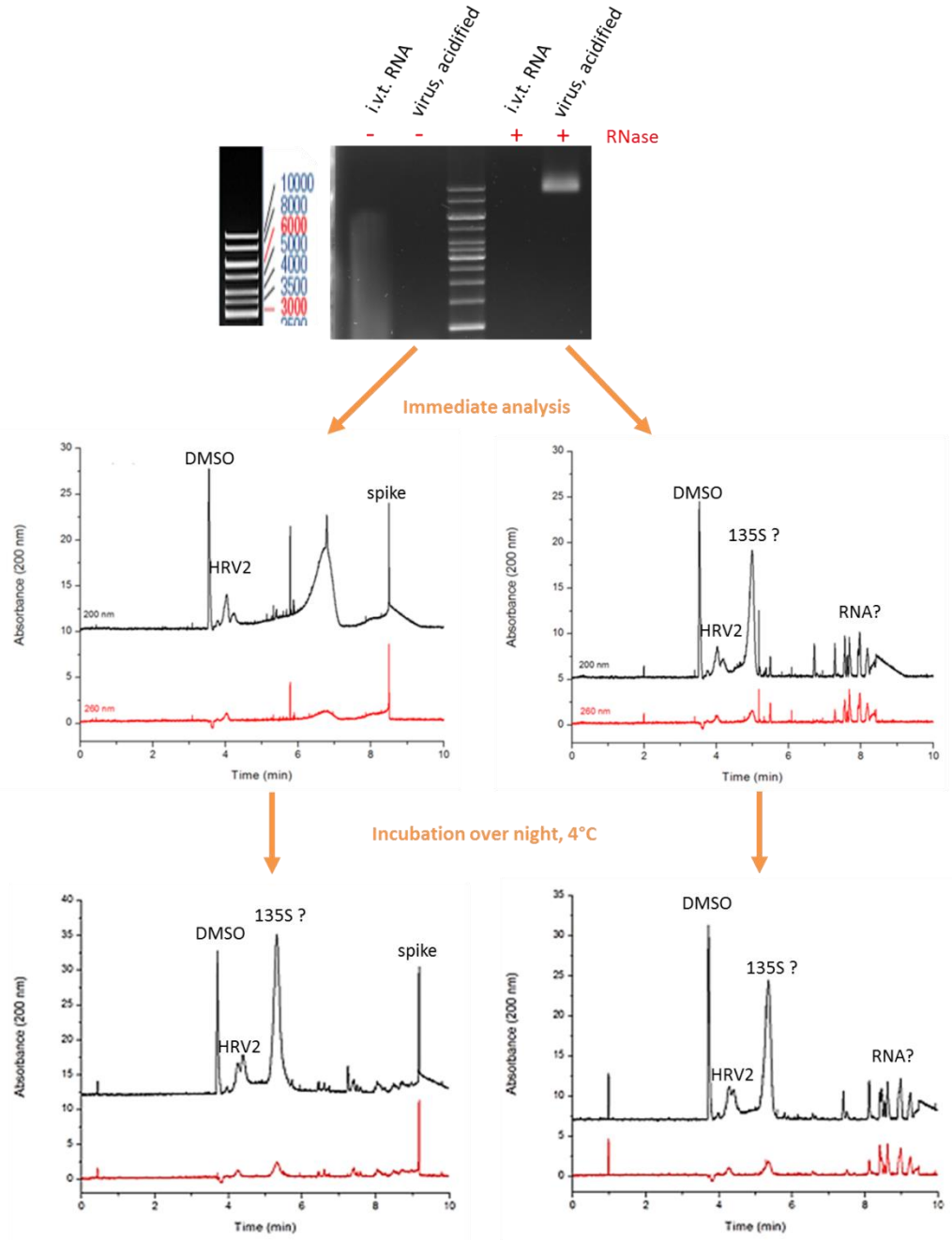


Figure 45: RNase A accelerates homogenization of the putative 135S population

Virus stock (~2mg/ml) was diluted 1:5 in $H_2O_{NF}$. Samples were acidified, one aliquot was digested with RNase A (~0.1mg/ml). Half of each sample was applied to an agarose gel; the other half was analyzed by CE. Analysis by CE was performed immediately after preparation and after incubation at 4°C over night. In GE, the RNase treated sample shows a defined band, whereas the non-digested sample does not show a band. In CE, the acidified sample without RNase shows a broad peak with absorbance at both 200nm and 260nm whereas the sample that was treated with RNase A shows a sharp peak most probably representing 135S particles. Both samples contain residual native HRV2. Following incubation over night, the RNase treated sample remains unaltered, whereas the peak in the sample that was solely acidified evolved into a sharp peak migrating identical to the putative 135S particle.
Gel electrophoresis: i.v.t. RNA: *in vitro* transcribed HRV2 RNA, M: Fermentas 1kb DNA Ladder #SM0311, gel: 1% agarose, 0.1% DEPC, 80V, 40min
CE: DMSO: neutral marker. Operator: Xavier Subirats, blue: 200nm, red: 260nm

#### 4.2.2.6 Analysis of the protein content of bands stained by both EtBr and Coomassie brilliant blue.

As shown by Coomassie staining of agarose gels used to visualize RNA “released” from the virus, protein(s) are not separated from RNA during gel electrophoresis (see Figure 36, Figure 37, Figure 39). Bands containing EtBr- stained material were excised from the agarose gels and the protein(s) associated with RNA were characterized by SDS- polyacrylamide gel electrophoresis (PAGE) and western blotting. Gel slices were heated in reducing sample buffer and loaded onto a 15% acrylamide gel. Following separation, proteins were transferred to a nitrocellulose membrane. Viral proteins were visualized using rabbit αHRV2 serum and HRP-conjugated α rabbit antibody. An EtBr band obtained from native virus as well as freshly thawed HRV2 were for comparison. No bands could be cut out for acidified samples without RNase incubation, because for those samples distinct bands could not be obtained. Following Western blotting, the polyacrylamide gel was stained with coomassie brilliant blue.

EtBr stained bands of acidified and RNase treated samples contain proteins of ~37, 25 and 20kD complying with VP1 (32kD) VP2 (29kD) and VP3 (26kD) (*Rossmann et al., 1985*), whereas the sample of native virus and freshly thawed virus show an additional band migrating at < 10kb matching VP4 with a size of 7.4kD. VP3 is only perceptible in the coomassie stained gel, whilst the <10kD protein is only visible on the X-ray film. Seemingly, incubation at low pH, even if the samples were diluted 1:5 beforehand, does not trigger complete uncoating of the HRV2 RNA, but transformation to 135S particles signified by loss of VP4 (*Korant et al., 1972*). Therefore, the idea that a specific protein interacts with the RNA in terms of RNP formation can be eliminated.

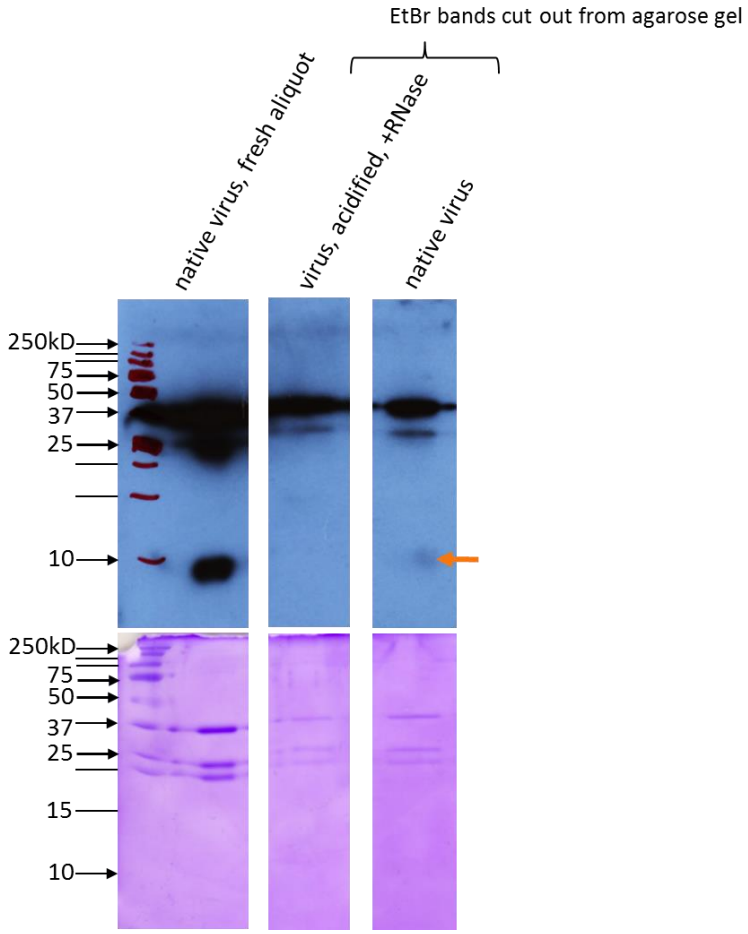


Figure 46: Analyzing the protein content of EtBr stained bands excised from agarose gel following acidification

Samples were prepared as outlined in Figure 43 and loaded to 1% agarose, 0.1% DEPC gels. Solely samples that were incubated along with RNase A and sometimes native virus showed sharp, bright bands that were cut out. Gel slices were heated with reducing sample buffer and loaded to a 15% polyacrylamide gel. Following separation, proteins were transferred to a PVDF membrane. Viral proteins were visualized using rabbit αHRV2 serum and HRP-conjugated α rabbit antibody. The polyacrylamide gel was stained with Coomassie brilliant blue subsequent to western blotting.
Rabbit αHRV2 antibodies visualize VP1, 2 and 4. Bands that were cut out from the agarose gel following acidification and RNase A digestion contain VP1, 2 and 3 but not VP4. Native virus shows VP4 as well (orange arrow).
Upper picture: chemiluminescence catalyzed by horse radish peroxidase coupled to the 2$^{nd}$ antibody, detected on an Agfa X-ray film, exposure: 5 seconds
Lower picture: the polyacrylamide gel, coomassie stained.
Gel: 15% polyacrylamide, 25mA, 300V
Marker: BIORAD precision plus protein standard all blue #161-0373.
Blotting conditions: 400mA, ~20V, 90 min

#### 4.2.2.7 Is part of the HRV2 genome sticking out of the 135S particle?

When samples containing heated virus were run in an agarose gel containing SDS instead of DEPC, RNA in RNase treated samples migrated all of a sudden with an apparent Mr corresponding to 4kb whilst RNA of solely heated virus migrated at a size corresponding to the full length RNA (not shown). Acidified, RNase A treated samples analyzed in DEPC-treated agarose gels showed bands migrating at 7kb (e.g. Figure 43). This change of migration behavior was interpreted as being founded by SDS, denaturing the 135S particle, thus ripping off the proteins from the RNA during electrophoresis. Further, it was hypothesized that in the 135S particle part of the RNA is accessible to RNase, ready for egress or even sticking out of the capsid.

To test this hypothesis, it was checked if one end- or both ends of the HRV2 genome is lost if the 135S particle is incubated along with RNase A using reverse transcription and PCR. HRV2 was diluted 1:5 and acidified. Following re-neutralization, the sample was split and one of the samples was incubated along with RNase A. Since RNase A is an extraordinarily resistant enzyme (*Raines, 1998*) and simple phenol /chloroform extraction proved to be insufficient to protect RNA from added RNase (results not shown) for purification of RNA, two protocols for extraction of RNA from tissue culture cells were adapted and tested. RNA was purified in half of the samples by the guanidine method for RNA extraction and in the other half by phenol/ chloroform/ SDS precipitation. Both extraction methods were adequate to inhibit RNase A, only results obtained from phenol/ chloroform/ SDS precipitated samples are shown. Extracted RNA was divided into two batches, and transcribed to cDNA. In one batch reverse transcription was primed by a primer binding 468nt apart from the 5´end, in the other batch reverse transcription was primed by a primer binding ~70nt proximal to the 3´end. Presence or absence of the 5´and 3´end was monitored by PCR. The primer pair HRV2_5´ab125 + HRV2_5´bis468, amplifies a ~340bp sequence close to the 5´end, the primer pair HRV2_7A (starting from nt 6126) + PR5 (ending with nt 6325), yields a 199bp product proximal to the 3´end. Formation of 135S particles was verified by applying the samples after acidification to an agarose gel. The sample where RNase A digestion was omitted shows a faint band whereas the sample that was incubated along with RNase A shows a sharp and bright band (Figure 47a). Following RNA extraction and reverse transcription an aliquot of each sample was analyzed in an agarose gel, but the concentration of both RNA and cDNA was too low to be visualized by EtBr (result not shown). PCR of the 5´proximal sequence yielded products, regardless if virus was incubated along with RNase A or not. PCR products derived from the 3´end were obtained exclusively for the undigested sample. The 3´end of the HRV2 genome is lost upon RNase A digestion.

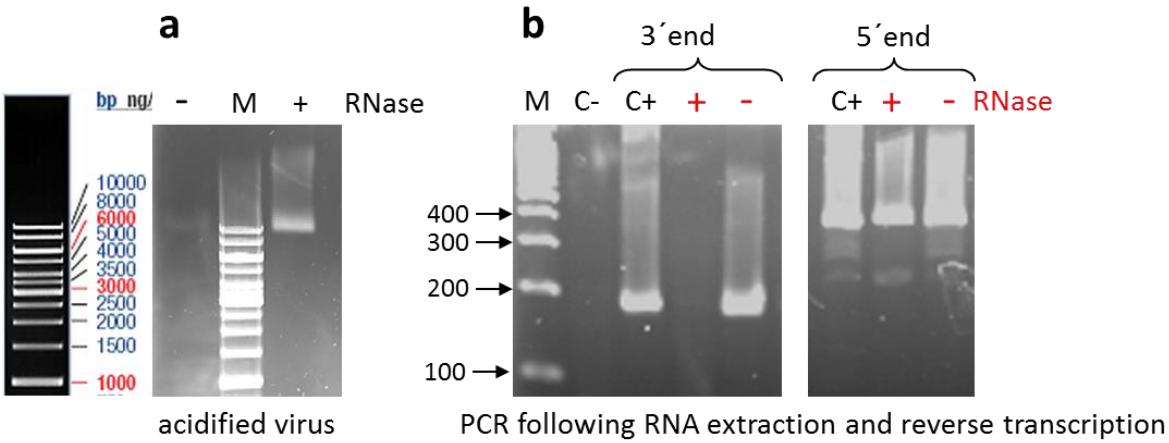


Figure 47: In the 135S particle, the 3´ end is accessible to RNase A digestion whereas the 5´ end is protected

a) Virus stock (~2mg/ml) was diluted 1:5 in $H_2O_{NF}$. Following acidification and reneutralization the sample was split, to one aliquot RNase A (c ~0.1mg/ml) was added, and both samples were incubated for further 20 minutes at 37°C. An aliquot of both samples was analyzed in an agarose gel.

b) RNA was purified and transcribed to cDNA using one primer binding near the 3´ end and another primer binding near the 5´end. Presence of the 3´ end and the 5´ end cDNA was checked by PCR. The primer pair binding near the 3´amplifies a 199bp product, the primer pair binding near the 5´ end amplifies a ~340bp product. PCR of the 5´ end sequence yields products, regardless if the 135S particle was incubated along with RNase or not. PCR of the 3´ sequence yields a product in the sample that was solely acidified, but no product in the sample that was retrieved from acidified virus incubated along with RNase A. The PCR from cDNA derived from by phenol/ chloroform/ SDS precipitation is shown.

C+: positive control, PCR using the plasmid HRV2_bluescript as template, linearized with *Kpn*I
C-: negative control, PCR without template
a: M: Fermentas 1kb DNA Ladder #SM0311, gel: 0,7% agarose, 0.1% DEPC, 80V, 40 min
b: M: new England Biolabs, quick loadTM 100bp DNA ladder #NO467G, gel: 2% agarose, 80V, 40 min

# 5 Discussion

Two methods were applied to tackling the question which end of the RNA genome leaves the capsid first: Selective 2´-Hydroxyl Acylation and Primer Extension (SHAPE) and Formaldehyde crosslinking followed by RNase A digestion.

## 5.1 Ad SHAPE

In SHAPE, an electrophile reagent reacts with the 2´hydroxyl group of RNA to form an ester, which is an obstacle to reverse transcriptase and causes it to stop. It was anticipated that the extruding end of the HRV genome is modified preferentially because the RNA that lags behind is protected by the capsid. To minimize diffusion of the reagent into the capsid, a fast reacting chemical was chosen. BzCN is rapidly inactivated by hydrolysis, and therefore RNA that is easily accessible is far more likely to be modified than RNA which is protected by a barrier.

### 5.1.1 Software

Resolution of cDNA fragments was outsourced to VBC-Biotech Service GmbH (VBC); VBC offers run-only service, leaving analysis of the data to the customer. A capillary electrophoresis instrument generates raw data, which plots relative fluorescence units for each data point. Analysis software then converts raw data into information about the reactivity of each nucleotide (ShapeFinder) or into information about the concentration and length of the fragments (PeakScanner, STRand). The main functions of data collection software and data analysis software are outlined in Figure 48.

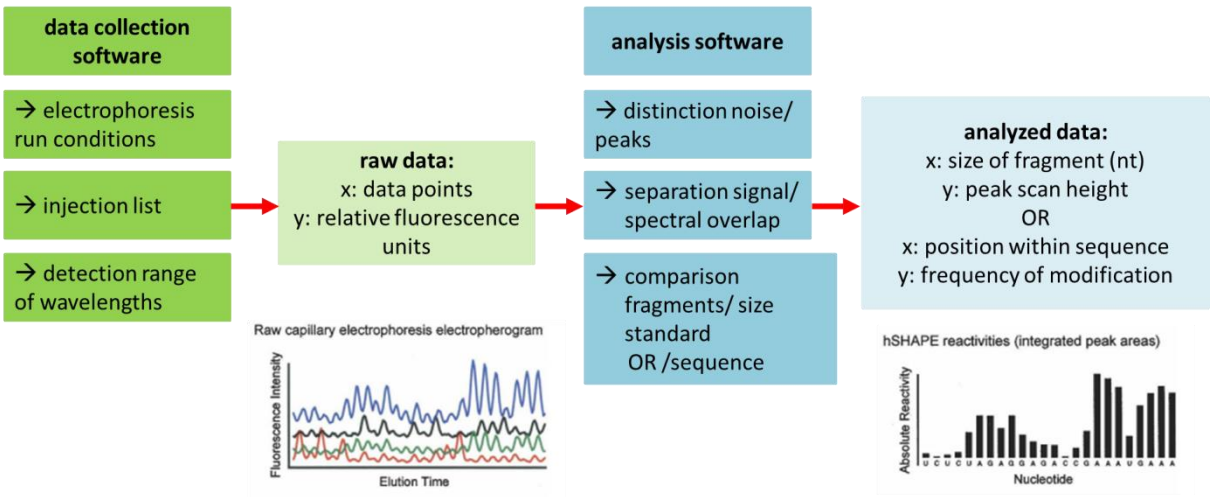


Figure 48: Outline of the main functions of data collection software and data analysis software

The data collection software operates electrophoresis run conditions, injection lists and detection range of wavelengths. The output of a sequencing instrument is raw data. Analysis software performs three primary functions: It differentiates between noise and peaks based on a threshold specified by the user, it separates actual signals from spectral overlap and it determines the size of the cDNA fragments or the position within a sequence.

VBC possessed an ABI Prism 310 Genetic Analyzer capable of performing fragment length analysis, a method used in genotyping. Analysis on this instrument requires addition of a specific size standard. ShapeFinder, the software designed for SHAPE analysis could not be

used to analyze the raw data, since it requires dideoxy sequencing reactions in order to map the cDNA fragments to the sequence of the input RNA (*Vasa et al., 2008*). Since it was not the goal to asses folding of the HRV2 genome accurately, but to rather find out which part of the RNA is modified (ergo solvent accessible), and which end is not (because of protection by the capsid) we first assessed fragment length analysis. There were two analysis programs freely available that were tested: Peak Scanner and STRand.

#### 5.1.1.1 Analysis of raw data using Peak Scanner™

Applied Biosystems offers the program Peak Scanner™ for download[19]. This free software was designed for DNA fragment length analysis using an ABI Prism 310 Genetic Analyzer. However, because of the presence of off-scale peaks Peak Scanner could not even open the files. Details on off-scale peaks are discussed below, in 5.1.2.4. For these reasons this software was found to be inadequate for the desired type of analysis.

#### 5.1.1.2 Analysis of raw data using STRand

STRand is an open-source program, provided by Davis' Veterinary Genetics Lab at the University of California[20]. It was designed for analysis of DNA fragment length polymorphism samples. This software was configured for analyzing files from Applied Biosystems instruments, including the ABI Prism 310 Genetic Analyzer. STRand could visualize all raw data obtained from VBC without exception. Unfortunately, analysis of raw data did malfunction. Evidence for dysfunctional data analysis is listed below, in Figure 49.

### 5.1.2 Problem analysis using a short RNA

An *in vitro* transcribed fragment of the HRV2 genome, 468nt in length was chosen for setting up conditions for modification and testing analysis software. Using this short RNA, it was possible to obtain reproducible fragment patterns for the modified samples, clearly differing from the no-reagent-control (Figure 29, Figure 30). However, upon closer examination, electropherograms showed

- bleed-through peaks
- baseline off-set
- diverging fluorescent intensity of different dyes and
- signal decay

Those phenomena are characteristics of raw data, indicating that STRand could not analyze the files obtained by VBC (*Vasa et al., 2008*). Further, vast peaks at the start of the electropherograms interfered with the recognition of the size standard (discussed in 5.1.2.4).

[19] http://www.appliedbiosystems.com/absite/us/en/home/support/software-community/free-ab-software.html May 2013

[20] http://www.vgl.ucdavis.edu/informatics/strand.php , May 2013 , Version 2.2.30

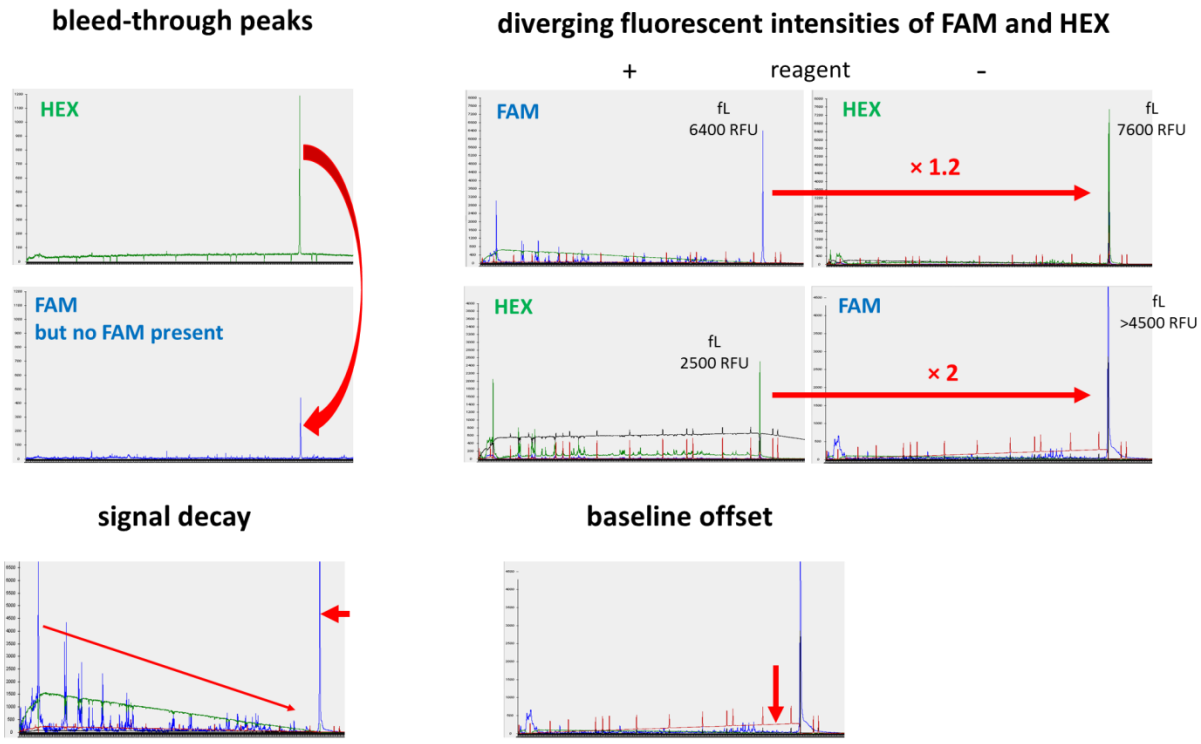


Figure 49: Indications for problems with the data analysis

Bleed-through peaks: both pictures show the same sample, containing only one fluorophore- HEX. The upper picture displays the HEX channel, supposedly showing a peak. The lower picture displays the FAM channel. Although in this sample no FAM was present, the FAM-channel shows a peak at exactly the same position as the HEX peak. It is a bleed through peak caused by spectral overlap.
Diverging fluorescent intensities of FAM and HEX: Since the reverse transcriptase stops elongation at sites of modification, untreated RNA is converted to cDNA to a far higher extent as modified RNA. When the (+) reagent sample is labeled with FAM and the no-reagent-sample is labeled with HEX, the intensities of the full length peaks are comparable, if the fluorophores are switched, the intensity of the full length peak in the no-reagent-control is about double. This indicates, that diverging emission intensities of FAM and HEX are not corrected.
Signal decay: In all (+) reagent traces, peaks at the start of the trace are far more intense than those at the end. Presence of a full length peak contraindicates degradation or excess modifications of RNA molecules. *Vasa et al.* (*2008*) describe signal decay of raw data such that peaks at the start of a trace are four times more intense than those towards the end. This is comparable with signal decay in the obtained traces.
Baseline offset: The size standard, displayed in red, shows an elevated baseline. This is also a sign of spectral overlap.

#### 5.1.2.1 Spectral overlap

Electropherograms showed bleed through peaks and often an elevated interpeak baseline (Figure 49). Both phenomena are a sign of poor correction of dye spectral overlap during data analysis. Bleed through peaks are caused by too little subtraction whereas an elevated interpeak baseline is caused by too much subtraction (*Applied Biosystems, 2000*).

In a multifluor run, when several dyes are combined in one sample, the dyes are chosen in a way that their excitation and emission wavelength are minimally interfering. Up to four different dyes are recommended to by combined, certain combinations are referred to as dye set. The CE instrument records fluorescence close to the emission maxima of the respective dyes, but with maximum possible separation among the emission maxima of different dyes.

Still, there is some overlap between wavelengths, for example FAM emission interferes with HEX detection. To eliminate this residual spectral overlap in order to produce peaks that can be attributed to one fluorescent dye, a computer algorithm- the matrix calculation- is utilized (outlined in Figure 50).

The matrix calculation is part of the analysis software, and is based on a matrix file. STRand automatically applies the respective matrix file to the raw data when the correct instrument and dye set is selected. However, deconvolution of spectral overlap was insufficient. It is mentioned in the ABI Prism 310 Genetic Reference Guide, that matrix files are susceptible to changes in run conditions. The emission spectra of the dyes vary with the physical environment, such as run temperature, the pH or polymer type and concentration. If run conditions change, the matrix file needs to be recreated (*Applied Biosystems, 2000*). Presumably, the conditions chosen by the Davis' Veterinary Genetics Lab at the University of California differ from the conditions chosen by VBC biotech; therefore it would have been necessary to recreate the matrix file. Recreation of the matrix is a calibration step, in which each relevant dye matrix standard is run separately (*Applied Biosystems, 2012*). We neither had access to the instrument nor to the valid matrix file.

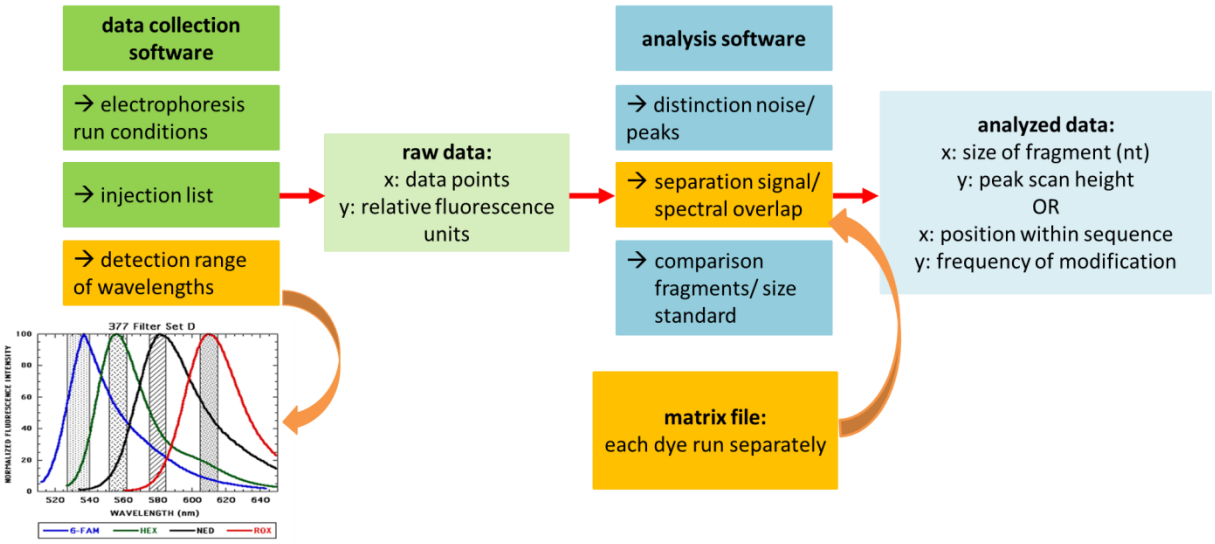


Figure 50: Contribution of data collection software and analysis software to elimination of spectral overlap

The data collection software controls detection range of wavelengths for a given dye set. Depending on the combination of dyes, the detector records light intensity in different regions of the spectrum (*Butler et al., 2004*). Those "windows" are chosen in a way, that they record wavelength close to the emission maxima of the respective dye, but with maximum possible separation among the emission maxima of different dyes (shaded areas in the graph). Still, there is some overlap between wavelengths, for example FAM emission interferes with HEX detection.
Separation of actual signals from residual spectral overlap is performed by the analysis software; the so called matrix calculation is based on a matrix file. The matrix file is generated by analyzing each dye relevant for a given dye set separately.
The graph was taken from the ABI PRISM 310 reference guide, *Applied Biosystems, 2000*

### 5.1.2.2 No correction for different emission intensity

Upon excitement by the laser of the ABI PRISM 310 Genetic Analyzer, different fluorophores show different intensity of fluorescence. Compared to FAM, the intensity of emitted

fluorescence by ROX is about eight times weaker. HEX also shows lower emission intensity than FAM (*Applied Biosystems, 2000*). It was tested if deviation in signal strength of the different dyes is corrected by STRand (example shown in Figure 49). Apparently signal intensity is not converted to the actual amount of dye. Therefore is not legitimate to deduce the degree of modification from signal intensity. Comparison of peaks in the (+) and (-) reagent trace is misleading if the samples are labeled with different dyes.

#### 5.1.2.3 Signal decay

In a raw trace obtained from a SHAPE experiment, peak intensities decline with increasing read length (example given in Figure 49). Vasa et al. describe signal decay such that peaks at the start of a trace are four times more intense as those towards the end. This is due to two effects, specifically encountered in SHAPE analysis. First, reverse transcriptase is not perfectly processive; the probability of adding an additional nucleotide to a cDNA is less than 1. Second, although the (+) reagent reaction is designed the way that, statistically, every RNA molecule is modified once, some RNAs react more than once. Reverse transcription stops at the first modification, therefore short RNAs are favored (*Vasa et al., 2008*). Both effects are not an issue in fragment length analysis, since the starting material is DNA. Therefore, neither STRand nor PeakScanner provide tools to correct for signal decay.

#### 5.1.2.4 Off-scale peaks

All electropherograms contained an enormous peak at the start of the traces (Figure 20, Figure 23 from results). To analyze the nature of those initial peaks, blanks and different ratios of primer: RNA were analyzed. Presence of an intense peak in the blank indicated that it is partially caused by the system and/ or by contaminations. Reduction of the amount of primer diminished, but did not eliminate the off-scale peak. Apart from contaminations and unbound primer, short fragments caused by pausing of the reverse transcriptase enzyme during the initiation process are part of the composition of this peak (*Wilkinson et al., 2006*).

Those off- scale peaks most certainly were the reason why the program Peak Scanner could not be used to analyze the raw data. Many files could not even be displayed. Therefore there was no way of removing primer peaks from the analysis range. Although it was possible to exclude initial peaks (i.e. to trim a trace) with the program STRand, the tail of the initial peaks most probably interfered with size standard recognition. If the initial peak migrates too close to the first size standard peak, the analysis software mistakes the spectral overlap for the first size standard peak, therefore the size-calling curve is inaccurate or cannot be calculated at all (*Applied Biosystems, 2000*). In Figure 51 electropherograms of samples containing different amounts of primer, a blank and a trimmed trace are shown. Even in the blank, where no primer is present, the tail of the initial peak comes very close to the first size standard peak.

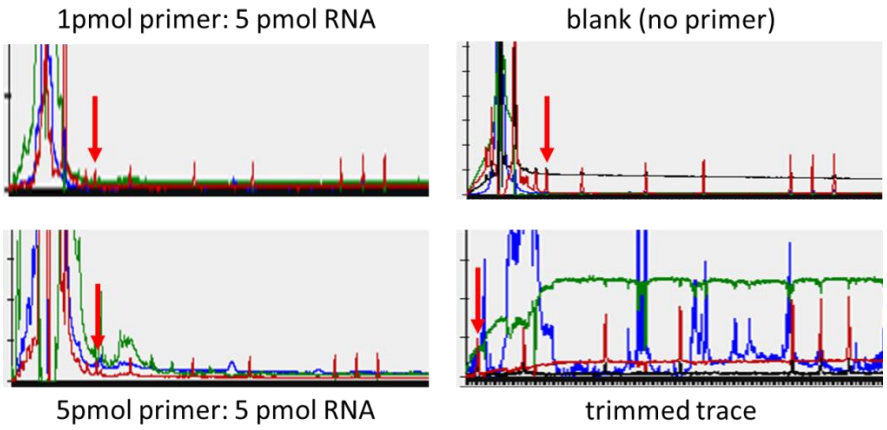


Figure 51: The initial peak interferes with size-calling

The first size standard peak is indicated with the red arrow. The vast peak at the onset of the trace migrates close to the initial size standard peak, even when 5× less primer than template is used and in the blank. Probably the tail of this peak interferes with the detection of the first size standard. In the trimmed electropherogram, all fragments that are shorter than the first size standard peak were computationally removed; nevertheless size calling was not possible.

### 5.1.3 Alterations possibly enabling analysis by Peak Scanner or STRand

Wilkinson et al. reduce the amount of unbound primer (contributing to the off-scale peak) by adding 3´and 5´ flanking sequences that contain an optimized primer binding site to the RNA of interest (*Wilkinson et al., 2006*). Addition of flanking sequences would not have met the purpose of this study. Addition of flanking sequences might have influenced positioning of the genome within the capsid and/ or egress. When designing the primer that was chosen for cDNA synthesis, HRV2_5´bis468rev, it was focused on selecting a region in the HRV2 RNA that melts easily. In order to match this request, it was necessary to cut back on recommendations regarding GC-content and melting temperature[21], which might have led to an increase of unbound primer. However, in the context of the extensively folded HRV2 genome it was regarded as the best option.

Another possibility to overcome interference of the initial peak with size calling (STRand) or analysis per se (Peak Scanner) would be choosing another size standard. The shortest fragment of the GeneScan -500 ROX size standard is 35nt in length (*Applied Biosystems, 2002*). In total, there are 7 size standards recommended for analysis with the ABI PRISM® 310 Genetic Analyzer (*Applied Biosystems, 2000*). Two of them are labeled on both strands, and are therefore designed to determine size of double stranded DNA. The output of a SHAPE experiment is single stranded cDNA. Among the size standards suitable for sizing single stranded DNA GeneScan-400HD is the only one that starts with a fragment larger than 35nt. The shortest fragment of the GeneScan-400HD is 50nt in length; therefore, the initial off-scale peak might not interfere with detection of the first size standard peak (Figure 52). At the other hand, using this size standard, only fragments up to 400nt can be analyzed because collection

[21] Recommendations primer design: http://www.premierbiosoft.com/tech_notes/PCR_Primer_Design.html (June 2013)

of data stops after detection of the last size standard peak. This would cause further reduction of the analyzable regions of the HRV2 genome.

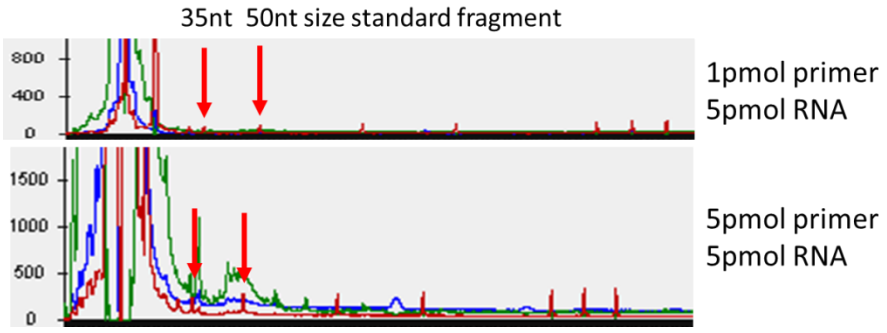


Figure 52: changing the size standard might improve size standard recognition

The off-scale peak composed of small fragments and contaminations migrates quite closely to the first size standard peak of the GeneScan-500 size standard, especially when equimolar amount of primer and template is used. Even if the initial peak is excluded, the tail of the peak might interfere with size standard recognition. The 50nt size standard fragment is further apart. Using a size standard that contains fragments no shorter than 50nt (GeneScan-400HD) size standard recognition could be improved. At the other hand, readout would be minimized to 400nt, in comparison to 500nt.

### 5.1.4 The solvent of BzCN might have an influence on RNA release

Angela Pickl-Herk monitored the effect of psoralen-crosslinking on RNA release via negative staining electron microscopy. She observed that DMSO has an effect on HRV2 RNA folding (data not shown). Both treatment with psoralen in DMSO and neat DMSO triggered rod-like appearance of RNA within the capsid (see **2.3.3**). The same effect was observed when virus was incubated in DMF. BzCN, the reagent used for modification of RNA, is solubilized in DMSO. If DMSO has an influence on folding of the HRV2 genome, it might as well affect egress of the genome and thereby impact on the results obtained via SHAPE analysis. If SHAPE analysis on HRV2 RNA will be pursued, the effect of DMSO on uncoating of HRV2 needs to be verified. If influence of DMSO on HRV2 RNA is confirmed, a non-interfering solvent for BzCN needs to be found.

### 5.1.5 Résumé

Performing DNA fragment length analysis on SHAPE samples was suboptimal. DNA fragment length analysis was designed for genotyping, such as amplified fragment length polymorphism (AFLP), microsatellite polymorphism genotyping and detection of loss of heterozygosity (LOH) (*Applied Biosystems, 2000*). All of those methods are based on amplification of genomic DNA and comparison of patterns/ length/ abundance of PCR products (*Jeffreys et al., 1985, Tautz, 1989, Croce CM., 1991, Vos et al. 1995*, *Canzian et al., 1996*). The major difference between fragment length analysis and SHAPE is the starting material. SHAPE acts on RNA, which is subjected to reverse transcription prior to analysis. In comparison to DNA polymerase, reverse transcriptase lacks proofreading activity and is more imprecise; features that are contributing to genetic variation of retroviruses (*reviewed in Svarovskaia et al., 2003*). At the other hand, in

the context of SHAPE analysis, diminished fidelity is contributing to signal decay. Further, short fragments caused by pausing of reverse transcriptase are not an issue when working on DNA.

In contrast to Peak Scanner or STRand, an off- scale peak at the beginning of a trace or an intense full length peak is not hindering analysis of raw data with ShapeFinder. Because sample peaks are not compared to size standard peaks but to a sequencing reaction, loosing peaks at the beginning or the end of the trace does not interfere with assignment of peaks. ShapeFinder provides tools for correction of all four characteristics of raw data obtained by a SHAPE experiment. Analysis software designed for fragment length analysis does not need to correct for signal decay, neither for presence of an intense peak of short fragments or an intense full length peak.

## 5.2 Ad halting egress and digesting protruding RNA

The second approach to identifying the exiting end of RNA in the uncoating process was to halt egress by formaldehyde crosslinking, digest the protruding part using bovine ribonuclease A and to characterize the remaining RNA.

### 5.2.1 Preliminary trials to halting egress by formaldehyde crosslinking

In preliminary test it was shown that

- RNase A as well as proteinase K is inhibited by formaldehyde, but addition of glycine sufficiently quenches the reaction to enable activity of the added enzymes.
- Proteinase K digestion followed by phenol-chloroform extraction is not adequate to retrieve RNA protected inside the viral shell after protruding sequences have been digested with RNase.
- Release of RNA from HRV2 in plain buffer solution is not complete

#### 5.2.1.1 The effect of formaldehyde on RNase A and proteinase K

If the crosslinking reaction is allowed to proceed during RNase A or proteinase K digestion, digestion by both RNase A and proteinase K is constrained. If the crosslinking reaction is quenched after 5 minutes by addition of saturated glycine in excess, RNase A and proteinase K activity is not inhibited. Hence, it is not necessary to remove formaldehyde by e.g. dialysis.

#### 5.2.1.2 Proteinase K and phenol-chloroform extraction do not inactivate RNase A

*Jackson et al.* (*1990*) compared different extraction methods to retrieve high quality DNA and RNA from formalin fixed samples and fresh tissue. Best protection from tissue-derived RNases was achieved by incubation with proteinase K for 1 h followed by phenol-chloroform extraction. However, when RNase A is added to the sample at the chosen concentration, digestion with proteinase K followed by phenol chloroform extraction was not sufficient to inactivate RNase A. Since proteinase K digests both RNase A as well as the capsid proteins, RNase gets access to the RNA during incubation with proteinase. Not even addition of proteinase K in excess protected the RNA from RNase A (data not shown). To obtain RNA from virus samples with added RNase, two protocols for extraction of RNA from tissue culture cells were adapted and tested. Using the guanidine method for RNA extraction as well as phenol/ chloroform/ SDS precipitation, RNA could be extracted from samples treated with RNase A.

### 5.2.2 RNA obtained from acidified HRV2 is not naked

Release of viral RNA into liposomes was reported to occur upon acidification of membrane-bound virus. When virus was acidified in the absence of liposomes and the material was analyzed by agarose gel electrophoresis, ethidium bromide (EtBr) staining revealed a band migrating to the same position as the full length HRV2 genome; however it was resistant to RNase A digestion.

- Protection of the HRV2 genome by a (viral) protein by formation of ribonucleoprotein was rejected
- Analysis by capillary electrophoresis (using the detergent Thesit) and SDS PAGE followed by western blotting revealed that uncoating of HRV2 under these conditions was incomplete; instead of the expected empty particles and free RNA, 135S particles were found.
- The two conditions reported to trigger RNA release from HRV2 (acidification and heating) were compared. Depending on the analysis method, different subviral particles were found.
- Digestion of acidified virus with RNase A results in conversion of a heterogeneous population of subviral particles to a homogenous population
- If the 135S particle is incubated with RNase A, the 3´ of the RNA is lost

#### 5.2.2.1 Testing formation of ribonucleoprotein

Sandy McGregor and Heather D. Mayor followed RNA release from poliovirus type LSc and HRV1B using negative stain electron microscopy. They observed formation of strands after 2min of heating to 50°C that elongated upon prolonged heating for up to 30 min. Enzymatic probing of those strands showed that they were resistant to RNase digestion unless pepsin, a proteinase, was added. They concluded that the long filaments seen in EM are ribonucleoprotein (RNP) and represent the viral genomes coated with a protein. Further, they observed that rhinovirus (HRV1B and HRV14) and poliovirus RNA were sensitive to RNase digestion if the enzyme was present during heat denaturation. They suggested that the protein involved in RNP formation is capsid-derived; in the time window between decomposition of capsid and assembly of RNP the RNA would be RNase sensitive. They stated that naked RNA is released from within the particle. It unfolds and associates with a protein; only after formation of RNP strands RNA is protected from RNase digestion (*McGregor & Mayor, 1968*, *McGregor & Mayor, 1971*).

Coomassie brilliant blue staining of agarose gels that showed EtBr stained, RNase A resistant material derived from acidified HRV2 revealed co-localization of proteins and RNA. To see, if RNP formation occurs following disassembly in the case of acidification, RNase A was added to the samples either during or after acidification. RNA within HRV2 is protected against RNase digestion both during and after incubation at low pH. Hence, the structural changes of HRV2 upon incubation at low pH must be different from this putative association of RNA and proteins occurring after RNA release triggered by heating as described by McGregor and D. Mayor. Detection of 135S particles in CE (see 5.2.2.3) indicated that protection from RNase A digestion is rather due to incomplete release than to association with a specific protein

forming RNPs. Further, the protein content of the ribonucleoprotein assembly resistant to RNase degradation was identified to be VP1, 2 and 3 by SDS-PAGE and western blotting (see 4.2.2.6) confirming its nature as 135S-particle and not as any other assembly of RNA and protein.

#### 5.2.2.2 Comparison of acidification and 56°C as trigger for conformational change analyzed via agarose gel electrophoresis

Lonberg-Holm and Yin report that acidification of concentrated HRV2 mainly produces 135S particles, whereas heating to 56°C mainly yields empty particles (*Lonberg-Holm & Yin, 1973*) whereas Gerhard Bilek reports that acidification is the more efficient trigger to stimulate transfer of the HRV2 genome into receptor-decorated liposomes (*Bilek, 2009*). The effects of heating and acidification on completion of RNA release of pure virus were compared. HRV2 samples were either heated to 56°C for 10 minutes or incubated at pH 5.2 for 15 minutes at 34°C. Association with proteins was monitored by agarose gel electrophoresis. Following visualization of the RNA by EtBr, agarose gels were stained by Coomassie brilliant blue. Regardless of the trigger, EtBr bands colocalized with Coomassie stained bands. Untreated virus showed two bands in coomassie staining, the ratio of upper and lower species differed between virus preparations. Upon heating or acidification, preferentially the lower band was converted to a species that is easily stained by EtBr, the upper band was unaltered by heating but was influenced by incubation at pH 5.2, 34°C. Also acidification on ice was tested (not shown); it had no effect on either band. The upper band, which is resistant to heating but susceptible to acidification could be the natural top component described by Korant et al. The natural top component does not contain RNA and contains VP0, the precursor of VP2 and VP4 instead of VP2 and VP4 (*Korant et al., 1972*).

#### 5.2.2.3 Comparison of acidification and 56°C as trigger for conformational change analyzed via CE

Heated or acidified virus was subjected to capillary electrophoresis. Depending on the detergent in the sample buffer and background electrolyte, different subviral particles can be separated. If samples are analyzed in presence of Thesit, native virions can be distinguished from 135S particles or empty capsids; if SDS is added, native virions or the individual viral proteins and the viral RNA can be detected (*Weiss, 2009*). When samples were analyzed in presence of SDS, there was no difference between HRV2 samples triggered by heat or acidification. Heating as well as acidification followed by addition of SDS destabilizes viral particles to an extent that they fall apart upon subjection to CE analysis. By contrast, different subviral particles were obtained from HRV2 by heating and acidification, when samples were analyzed in presence of Thesit. In heated samples empty particles were observed, whereas the acidified sample showed a peak with absorption at both 200nm and 260nm that migrated at a position that is different from native virus. This peak is derived from 135S particles that have lost VP4, but still contain the RNA. Further, the acidified sample changed over time. Within one hour a very broad peak developed to a sharp peak with both 200 and 260nm absorbance.

#### 5.2.2.4 Dilution has no effect on uncoating upon acidification

Korant et al. found that acidification of HRV2 yields both empty 80S particles as well as 135S particles (*Korant et al., 1972*). Lonberg-Holm & Yin as well as Victor Weiss described that

dilution of virus samples prior to triggering RNA release shifts the equilibrium of subviral particles towards formation of empty 80S particles (*Lonberg-Holm & Yin, 1973*, *Weiss, 2009*). If HRV2 is diluted 1:2 in boric acid prior to heating, mainly 80S particles are detected by capillary electrophoresis (*Weiss, 2009*). This is not true for acidification of HRV2 analyzed using agarose gel electrophoresis. Even after diluting HRV2 1:5 in water and acidification, RNA was not accessible to RNase, indicating formation of 135S particles instead of uncoating. Also prolonged incubation of diluted samples at pH 5.2 for up to 30 minutes at 37°C did not trigger RNA release.

#### 5.2.2.5 RNase A has an accelerating effect on homogenization of the 135S population

Reproducibly, samples treated with RNase following acidification showed more distinct, brighter bands than samples, which have been acidified without RNase treatment. It was tested, if formation of sharp bands interpreted as homogenous population of 135S particles is caused by the prolonged incubation at 37°C or actually by RNase A itself. Prolonged incubation at 37°C without addition of enzyme or with addition of DNase (as a control) does not show the same effect. In parallel, the effect of RNase A treatment on acidified HRV2 was monitored using capillary electrophoresis. HRV2 that was nothing but acidified migrates as a broad peak with absorbance at both 200nm and 260nm directly after preparation, during incubation at 4°C over night this broad peak converts into a well-defined peak, most probably representing homogeneous 135S particles. The acidified and RNase A treated HRV2 shows immediately after preparation a sharp peak with both 200nm and 260nm absorbance matching the 135S particle, that does not change upon incubation over night. An explanatory model for the homogenizing effect of RNase A on the 135S population could be the following: In the process of conversion from native virus to 135S particles part of the RNA is already extruded. Different 135S particles are interacting via partially extruded genomes and aggregates of indeterminate number generate an inhomogeneous population. RNase A cleaves the protruding part of RNA, thus clipping the conjunctions and leading to isolated 135S particles.

It is noteworthy that the RNase A treated sample showed five distinct RNA peaks with no apparent protein content, which were not altered upon incubation along with RNase A overnight. As long as the ionic strength is not lowered significantly, bovine RNase A acts on single stranded RNA (*Libonati & Sorrentino, 1992*, *Libonati & Palmieri, 1978*). Further, it strongly prefers a cytosine followed by two purines as cleavage site (*Raines, 1998*). Persistence of 5 distinct RNA peaks in presence of RNase A could indicate that a part of the HRV genome is exposed, and that the externalized RNA is predominantly double stranded, with the folding of one conformation is strongly preferred and few loops where a cytosine is followed by two purines are presented to RNase A. At the other hand, it was hypothesized that RNase A is capable of unwinding double stranded RNA by binding to single stranded regions exposed by thermal fluctuations, and RNase A was even reported to melt double stranded DNA (*Jensen & von Hippel, 1976*, *Yakovlev et al., 1995*). Acidified HRV2 was incubated along with RNase A at 37° for 20 minutes- thermal fluctuations of RNA structure are highly probable under those conditions. Further, in agarose gel electrophoresis 5 distinct RNA bands never became apparent. Probably the signal of those RNA fragments is under the detection limit of agarose gel electrophoresis. Probably analysis by CE further destabilizes some 135S particles that have extruded their genome until 5 different putative halting points, setting free HRV2 RNA

degraded to different degrees. Alternatively, RNase A can access RNA in the 135S particle, but can cleave it only at 4 sites because the genome is extensively folded, and if 135S particles fall apart during CE, 5 fragments are released.

#### 5.2.2.6 Is part of the HRV2 genome sticking out of the 135S particle?

When heated HRV2 incubated along with RNase A was analyzed in an agarose gel that was treated with SDS instead of DEPC, RNA migrated at 4kb instead of 7kb, whereas RNA obtained from solely acidified HRV2 still migrated at about 7kb. This was interpreted as an effect of SDS, denaturing the 135S particle and setting free partially degraded RNA. Together with the observation that RNase A has an accelerating effect on homogenization of the 135S particle population, shortening of the RNA upon incubation with RNase A led to the hypothesis that in the 135S particle part of the RNA is accessible to RNase or even sticking out. To test this hypothesis, HRV2 was acidified, incubated with RNase A or not, RNA was retrieved, transcribed to cDNA and presence or absence of the 5´and 3´end was monitored with PCR. PCR of a 5´proximal sequence yielded products, regardless if virus was incubated along with RNase A or not. PCR products derived from the 3´end were obtained exclusively for the undigested sample. The 3´end of the HRV2 genome is lost upon RNase A digestion of 135S particles.

As only the far ends of the RNA were analyzed, it is unclear, if part of the HRV2 genome was actually sticking out of the virus or if RNase A had access to RNA in the 135S particle. It is not clear if just the 3´end is missing, or if the genome was fragmented. If HRV2 is psoralen-UV-crosslinked and heated to 56°C for 10 min, exit of RNA is halted at secondary structures fixed by crosslinking. Subsequent digestion with micrococcal nuclease, purification of RNA and RT-PCR using multiple primer pairs showed that about 1000 nucleotides are missing at the 3´end (*Harutyunyan et al., 2013).*

### 5.2.3 Résumé

If HRV2 was acidified or heated and analyzed in a DEPC-treated agarose gel, 135S particles were found. Capillary electrophoresis detected the individual viral proteins and free RNA for both treatments if the detergent SDS was added; if the detergent Thesit was added instead, empty particles for heating and 135S particles for acidification were found. Depending on the analysis method, different subviral particles were in the same sample. The data presented in this thesis suggest that if pure virus is heated or acidified, uncoating does not proceed to completion. The particle is destabilized, but release is stuck in the stage of the 135S particle. Some analysis methods further destabilize the 135S particle, and empty particles are detected. Apparently, agarose gel electrophoresis (if the gel is treated with DEPC instead of SDS) is very mild and does not further influence viral particles in the sample. In capillary electrophoresis the detergent seems to differentially influence stability of the 135S particle. Further, heating and acidification seem to destabilize HRV2 to a different extent- heated samples are converted to empty particles during CE in presence of Thesit, whereas acidified samples remain in the stage of 135S particles.

A piece of the puzzle is missing in the reaction tube. Bilek et al. showed that HRV2 transfers its genome into liposomes that display ligand binding modules of VLDLR. Liposomes are artificial membrane compartments, composed of a defined lipid composition. Since no host-cell derived

proteins were present, a facilitator, like a host cell factor, could be excluded. They also showed that acidified HRV2 is capable of transferring its genome into bare liposomes that lack the receptor (*Bilek et al., 2011*). So, the minimal requirements for HRV2 uncoating are virus + liposome + acidification. Further, free RNA obtained from acidified HRV2 was detected when SDS was used in capillary electrophoresis. Liposomes used by Bilek et al. were composed of 3 lipids and cholesterol, plus two functionalized lipids (see Table 2). A characteristic of lipids is their amphiphilic nature. Although both detergents used in capillary electrophoresis for analysis of HRV2 share the amphiphilic nature of lipids, only SDS destabilizes the 135S particle, obtained from acidified HRV2. The two detergents do not differ in their hydrophobic moiety, but the hydrophilic moiety of SDS is more similar to the polar head group of lipids than the hydrophilic part of Thesit (see Figure 53). SDS consists of a negatively charged molecule associated with a sodium ion whereas Thesit is polar but not charged.

| abbrev. | structural formula<br>hydrophobic moiety hydrophilic moiety | formal charge |
|---|---|---|
| POPC | 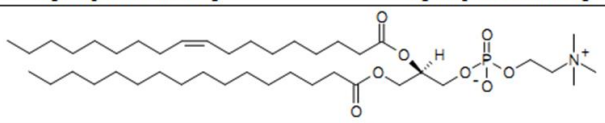 | 0 |
| PE | 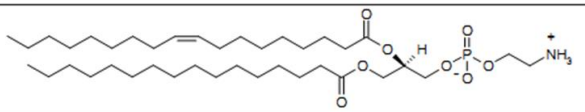 | 0 |
| SM | 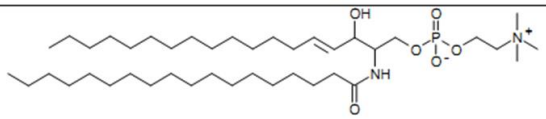 | 0 |
| Ch | 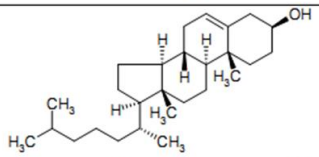 | 0 |
| DOGS-NTA | 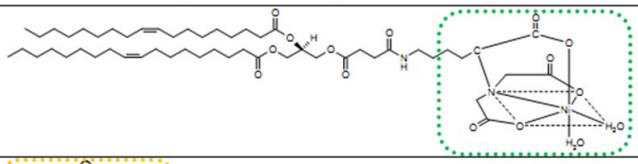 | -1 |
| NBD-PC | 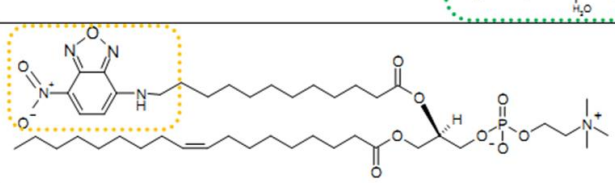 | 0 |

Table 2: Lipids used for liposome preparation

POPC: 1- palmitoyl-2-oleoyl-sn-glycero-3-phosphocholine
PE: L-α-phosphatidylethanolamine
SM: sphingomyelin, Ch: cholesterol
DOGS-NTA: 1,2-dioleoyl-sn-glycero-3-[(N-(5-amino-1-carboxypentyl)iminodiacetic acid)succinyl]
NBD-PC: 1-oleoyl-2-[12-[(7-nitro-2-1,3-benzoxadiazol-4-yl)amino]dodecanoyl]-sn-glycero-3-phosphocholine
Colored boxes indicate functional domains. Table taken from (*Bilek, 2009*)

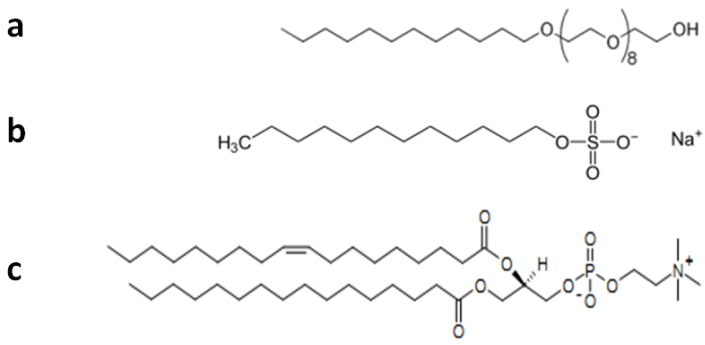


Figure 53: SDS and Thesit in comparison with POPC, a component of liposomes

a: Thesit (Polidocanol)
b: SDS (sodium dodecyl sulphate)
c: POPC
Structural formula of Thesit taken from http://de.wikipedia.org/wiki/Polidocanol [August 2013], structural formula of SDS taken from http://de.wikipedia.org/wiki/Natriumlaurylsulfat [August 2013], POPC and DOGS-NTA see Table 2.

Kremser et al. observed that HRV analyzed in the presence of SDS shows an increased electrophoretic mobility in comparison to HRV analyzed in the presence of Thesit. They concluded that SDS is forming charged micelles that attach to the virus, thereby causing a mobility shift in CE (*Kremser et al., 2009*). Depending on the concentration, Thesit (or Polidocanol) is also forming micelles[22], but they are not charged. Probably interaction with a membrane or a micelle in combination with close proximity of charged moieties is the final push to trigger genome release from the 135S particle. Given that release of the RNA into the hostile environment of the late endosome would terminate the life cycle of the virus, it would be of evolutionary benefit to ensure that the genome is only released when virus is in contact with the membrane from a membrane- proximal pore. Contribution of the membrane to uncoating of minor group HRVs would make sense. For major group HRVs, it was hypothesized that binding of the receptor decides about the point of egress, ensuring that the genome is released into the cytosol instead of into the endosome (*Xing et al., 2003*). Minor group viruses dissociate from their receptor during the progression from early to late endosomes (*Brabec et al., 2003*), thus other means of directing the genome into the cytosol would be necessary. Probably amphiphilic environments are implicated in sequestering the pocket factor stabilizing the capsid. Close proximity of charged moieties might influence complexation of divalent cations, which were suggested to regulate stability and uncoating of naked viruses (*Zhao et al., 1997, Banerjee et al., 2010*).

Concerning directionality of release, exposal of the 3´ end and protection of the 5´ end of the HRV2 genome in the 135S subviral particle comes as a surprise. Since the capsid constitutes a limitation to genome size, small icosahedral viruses are under evolutionary pressure to keep their genomes small. Usually, viruses are an amazing example of efficiency, exemplified by sequential cleavage of the proteins to yield a variety of biochemically active as well as structural proteins. In the picornaviral life cycle, the next step to uncoating is translation. Translation starts at the IRES located at the 5´ end; therefore, virus gene expression could start

[22] Mode of action of Polidocanol in drugs: http://kreussler-pharma.de/zugang-fuer-aerzte-und-apotheker-fachkreise/phlebologie/2012-09-15-16-46-41/polidocanol.html [August 2013]

immediately if the 5´ was exposed first. If the 5´ end exits the capsid last, initiation of translation needs to await complete release of the genome.

According to folding predictions, picornaviral genomes adopt an elongated conformation with protruding stems in which the two ends of the picornaviral genome are located close to each other (*Palmenberg & Sgro, 1997*, Figure 54). Either, those folding predictions do not reflect the folding RNA undergoes when packed inside the capsid or conformational changes of the capsid during uncoating affects folding of RNA. Further, these RNA secondary structures were computed without the VPg, which might significantly influence folding.

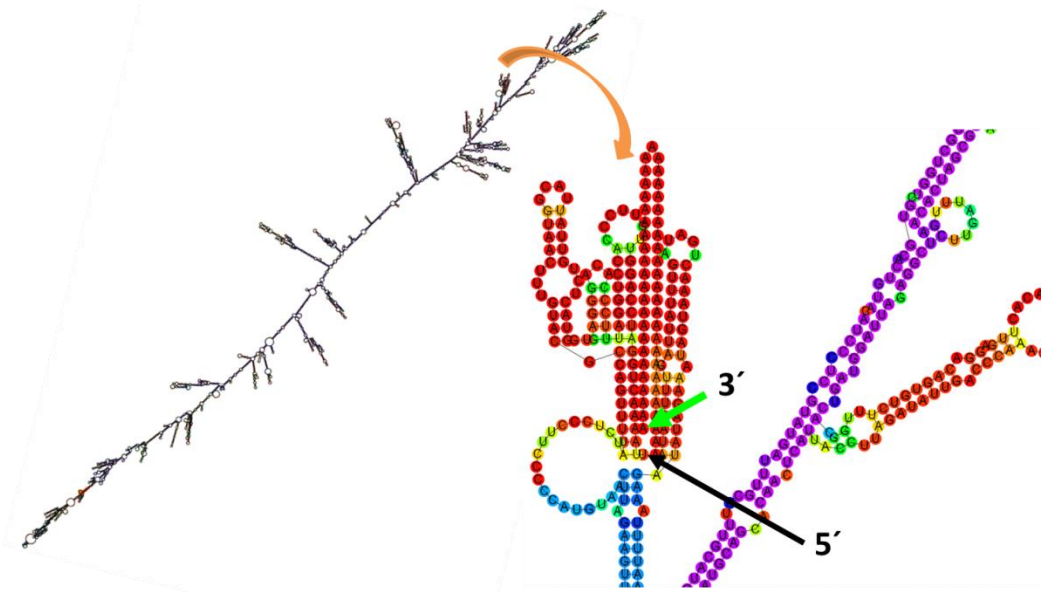


Figure 54: In the folding prediction of HRV2 RNA, the 3´end and the 5´end are located in close proximity

The folding of the HRV2 genome was calculated by the RNAfold Webserver[23]. In the sequence of the HRV2 cDNA (GenBank accession no. X02316) T was replaced by U using the life science tools of fr33.net[24] and 50 A residues were added.

[23] RNAfold Webserver: http://rna.tbi.univie.ac.at/cgi-bin/RNAfold.cgi [August 2013]

[24] Complementary sequence, T → U http://www.fr33.net/seqedit.php [August 2013]

# 6 References

Ich habe mich bemüht, sämtliche Inhaber der Bildrechte ausfindig zu machen und ihre Zustimmung zur Verwendung der Bilder in dieser Arbeit eingeholt. Sollte dennoch eine Urheberrechtsverletzung bekannt werden, ersuche ich um Meldung bei mir.


Abraham G. & Colonno RJ: Many rhinovirus serotypes share the same cellular receptor. *J. Virol*. 1984, **51:** 340-345

Ahlquist P and Kaesberg P: Determination of the length distribution of poly(A) at the 3' terminus of the virion RNAs of EMC virus, poliovirus, rhinovirus, RAV-61 and CPMV and of mouse globin mRNA. *Nucleic Acids Res*. 1979, **7:** 1195-1204

Andries K, Dewindt B, Snoeks J, Wouters L, Moereels H, Lewi PJ, Janssen PA: Two groups of rhinoviruses revealed by a panel of antiviral compounds present sequence divergence and differential pathogenicity. *J Virol.* 1990, **64(3):** 1117-23.

Applied Biosystems, 2000: GeneScan® Reference Guide, Chemistry Reference for the ABI PRISM® 310 Genetic Analyzer, Part Number 4303189B, Printed in the USA, 10/2000. Foster City, CA: Applied Biosystems.

Applied Biosystems, 2002: GeneScan™ -500 ROX™ STANDARD product insert information sheet, Printed in the USA, 12/2002, Foster City, CA: Applied Biosystems

Applied Biosystems, 2006: Reference Guide Peak Scanner™ Software Version 1.0, Printed in the USA, 12/2006, Foster City, CA: Applied Biosystems

Arruda E, Boyle TR, Winther B, Pevear DC, Gwaltney JM, Jr, Hayden FG: Localization of human rhinovirus replication in the upper respiratory tract by *in situ* hybridization. *J Infect Dis* 1995; **171:** 1329–1333.

Bacher G, Szymanski WW, Kaufman SL, Zöllner P, Blaas D, Allmaier G: Charge-reduced nano electrospray ionization combined with differential mobility analysis of peptides, proteins, glycoproteins, noncovalent protein complexes and viruses. *J Mass Spectrom*. 2001; **36(9):** 1038-1052.

Banerjee M, Johnson JE: Activation, exposure and penetration of virally encoded, membrane-active polypeptides during non-enveloped virus entry. *Curr Protein Pept Sci* 2008; **9:** 16–27.

Banerjee M, Speir JA, Kwan MH, Huang R, Aryanpur PP, Bothner B, Johnson JE: Structure and Function of a Genetically Engineered Mimic of a Nonenveloped Virus Entry. *J Virol.* 2010; **84(9):** 4737-4746.

Bardin PG, Johnston SL, Sanderson G: Detection of rhinovirus infection of the nasal mucosa by oligonucleotide *in situ* hybridization. *Am J Respir Cell Mol Biol* 1994; **10:** 207–213.

Bayer N, Prchla E, Schwab M, Blaas D, Fuchs R. Human rhinovirus HRV14 uncoats from early endosomes in the presence of bafilomycin. *FEBS Lett.* 1999; **463:** 175-178.

Bayer N, Schober D, Prchla E, Murphy RF, Blaas D, Fuchs R: Effect of bafilomycin A1 and nocodazole on endocytic transport in HeLa cells: implications for viral uncoating and infection, *J. Virol*. 1998, **72:** 9645–9655.

Bilek G.: Functionalized Liposomes as a Model to Reveal Cell-Surface Associated Events of the Human Rhinovirus Infection-Pathway, Wien, Universität Wien, Diss., 2009.

Bilek G, Matscheko NM, Pickl-Herk A, Weiss VU, Subirats X, Kenndler E, Blaas D: Liposomal nanocontainers as models for viral infection: monitoring viral genomic RNA transfer through lipid membranes. *J Virol*. 2011; **85(16):** 8368-8375.

Bostina M, Levy H, Filman DJ, Hogle JM. Poliovirus RNA is released from the capsid near a twofold symmetry axis*. J Virol.* 2011; **85(2):** 776-783

Brabec M, Baravalle G, Blaas D, Fuchs R: Conformational Changes, Plasma Membrane Penetration, and Infection by Human Rhinovirus Type 2: Role of Receptors and Low pH*, J. Virol*. 2003, **77:** 5370–5377.

Brabec M, Schober D, Wagner E, et al. Opening of size-selective pores in endosomes during human rhinovirus serotype 2 in vivo uncoating monitored by single-organelle flow analysis. *J Virol* 2005; **79:** 1008–1016.

Butler JM, Buel E, Crivellente F, McCord BR: Forensic DNA typing by capillary electrophoresis using the ABI Prism 310 and 3100 genetic analyzers for STR analysis. *Electrophoresis* 2004, **25:** 1397–1412.

Canzian F, Salovaara R, Hemminki A, Kristo P, Chadwick RB, Aaltonen LA, de la Chapelle A: Semiautomated assessment of loss of heterozygosity and replication error in tumors. *Cancer Res*. 1996; **56:** 3331–3337.

Chien RL, Burgi DS: Field amplified sample injection in high-performance capillary electrophoresis. *Journal of Chromatography A* 1991, **559:** 141–152

Colonno RJ, Condra JH, Mizutani S, Callahan PL, Davies ME, Murcko MA: Evidence for the direct involvement of the rhinovirus canyon in receptor binding. *Proc Natl Acad Sci U S A* 1988; **85:** 5449–5453.

Compton SJ, Jones CG: Mechanism of dye response and interference in the Bradford protein assay. *Anal Biochem.* 1985; **151:** 369-74.

Croce CM: Genetic approaches to the study of the molecular basis of human cancer. *Cancer Res. 1991*; **51(18 Suppl):**5015s-5018s.

Dreschers S, Franz P, Dumitru C, Wilker B, Jahnke K, Gulbins E: Infections with Human Rhinovirus Induce the Formation of Distinct Functional Membrane Domains. *Cell Physiol Biochem.* 2007; **20:** 241-54.

Duechler M, Skern T, Blaas D, Berger B, Sommergruber W, Kuechler E: Human Rhinovirus Serotype 2: *In Vitro* Synthesis of an Infectious RNA. *Virology* 1989, **168:** 159-161.

Ehresmann C, Baudin F, Mougel M, Romby P, Ebel JP, Ehresmann B: Probing the structure of RNAs in solution. *Nucleic Acids Res*. 1987, **15:** 9109-9128.

Fendrick AM, Monto AS, Nightengale B, Sarnes M: The Economic Burden of Non–Influenza-Related Viral Respiratory Tract Infection in the United States. *Arch Intern Med*. 2003; **163:** 487-494

Fuchs R, Blaas D: Uncoating of human rhinoviruses. *Rev. Med. Virol.* 2010; **20:** 281–297.

Garriga D, Pickl-Herk A, Luque D, Wruss J, Castón JR, Blaas D, Verdaguer N: Insights into Minor Group Rhinovirus Uncoating: The X-ray Structure of the HRV2 Empty Capsid. *PLoS Pathog.* 2012; **8(1):** e1002473

Gerber K, Wimmer E, Paul AV: Biochemical and Genetic Studies of the Initiation of Human Rhinovirus 2 RNA Replication: Identification of a cis-Replicating Element in the Coding Sequence of 2Apro. *J Virol*. 2001, **75(22)**:10979-10990.

Gern JE, Galagan DM, Jarjour NN, Dick EC, Busse WW: Detection of rhinovirus RNA in lower airway cells during experimentally induced infection. *Am J Respir Crit Care Med* 1997; **155:** 1159–1161.

Golini F, Nomoto A, and Wimmer E: The genome-linked protein of picornaviruses. IV. Difference in the VPg's of encephalomyocarditis virus and poliovirus as evidence that the genome-linked proteins are virus-coded. *Virology* 1978, **89:** 112-118

Greve JM, Davis G, Meyer AM, Forte CP, Yost SC, Marlor CW, Kamarck ME, McClelland A: The major human rhinovirus receptor is ICAM-1. *Cell*. 1989; **56(5):** 839-847.

Grunert H, Wolf K, Langner K, Sawitzky D, Habermehl K, Zeichhardt H: Internalization of human rhinovirus 14 into HeLa and ICAM-1-transfected BHK cells. *Med Microbiol Immunol Berl* 1997; **186:** 1–9.

Harutyunyan S, Kumar M, Sedivy A, Subirats X, Kowalski H, Köhler G, Blaas D: Viral Uncoating Is Directional: Exit of the Genomic RNA in a Common Cold Virus Starts with the Poly-(A) Tail at the 3'-End. *PLoS Pathog*. 2013; **9(4):** e1003270.

Hayden FG.: Rhinovirus and the lower respiratory tract. *Rev Med Virol* 2004; **14:** 17–31

Heikkinen T, Jarvinen A: The common cold. *Lancet* 2003; **361:** 51–59.

Hewat EA, Neumann E, Conway JF, Moser R, Ronacher B, Marlovits TC, Blaas D: The cellular receptor to human rhinovirus 2 binds around the 5-fold axis and not in the canyon: a structural view *EMBO J.* 2000; **19(23):** 6317–6325

Hewat EA, Neumann E, Blaas D: The concerted conformational changes during human rhinovirus 2 uncoating. *Mol Cell* 2002; **10:** 317–326.

Hewat EA, Blaas D. Cryoelectron microscopy analysis of the structural changes associated with human rhinovirus type 14 uncoating. *J Virol* 2004; **78:** 2935–2942

Hofer F, Gruenberger M, Kowalski H, Machat H, Huettinger M, Kuechler E, Blaas D: Members of the low density lipoprotein receptor family mediate cell entry of a minor-group common cold virus. *Proc Natl Acad Sci U S A*. 1994; **91(5):** 1839-1842.

Hogle JM: Poliovirus cell entry: common structural themes in viral cell entry pathways. *Annu. Rev. Microbiol*. 2002, **56:** 677-702

Jackson, D.P., Lewis, F. A., Taylor, G.R., Boylston, A.W. and Quirke, P: Tissue extraction of DNA and RNA and analysis by the polymerase chain reaction. *J. Clin. Pathol.* 1990, **43**, 499-504.

Jacobs SE, Lamson DM, St George K, Walsh TJ: Human rhinoviruses. *Clin Microbiol Rev*. 2013; **1:**135-162

Jeffreys AJ, Wilson V, Thein SL: Hypervariable 'minisatellite' regions in human DNA., *Nature*. 1985 **314(6006):** 67-73.

Jensen DE, von Hippel PH: DNA "melting" proteins. I. Effects of bovine pancreatic ribonuclease binding on the conformation and stability of DNA. *J Biol Chem*. 1976; **251(22):** 7198-214.

Khan AG, Pichler J, Rosemann A, Blaas D: Human rhinovirus type 54 infection via heparan sulfate is less efficient and strictly dependent on low endosomal pH. *J Virol* 2007; **81:** 4625–4632.

Khan AG, Pickl-Herk A, Gajdzik L, Marlovits T, Fuchs R, Blaas D: Human rhinovirus 14 enters RD cells expressing ICAM-1 by a non-clathrin, non-caveolin dependent pathway. *J Virol* 2010; **84(8):** 3984–3992.

Kiernan JA: Preservation and retrieval of antigens for immunohistochemistry - methods and mechanisms. 1: Effects of formaldehyde fixation. *The Cutting Edge* (National Society for Histotechnology, Newsletter for Region IX, Canada) January 2005, pp. 5-9.

Kim YC, Russell WK, Ranjith-Kumar CT, Thomson M, Russell DH, Kao CC: Functional analysis of RNA binding by the hepatitis C virus RNA-dependent RNA polymerase. *J Biol Chem.* 2005; **280(45):** 38011-38019

Korant BD, Lonberg-Holm K, Noble J, Stasny JT. Naturally occurring and artificially produced components of three rhinoviruses. *Virology.* 1972; **48(1):** 71-86.

Krasilnikov AS, Yang X, Pan T, Mondragón A: Crystal structure of the specificity domain of ribonuclease P. *Nature* 2003; **421(6924):** 760-764

Kremser L, Blaas D, Kenndler E: Virus analysis using electromigration techniques. *Electrophoresis* 2009, **30:** 133–140

Lewis JK, Bothner B, Smith TJ, Siuzdak G: Antiviral agent blocks breathing of the common cold virus. *Proc. Natl. Acad. Sci. USA* 1998, **95:** 6774-6778.

Li QA, Yafal G, Lee YM, Hogle J, Chow M: Poliovirus neutralization by antibodies to internal epitopes of VP4 and VP1 results from reversible exposure of these sequences at physiological temperature. *J. Virol*. 199, **68:** 3965-3970.

Libonati M, Palmieri M. How much is secondary structure responsible for resistance of double-stranded RNA to pancreatic ribonuclease A? *Biochim Biophys Acta*. 1978; **518(2):** 277-89.

Libonati M, Sorrentino S. Revisiting the action of bovine ribonuclease A and pancreatic-type ribonucleases on double-stranded RNA. *Mol Cell Biochem.* 1992; **117(2):** 139-51.

Lin JY, Chen TC, Weng KF, Chang SC, Chen LL, Shih SR. Viral and host proteins involved in picornavirus life cycle. *J Biomed Sci.* 2009, **16:** 103

Lonberg-Holm K, Gosser LB, Shimshick EJ: Interaction of liposomes with subviral particles of poliovirus type 2 and rhinovirus type 2. *J Virol*. 1976; **19(2):** 746–749

Lonberg-Holm K, Yin FH: Antigenic determinants of infective and inactivated human rhinovirus type 2. *J Virol*. 1973; **12(1):** 114-123.

López-Lastra M, Rivas A, Barría MI: Protein synthesis in eukaryotes: The growing biological relevance of cap-independent translation initiation. *Biol Res*, 2005, **38:** 121-146

Marsh M, Helenius A: Virus Entry: Open Sesame. *Cell* 2006, **124:** 729–740.

Martín-Acebes MA, Vázquez-Calvo Á, Caridi[1] F, Sobrino[1] F and Saiz JC: Lipid Involvement in Viral Infections: Present and Future Perspectives for the Design of Antiviral Strategies. *Lipid Metabolism*, edited by Rodrigo Valenzuela Baez, ISBN 978-953-51-0944-0, chapter 13, DOI: 10.5772/51068. Published: January 23, 2013 under CC BY 3.0 license

Masuda N, Ohnishi T, Kawamoto S, Monden M, Okubo K: Analysis of chemical modification of RNA from formalin-fixed samples and optimization of molecular biology applications for such samples. *Nucleic Acids Res*. 1999; **27(22):** 4436-4443.

McErlean P, Shackelton LA, Andrews E, Webster DR, Lambert SB, et al.: Distinguishing molecular features and clinical characteristics of a putative new rhinovirus species, human rhinovirus C (HRV C). *PLoS ONE*. 2008; 3:e1847.

McGhee JD, von Hippel PH: Formaldehyde as a probe of DNA structure. I. Reaction with exocyclic amino groups of DNA bases. *Biochemistry*. 1975; **14(6):** 1281-96.

McGhee JD, von Hippel PH: Formaldehyde as a probe of DNA structure. II. Reaction with endocyclic imino groups of DNA bases. *Biochemistry*. 1975; **14(6)**: 1297-303.

McGregor S, Mayor HD: Biophysical studies on rhinovirus and poliovirus. I. Morphology of viral ribonucleoprotein. *J Virol*. 1968; **2(2):** 149-154.

McGregor S, Mayor HD: Internal components released from rhinovirus and poliovirus by heat. *J Virol*. 1971; **10(2):** 203-207.

Merino EJ, Wilkinson KA, Coughlan JL, Weeks KM: RNA Structure Analysis at Single Nucleotide Resolution by Selective 2´- Hydroxyl Acylation and Primer Extension (SHAPE). *J Am Chem Soc*. 2005; **127:** 4223-4231

Metz B, Kersten GF, Hoogerhout P, Brugghe HF, Timmermans HA, de Jong A, Meiring H, ten Hove J, Hennink WE, Crommelin DJ, Jiskoot W: Identification of formaldehyde-induced modifications in proteins: reactions with model peptides. *J Biol Chem*. 2004; **279(8):**6235-6243.

Mortimer SA, Weeks KM: A fast-acting reagent for accurate analysis of RNA secondary and tertiary structure by SHAPE chemistry. *J Am Chem Soc*. 2007; **129(14):** 4144-4145.

Mortimer SA, Weeks KM: Time-resolved RNA SHAPE chemistry. *J Am Chem Soc*. 2008; **130(48):** 16178-16180

Moscufo N, Simons J, Chow M. Myristoylaton is important at multiple stages in poliovirus assembly. *J. Virol*. 1991, **65:** 2372-2380.

Nurani G, Lindqvist B, Casasnovas JM. Receptor priming of major group human rhinoviruses for uncoating and entry at mild low-pH environments. *J Virol* 2003; **77:** 11985–11991.

Ogram SA and Flanegan JB: Non-Templated Functions of Viral RNA in Picornavirus Replication. *Curr Opin Virol*. 2011, **1(5):** 339–346

Okun VM, Ronacher B, Blaas D, Kenndler E: Analysis of Common Cold Virus (Human Rhinovirus Serotype 2) by Capillary Zone Electrophoresis: The Problem of Peak Identification. *Anal Chem* 1999, **71(10):** 2028-2032.

Olson NH, Kolatkar PR, Oliveira MA, et al.: Structure of a human rhinovirus complexed with its receptor molecule. *Proc Natl Acad Sci USA* 1993; **90:** 507–511.

Orlando V, Strutt H, Paro R: Analysis of chromatin structure by in vivo formaldehyde cross-linking. *Methods*. 1997; **11(2):** 205-214.

Palmenberg AC, Sgro J-Y: Topological organization of picornaviral genomes: statistical prediction of RNA structural signals. *Seminars in Virology* 1997; **8:** 231–41.

Palmenberg AC, Spiro D, Kuzmickas R, Wang S, Djikeng A, Rathe JA, Fraser-Liggett CM, Liggett SB: Sequencing and analyses of all known human rhinovirus genomes reveal structure and evolution. *Science* 2009, **324:**55-59.

Palmenberg A, Rathe J, Liggett S: Analysis of the complete genome sequences of human rhinovirus. *J. Allergy Clin. Immunol*. 2010, **125**: 1190–1201.

Peltola V*,* Waris M*,* Osterback R*,* Susi P*,* Hyypia T*,* Ruuskanen O: Clinical effects of rhinovirus infections*. J Clin Virol* 2008*;* **43***:* 411–414

Prchla E, Kuechler E, Blaas D, Fuchs R: Uncoating of human rhinovirus serotype 2 from late endosomes. *J. Virol*. 1994, **68:** 3713- 3723

Prchla E, Plank C, Wagner E, Blaas D, Fuchs R: Virus-mediated release of endosomal content in vivo: different behaviour of adenovirus and rhinovirus serotype 2. *J. Cell. Biol*. 1995, **131:** 111-123

Raines RT: Ribonuclease A. Chem Rev. 1998 May 7;98(3):1045-1066.

Register RB, Uncapher CR, Naylor AM, Lineberger DW, Colonno RJ: Human-murine chimeras of ICAM-1 identify amino acid residues critical for rhinovirus and antibody binding. *J Virol* 1991; **65:** 6589–6596.

Richards AL, Jackson WT: Behind Closed Membranes: The Secret Lives of Picornaviruses? *PLoS Pathog*. 2013; **9(5):** e1003262.

Rossmann MG, Arnold E, Erickson JW, Frankenberger EA, Griffith JP, Hecht HJ, Johnson JE, Kamer G, Luo M, Mosser AG, et al.: Structure of a human common cold virus and functional relationship to other picornaviruses. *Nature* 1985; **317:** 145-153.

Schmiedeberg L, Skene P, Deaton A, Bird A: A temporal threshold for formaldehyde crosslinking and fixation. *PLoS One*. 2009; **4(2):**e4636. doi: 10.1371

Schober D, Kronenberger P, Prchla E, Blaas D, Fuchs R: Major and minor receptor group human rhinoviruses penetrate from endosomes by different mechanisms. *J. Virol*. 1998, **72:** 1354-1364

Sieczkarski SB, Whittaker GR: Viral entry*. Curr Top Microbiol Immunol.* 2005; **285:** 1-23.

Skern T, Sommergruber W, Blaas D, Pieler C, Kuechler E: Relationship of human rhinovirus strain 2 and poliovirus as indicated by comparison of the polymerase gene regions. *Virology* 1984; **136:** 125-132

Skern T, Sommergruber W, Blaas D, Gruendler P, Fraundorfer F, Pieler C, Fogy I, Kuechler E: Human rhinovirus 2: complete nucleotide sequence and proteolytic processing signals in the capsid protein region., *Nucleic Acids Res.* 1985; **13(6):** 2111-2126.

Skern, Tim: Coffee House Notes on Virology (1), Wien, 2006

Snyers L, Zwickl H, Blaas D: Human rhinovirus type 2 is internalized by clathrin-mediated endocytosis*. J Virol* 2003; **77:** 5360–5369.

Solomon MJ, Varshavsky A: Formaldehyde-mediated DNA-protein crosslinking: a probe for in vivo chromatin structures. *Proc Natl Acad Sci U S A*. 1985; **82(19):** 6470-6474.

Sutherland BW, Toews J, Kast J: Utility of formaldehyde cross-linking and mass spectrometry in the study of protein-protein interactions. *J Mass Spectrom*. 2008; **43(6):** 699-715.

Svarovskaia ES, Cheslock SR, Zhang WH, Hu WS, Pathak VK: Retroviral mutation rates and reverse transcriptase fidelity. *Front Biosci*. 2003; 8:d117-134.

Tautz D: Hypervariability of simple sequences as a general source for polymorphic DNA markers. *Nucleic Acids Res*. 1989; **17(16):** 6463-71.

Toonen RJ and Hughes S: Increased Throughput for Fragment Analysis on ABI Prism 377 Automated Sequencer Using a Membrane Comb and STRand Software. *Biotechniques* 2001, **31:** 1320-1324

Tsai B: Penetration of nonenveloped viruses into the cytoplasm. *Annu Rev Cell Dev Biol* 2007; **23:** 23–43.

Uncapher CR*,* Dewitt CM*,* Colonno RJ: The major and minor group receptor families contain all but one human rhinovirus serotype*. Virology* 1991*;* **180***:* 814–817*.*

Vasa SM, Guex N, Wilkinson KA, Weeks KM, Giddings MC: ShapeFinder: A software system for high-throughput quantitative analysis of nucleic acid reactivity information resolved by capillary electrophoresis. *RNA* 2008; **14(10):** 1979-1990

Verdaguer N, Blaas D, Fita I: Structure of human rhinovirus serotype 2 (HRV2). *J Mol Biol* 2000; **300:** 1179–1194.

Vlasak M, Roivainen M, Reithmayer M: The minor receptor group of human rhinovirus (HRV) includes HRV23 and HRV25, but the presence of a lysine in the VP1 HI loop is not sufficient for receptor binding. *J Virol* 2005; **79:** 7389–7395.

von Ahlfen S, Missel A, Bendrat K, Schlumpberger M: Determinants of RNA quality from FFPE samples. *PLoS One*. 2007**; 2(12):** e1261.

Vos P, Hogers R, Bleeker M, Reijans M, van de Lee T, Hornes M, Frijters A, Pot J, Peleman J, Kuiper M, et al.: AFLP: a new technique for DNA fingerprinting. In: *Nucleic Acids Res*. 1995, **23(21):** 4407-4414.

Weiss, Victor U.: Chip Electrophoresis of Human Rhinovirus and Receptor Decorated Liposomes as Model Membranes for the Analysis of Key Steps in the Viral Infection Pathway, Wien, Universität Wien, Diss., 2009.

Weiss VU, Subirats X, Pickl-Herk A, Bilek G, Winkler W, Kumar M, Allmaier G, Blaas D, Kenndler E: Characterization of rhinovirus subviral A particles via capillary electrophoresis, electron microscopy and gas-phase electrophoretic mobility molecular analysis: Part I *Electrophoresis* 2012, **33:** 1833–1841

Wilkinson KA, Merino EJ, Weeks KM: Selective 2'-hydroxyl acylation analyzed by primer extension (SHAPE): quantitative RNA structure analysis at single nucleotide resolution. *Nat Protoc*. 2006; **1(3):** 1610-1616.

Xing L, Casasnovas JM, Cheng RH: Structural analysis of human rhinovirus complexed with ICAM-1 reveals the dynamics of receptor-mediated virus uncoating. *J Virol* 2003; **77:** 6101–6107.

Yakovlev GI, Sorrentino S, Moiseyev GP, Libonati M. Double-stranded RNA: the variables controlling its degradation by RNases. *Nucleic Acids Symp Ser*. 1995; **33:** 106-108.

Yin FH & Knight CG: *In vivo* and *in vitro* synthesis of human rhinovirus type 2 ribonucleic acid. *J Virol* 1972; **10:** 93–98.

Zhao R, Hadfield AT, Kremer MJ, Rossmann MG: Cations in human rhinoviruses. *Virology*. 1997; **227(1):** 13-23.

# 7 Appendixes

## 7.1 Zusammenfassung

Die Vermehrung von Viren ist von einer Wirtszelle abhängig. Humane Rhinoviren (HRVs) vermehren sich vorzugsweise in Epithelzellen des oberen Atmungstraktes, sie sind die Ursache für circa 50% an milden Infektionen des oberen Respirationstraktes. Rhinoviren setzen sich aus einem RNA-Genom und einer schützenden Proteinhülle (Capsid) zusammen. Diese Arbeit konzentriert sich auf den Vorgang des Genomtransfers. Wenn HRV den Rezeptor einer Wirtszelle bindet wird es durch Endozytose in die Zelle aufgenommen. In die Zelle aufgenommene Vesikel werden angesäuert, dieser Abfall des pH-Wertes induziert Konformationsänderungen des Capsids. Dadurch werden Poren in der Hülle geöffnet und das Genom wird entlassen. Die Proteinhülle ist aus sich wiederholenden Untereinheiten zusammengesetzt, die sich gleichzeitig umorganisieren. Das bewirkt ein simultanes Öffnen einer Vielzahl an Poren. Das Ziel dieser Arbeit war herauszufinden ob das Genom durch eine oder mehrere Poren entlassen wird. Des Weiteren sollte geklärt werden, ob es eine bestimmte Richtung gibt mit der der Ausstoß der RNA erfolgt. Ist ein bestimmtes Ende dafür vorgesehen zuerst in die Wirtszelle zu gelangen?

Um Antworten auf diese Fragen zu erhalten wurden zwei chemische Methoden angewandt. Bei der einen Methode (SHAPE) modifiziert eine Chemikalie RNA am 2´OH, aber nur dann, wenn das betreffende Nucleotid nicht in Sekundär- oder Tertiärinteraktionen involviert ist. Es gibt verschiedene Chemikalien, die RNA auf diese Art modifizieren, einige davon mit hoher Reaktionsgeschwindigkeit. Aufgrund dieser hohen Reaktionsgeschwindigkeit ist eine Momentaufnahme des Transfers möglich, des Weiteren gibt die Methode Aufschluss darüber, ob die RNA einzel- oder doppelsträngig das Capsid verlässt. Modifikationen sind ein Hindernis für das Enzym Reverse Transcriptase, wenn modifizierte RNA in cDNA umgeschrieben wird, bricht die cDNA Synthese bei Modifikationen ab. cDNA Fragmente verschiedener Länge erlauben Rückschluss auf die Zugänglichkeit für die Chemikalie – doppelsträngige und vom Capsid geschützte RNA sollte nicht reagieren. cDNA Fragmente unterschiedlicher Länge werden mittels Kapillarelektrophorese aufgetrennt. Um die Analyse mittels eines ABI PRISM®310Genetic Analyzers zu ermöglichen mussten Änderungen an der Methode vorgenommen werden, wodurch die Auswertung der Daten mit dem dafür vorgesehenen Computerprogramm verhindert wurde. Ein alternatives Programm konnte die Daten ebenfalls nicht auswerten.

Die zweite Methode basiert auf der Vernetzung von Proteinen und RNA durch Formaldehyd. Formaldehyd reagiert sowohl mit Aminosäuren als auch mit den Basen von Nucleinsäuren. Wenn die Pore um die herausragende RNA herum oder sogar mit der austretenden RNA selbst vernetzt wird, dann sollte der Transfer unterbrochen werden. Charakterisierung der im Capsid zurückgebliebenen RNA sollte aufklären ob ein bestimmtes Ende zuerst entlassen wird. Im Verlauf der Untersuchungen stellte sich heraus, dass HRV2 in Pufferlösung sein Genom nicht vollständig ausstößt, somit erübrigt sich Vernetzung. Die Konformationsänderungen, die den Genomtransfer bedingen laufen über eine Zwischenstufe- das 135S Partikel ab. Wird HRV2 in reiner Pufferlösung angesäuert, so läuft die Freisetzung des Genoms nur bis zu dieser Zwischenstufe ab. Das 135S Partikel hat allerdings einen Teil der RNA freigesetzt. Mithilfe von RNase A und RT-PCR konnte festgestellt werden, das das 3´Ende des Genoms RNase A zugänglich ist, während das 5´ Ende geschützt ist.

## 7.2 Curriculum Vitae

Huszar Katharina

Siebenbürgerstr. 2-12/1/11, 1220 Wien

Phone.: 0650 283 85 46

e-mail: katharina_huszar@gmx.net

Date of birth: 30.04.1981 in Vienna

### *Education*

| | |
|---|---|
| 1999- 2013 | University of Vienna, Vienna, Austria. Biology, focus on immunology, virology and biochemistry. Diploma thesis title: Investigating directionality of genome release from Human Rhinovirus A 2 |
| 1991- 1999 | Bundesgymnasium Bernoullistrasse, Vienna, Austria, graduation: Matura |
| 1987- 1991 | private Volksschule der Schwestern „zum armen Kinde Jesu“ |

### *Scientific work experience*

| | |
|---|---|
| 08/ 2007 | Medical University of Vienna, Department of the Pathobiology of the Nervous System, Univ.-Prof. Johannes Berger, Dr. Markus Kunze. Research practical on targeting signals of insulin degrading enzyme. |

| | |
|---|---|
| 03/ 2006 | Medical University of Vienna, Department Virology (Klinisches Institut für Virologie), Univ. Prof. DDr. Christian Mandl, Mag. Verena Hönninger. Research practical on influence of sequence elements of the 5´- and 3´NCR of TBE virus on translation and replication |
| 08/ 2005 & 2006 | Baxter Healthcare GmbH, Orth a. d. Donau, Department workplace hygiene, Dr. Marina Jarosch. Holiday internship |

### *Personal skills*

| | |
|---|---|
| Sept/ 2005 | Mitarbeiterführung I- Der Chef als Coach, Gloggnitz, Austria. Ing. Robert Graf |
| Mother tongue | German |
| Foreign languages | English (excellent)<br>French: Certificat pratique de langue francaise, 1$^{er}$ degré, Université Paris-Sorbonne |

### *Occupations*

| | |
|---|---|
| 01/2013- 09/2013 | Confare GmbH, 1210 Vienna, Austria. Customer relationship management |
| 11/2002- 01/2011 | BP-Tankstelle Stefan Huszar, 1200 Vienna, Austria. Controlling, human resource management, ordering |
| 10/2000- 03/2001 | Paris, fille Au-pair |
| Since 1997 | Segelschule Hofbauer, 1220 Vienna, Austria. Sailing teacher for children and adults |